N° Ordre...../Institut/UMBB/2022

PEOPLE'S DEMOCRATIC REPUBLIC OF ALGERIA

MINISTERY OF HIGHER EDUCATION AND SCIENTIFIC RESEARCH

UNIVERSITY M'HAMED BOUGARA-BOUMERDES

Institute of **E**lectrical and **E**lectroni**c** **E**ngineering

Doctorate Thesis

Presented by:

AHCENE Fazia

For a **PhD Degree** in**:**

***Filière :*Génie électrique**

***Option :*Electrotechnique**

Title: Automatic Voltage Regulator Performance Enhancement in Power Generation Plant

To be defended before the jury composed of :

Mr	BENAZZOUZ Djamel	Prof	(UMBB)	President
Mr	BENTARZI Hamid	Prof	(UMBB)	Supervisor
Mr	KARA Kamel	Prof	(Blida)	Examinateur
Mr	KARA Redouane	Prof	(UMMTO)	Examinateur

Année Universitaire 2021/2022

ABSTRACT

The generation of electrical energy in power systems and islanded networks is generally ensured by the synchronous machine, and hence the enhancement of its dynamic performance during disturbances is increasingly required. The main objective of this research work is to enhance the dynamic performance by maintaining its terminal voltage constant during any instability. This voltage regulation can be ensured via a well-known controller named automatic voltage regulator (AVR) that is generally based on proportional integral (PI) controller. In the first proposed approach, an optimization method such as the particle swarm optimization algorithm (PSO) has been applied to determine the regulator parameters. However, in the second developed method, the AVR is based on Active Disturbance Rejection Control (ADRC) that allows controlling uncertain systems, where the dynamic is not well known such as in this application.

Both approaches are tested using different generators with two different ratings under different operating conditions. The first designed AVR is implemented; simulation and test have been carried out under three different operating load conditions using micro-generators such as a 1.5 kVA and 175 W synchronous laboratory power machine with salient pole. This AVR is based on PI controller tuned by PSO algorithm; the obtained simulation and experimental results validate the use of the designed AVR. Then, the second designed AVR test of a second generator of 187 k VA with different exciting system is investigated. However, the designed AVR of the second machine is tested using both techniques PSO base PI and ADRC, the obtained simulation results encourage to use the ADRC control in such application.

Key-words: Synchronous Generator; Automatic Voltage Regulator(AVR); Particle Swarm Optimization(PSO); excitation system; modeling and linearization; Active Disturbance Rejection Control (ADRC)

خلاصة

يتم بشكل عام ضمان توليد الطاقة الكهربائية في أنظمة الطاقة وشبكات بواسطة الآلة المتزامنة ، وبالتالي فإن تحسين أدائها الديناميكي أثناء الاضطرابات مطلوبة بشكل متزايد. الهدف الرئيسي من هذا العمل البحثي هو تحسين الأداء الديناميكي من خلال الحفاظ على الجهد ثابتًا أثناء عدم استقرار. يمكن ضمان تنظيم الجهد هذا من خلال وحدة تحكم معروفة تسمى منظم الجهد الأوتوماتيكي AVR والتي تعتمد بشكل عام على وحدة تحكم متكاملةPI في النهج الأول المقترح، تم تطبيق طريقة تحسين مثل خوارزمية PSOلتحديد معلمات المنظم. ومع ذلك، في الطريقة الثانية المطورة، يعتمدAVRعلى التحكم في رفض الاضطراب النشطالذي يسمح بالتحكم في الأنظمة غير المؤكدة، حيث لا تكون الديناميكية معروفة جيدًا كما هو الحال في هذا التطبيق.

كلمات مفتاحية: مولد متزامن ؛ منظم الجهد الأوتوماتيكي AVR,خوارزمية PSO؛ نظام الإثارة؛ النمذجة والخطية. التحكم النشط في رفض الاضطراب ADRC

Résumé

La génération d'énergie électrique dans les systèmes électriques et les réseaux îlotés est généralement assurée par la machine synchrone, et donc l'amélioration de ses performances dynamiques lors des perturbations est de plus en plus demandée. L'objectif principal de ce travail de recherche est d'améliorer les performances dynamiques en maintenant sa tension aux bornes constante pendant toute instabilité. Cette régulation de tension peut être assurée via un contrôleur bien connu nommé régulateur automatique de tension (AVR) qui est généralement basé sur un contrôleur proportionnel intégral (PI). Dans la première approche proposée, une méthode d'optimisation telle que l'algorithme d'optimisation par essaim de particules (PSO) a été appliquée pour déterminer les paramètres du régulateur. Cependant, dans la deuxième méthode développée, l'AVR est basé sur le contrôle actif de rejet de perturbations (ADRC) qui permet de contrôler des systèmes incertains, où la dynamique n'est pas bien connue comme dans cette application.
Les deux approches sont testées dans des conditions de fonctionnement différentes. Tout d'abord, l'AVR conçu est testé sous trois charges différentes à l'aide d'une machine de laboratoire synchrone de 1,5 kVA avec pôle saillant. Ensuite, le test d'un deuxième générateur de 187 k VA avec un système d'excitation différent est étudié. Dans le premier test utilisant la première méthode, les résultats de simulation obtenus valident l'utilisation de l'AVR conçu. Cependant, la deuxième machine est testée avec les deux approches proposées, les résultats de simulation obtenus encouragent à utiliser le contrôle ADRC dans une telle application.

Mots-clés : Régulateur de tension automatique AVR ; générateur synchrone ; Optimisation de l'essaim de particules PSO ; système d'excitation ; modélisation et linéarisation ; Contrôle actif du rejet des perturbations ADRC

ACKNOWLEDGMENT

First and foremost, we are very thankful to Allah for helping us finish this modest work.

This thesis is a result of six long years of hard work, and with the help of people who did not give up. During these years I learned a lot in my field and that is what leads me to make contributions, to continue research so as to improve my knowledge and to be a specialist in this field either if i have not get chance to validate all my results experimentally

We would like to specially thank our Parents who helped us in every possible way during studies and to express our deep gratitude to our Supervisor Mr. BENTARZI HAMID for his support and guidance throughout the study and realization of this thesis.

*My sincere thanks also go to the members of the jury: Mr*BENAZZOUZ Djamel*, Mr MANSOURI Rachid and Mr KARA Redouane,for agreeing to examine and evaluate my work.*

*I would like to warmly and particularly thank MANSOURI Rachid,Mr*OUADI Abderrahmane *and Mr REZEGUI Slimane for their precious help, presence and advice.*

We would like to extend our thanks to everyone who has been a support and to all friends.

At last but not least, I would like that my dear parents, my husband Ali, my son Sido, my sisters (Nadjet, Farida, Wassila, Karima, Maria) and my brother Rostom, find here the expression of my most sincere and deep thanks in recognition of their sacrifices, encouragement, their prayers, helpers and support to ensure this work in the best conditions.

THANK YOU.

DEDICATION

To my dear Parents

To my husband Ali

To my Family and Friends

To the special person in my life, my son sido

Table of Contents

Table of Contents

LIST OF ILLUSTRATIONS, GRAPHICS AND TABLES

LIST OF ILLUSTRATIONS, GRAPHICS AND TABLES

List of Symbols and Abbreviations

List of Abbreviations

AVR: Automatic Voltage Regulator

PI: Proportional Integral

PID: Proportional Integral Derivation

GA: Genetic Algorithm

BF:Bacterial Foraging

PSO:Particle Swarm Optimization

CRPSO: Craziness Based Particle Swarm Optimization

RGA: Real-Value Genetic Algorithm

ADRC:Active Disturbance Rejection Control

E.M.F: Electro-Motive Forces

RLmodel: Model expressed by resistances and inductances

XT model: Models expressed by reactances and time constants

PS: Power Stability

PSS:Power System Stabilizer

DC: Direct Current

AC: Alternatif Current

ST: Static excitation system

EM:Excitation Machine

GP: Principal Generator

HT: High Voltage

SGs: Synchronous Generators

SSFR: Short-Circuit Tests, Standstill Frequency Response

OCFR: Open Circuit Frequency Response

LFO: Low Frequency Oscillations

4SID:Subspace Slate Space (4SID, Pronounced 'Forsid')

LS: Least Squares

HN:identificationmethod

IEEE The Institute of Electrical and Electronics Engineers

PMSM: permanent magnet synchronous machine

OCC:Open-Circuit Characteristic

SCC: Short-Circuit Characteristic

ITSE: Integrated of Time weight Square Error

ISE: Integrated Square Error

IAE: Integrated Absolute Error

TD : tracking differentiator

ESO :extended state observer

NLSEF: nonlinear state error feedback

LADRC: linearActive Disturbance Rejection Control

VP :Eigenvalue

SISO: single input single output

ST1A : the Excitation System

PWM:pulse width modulation signal

List of Symbols

(d, q, 0): model described in the Park's coordinate system

θ : an electrical angle

nd, nq: number of equivalent damping circuits in the d and q axes of the rotor

X_d, X'_d, X''_d, T_{do}, T'_{do}: reactances and time constants of sub-transient, transient and steady states

Ld: shunt self-excitation winding

Ls: separate excitation winding

V : Voltage

Vc: voltage at a fictitious point

ω: The angular velocity of the rotor (rad/s)

(Slip): Slip test

Max: maximum

Min: minimum

I_{sc}: current of short-circuit occurrence

E_o :is the rms line-to-neutral open circuit pre-fault terminal voltage

$Z_{d\ (unsat)}$:The d-axis unsaturated impedance

$X_{d\ (unsat)}$:The direct-axis unsaturated synchronous reactance

S_n : Nominal power

I_D and I_Q :damper currents

rms: effective value

V_o:voltage set point

Vf: excitation voltage

If: excitation current

Zc: compensation impedance

Ifmax: maximum permanently admissible current.
a, b and c: The three-phase windings of the armature
d-axis: direct-axis
q-axis: orthogonal quadratic-axis
mmf: magneto-motive force
f, *D* and *Q* : The rotor windings
$I_{A,B,C}$: The phase currents respectively phase A, phase B and phase C

Ψ: the magnetic flux linking the windings
T_m : mechanical torque

U_n : Nominal rms line-to-neutral voltage

f_n : Frequency

R_s : Stator resistance

R_f : Rotor resistance

X_d :Direct-axis synchronous reactance (unsaturated)

X_q : Quadrature-axis synchronous reactance (unsaturated)

T_{do}' : Direct-axis open-circuit time constant

X_d' : Direct-axis transient reactance

T_d' : Direct-axis transient time constant

X_d" : Direct-axis sub-transient reactance

X_q" : Quadrature-axis sub-transient reactance

T_d" : Direct-axis sub-transient time constant

K_f, K_D and K_Q: Reduction Coefficients

Xd Steady-state direct axis synchronous reactance

X_l Stator leakage reactance

$(I,\Psi, R,V)^r$:magnitude with stator axes fixed magnetically to the rotor d- and q-axes

M: mutual reactance

V_t : The input voltages

V_{ref} : voltage reference

V_r : The output voltage of the PI controller

KA gain

TA: time constant

VRMAX and VRMIN: saturation limits.
The indices 1 and 2: transformer's primary and secondary
R: resistance
L: leakage induction

M: mutual induction

s : Laplace domain

$V_{con\ (AVR)}$: control voltage

K_P :proportional gain

T_I :integral constant time

T_D :derivative constant time.

e(t) : error voltage.

$()_{FP}$: forward-path index

ω_n : nominal pulse

ζ:damping coefficient

()G: generator index

V_f: voltage applied to the field winding.

V_2: the rms value of the secondary winding of the excitation transformer.

V_{tb}: maximum generator output voltage.

Pbest: The best staff

Gbest:Global Best

c1 & c2: Acceleration parameters

V_i^t: Velocity

X: constriction factor

v_x:the speed of the X axis

v_y :the speed of the Y axis

w :The inertial weight

i: particle index

V_i: Movement Speed

x_i : position

t: iteration number

n : population size

ˆf :estimated disturbance

ωc: controller bandwidth

ωo : observer bandwidth

y (t) :output quantity

u (t): control quantity

f (t): total disturbances

$f_0(t)$: estimate of the total disturbance

A,B, C,E: matrix

$\varepsilon(t)$:The error

$\hat{x}(t)$, $\hat{y}(t)$:respectively the dynamics and the output of ESO

L :Correction gain matrix

$\dot{\varepsilon}(t)$:derivation of this error

P(s): first-order process

b: adrc parameter

s^{CL} : pole

$s_{1/2}^{ESO}$:the observer poles

T_{settle} : settling time

r(t): reference value

K_p and K_D: ADRC gains

λd :Increase the time constant

r_{exc} :star-connected resistances

Chapter 1

Introduction

Chapter 1

Introduction

1.1 Context

Electric energy is a vital element in our modern life. Around the world, electricity has found many applications in various areas. However, since energy is a scarce and precious resource, the investigation of its use may be performed through the use of the most optimal possible way. For two centuries ago, the consumption of electricity globally has increased by a factor of 70. This leads to increase the mode of living and life expectancy of the people in the earth. However, these tremendous advances in this field have been made with an increasingly significant impact on the environment, whether in the production, transport or/and distribution level of the electrical energy.

While waiting for renewable energies to take a place at the worldwide level, a thought about minimizing the effect of the conventional electrical energy; for example, more attention should be paid to reducing consumption, improving the efficiency of power plants and distribution, and also adopting specific compensation programs for co_2 gases. Over the past decade, power utilities in Algeria have operated their power systems at full power and often closer to their stability limits. This can damage the generator and the power grid.

Today most of this energy is produced by synchronous machines in thermal and hydraulic power plants. Thus, synchronous machines play an important role to provide the power system with an energy compensation making its voltage level possible constant, in the first moments, during a transient condition of imbalances between production and consumption, through the control of the machine exciter [1, 2, 3].

The efficiency of electric power system and the stability of the synchronous generator are highly dependent on the reliability of the exciter that is considered as the main power source for the whole system. Because the excitation supports the stator and the rotor, however, the loss of excitation of the generator weakens the various parts of the machine and hence leads to an imbalance of mechanical and electrical power and the speed of the rotor increases beyond the synchronous speed. This phenomenon can damage the generator and the power grid.

Consequently, the regulation of the voltage at the terminals of the generator, despite the presence of disturbances has become a priority and a great concern. In practice, this role is devoted to the generator excitation system [4].

The excitation system reduces the above mentioned risks, the generator itself is a source of energy or the generator is self-excited. The significant advantage of this type of excitation system can generate negative excitation current. Thus, it allows a rapid de-excitation which may be necessary in the event of an internal fault of the generator and also reduces the response time and the size of the installation. Therefore, a voltage regulator is essential to achieve satisfactory system performance. Voltage regulation is provided by a well-known controller called an Automatic Voltage Regulator (AVR).

A typical power conditioner device is an AVR combined with one or more of the following: Surge suppression, short-circuit protection, line noise reduction, phase-to-phase voltage balancing, harmonic filtering, etc. The AVR is mainly used for safety and financial reasons. The deviation from the desired output value may cause malfunction or permanent failure to the supplied electrical equipment that will result in extra costs and downtime. Thus, the AVR is used to primarily maintain voltage within a range of 5% error for safety purposes of the equipment. In order to remedy this drawback, a PID Controller for an AVR has been used. Besides, many approaches have been developed by several researchers in previous years for tuning the parameters of this controller. We can cite some works such as:PSO-based PID type controller presented by Gaiang[5]; Hybrid genetic algorithm (GA), bacterial foraging (BF) technique developed by Kim and Cho [6],Craziness Based Particle Swarm Optimization (CRPSO) presented by Mukherjee and Ghoshal and binary encoded genetic algorithm[7].Ching-Chang proposed a PID controller for the AVR system based on a real-value genetic algorithm (RGA) and a particle[8] and Dadashpour implemented a PID based on the company's optimization lawless [9], also PID for AVR system designed using Taguchi Combined Genetic Algorithm[10], Jingquin Han published several papers on a new unconventional control method ADRC [11, 12]. Moreover, the application of a PSO algorithm for the determination of the parameters of the corrector offered precision can be found in [2, 8, 12].

1.2 The Objectives of this research work:

The main contribution of our work is to propose two approaches which can be used to enhance the dynamic performance by maintaining its terminal voltage constant. This research work is divided into two parts. In the first part, a voltage controlling system named automatic voltage regulator (AVR) that is generally based on proportional integral (PI) controller is investigated. In this approach, an optimization method such as the particle swarm optimization algorithm (PSO) has been used to tune the regulator parameters. Then, an AVR based on Active Disturbance Rejection Control (ADRC) that allows controlling uncertain systems when the dynamic is not well known as in this application, is developed.

In the second part, validation tests have been investigated using both approaches. In the first test, the output voltage is regulated by acting on the excitation voltage for a synchronous machine with salient pole of power 1.5 KVA by adopting a static excitation. For the control purpose, two control methods are used. The first method is a conventional method the PSO to optimize the parameters of the PI regulator; however, the second one is a digital ADRC method. In the second test, same control methods are applied to a self-excited synchronous

machine with a power of 187 MVA. The results obtained by the ADRC are very satisfactory compared to the PSO-PI method.

1.3 Thesis Outline

After the first chapter introduction summarizes the motivation of this research work and methodology to achieve the objectives and the last chapter deals with A summary of the contributions, implications, and limitations of the study and future research directions. It is useful to organize the remaining chapters as follows:

The second chapter presents a state of the art where we have summarized all the parts of our work such as the presentation of the synchronous machine and its different parts,

In third chapter, the modeling followed by a study on the different existing excitation systems was presented. Besides, for test purpose, two different systems are used; including a power synchronous generator of 1.5 KVA with static excitation represented by its transfer function and a self-excited system containing a generator of 187MVA represented by its Simulink model.

The parameters of the two machines are given in the appendix (A).

The fourth chapter deals with the application of a PI based AVR controller; where its parameters optimized by the PSO method. Before carrying out various tests on the turbine-alternator associated with excitation system, the modeling of each block is essential. The model of the generator is presented, and adapted to the issue of the topic. And finally, the modeling of the excitation system, which presents the most important part in our work, before assembling and putting of the different models, in a single global model.

In chapter five, the ADRC method principle and its implementation in the system is discussed. Some important aspects of this method are presented, followed by concluding observations.

In chapter six, the two techniques are analyzed and compared in order to validate our contribution and justify our choice. The test that has been carried out consists of regulation via well-chosen PI-based AVR controllers, which will be introduced into the exciting circuit of the overall system. The obtained study results using two generators are illustrated and analyzed.

1.4 Publications

The thesis is developed from the peer-reviewed journal and conference papers which are listed below.

Journal papers

1. AHCENE Fazia, BENTARZI Hamid OUADI Abderrahmane « automatic voltage regulator design enhancement taking into account different operating conditions and environment disturbances » journal ALJEST Algerian journal of environmental science and technology ISSN 2437-1114. e-ISSN: 2478-0030
2. AHCENE Fazia, BENTARZI Hamid « Synthesis of ADRC and its Application to an Electrical Power System », submitted to Algerian journal of signals and systems september 2022.

Conference papers

1. AHCENE Fazia, BENTARZI Hamid OUADI Abderrahmane the international conference « Computational methods in applied sciences » Istanbul, Turkey Juilly 2019.
2. AHCENE Fazia, BENTARZI Hamid OUADI Abderrahmane « automatic voltage regulator design using particle swarm optimisation technique » 6th international conference on electrical engineering (ICEE-2020) septembre 2020 Istanbul Turkey.

Chapter 2

Review of Synchronous Generator and its Exciting Circuit

Chapter 2

Review of Synchronous Generator and Its Exciting Circuit

2.1 Introduction

Our modern daily life revolves around electrical energy. Electricity has many uses in various areas of life such as industry, agriculture, transportation, and residential applications. Electrical power is considered as the most adaptable and versatile type of energy. Because it is derived from abundant primary sources such as coal, gas, oil, hydroelectricity, wind, and solar radiation. Electricity is a well-suited energy source for consumption-driven applications due to the various conversion possibilities. Since energy is an intermittent and precious resource, the focus must be on its optimal use [13].

A power system is sized to provide the desired electricity capacity at all times under acceptable quality requirements with the ability to keep voltage and frequency levels within acceptable limits. An electrical energy system can return to the same state or another state of equilibrium after disturbances, by keeping most system variables within their limits and the entire system remains in normal operation condition. This ability is referred to as power system stability which can be classified into three types: Rotor angle stability (angular stability), voltage stability, and frequency stability [15].

The modeling of a synchronous machine helps to develop a system that would allow the machine's static and dynamic functioning to be represented. Analysis knowledge, identification, simulation, diagnosis, control, and prototype design are all tasks can be investigated by the modeling. The mathematical method that can be adopted as well as the simplifying assumptions can be taken into account, have a direct impact on the model's complexity and precision [16]. The stability is ensured via regulatory and control systems. To improve network stability, the alternator will be equipped with an excitation system with an automatic voltage regulation circuit (AVR) for improving performance in a permanent state; however, this has not been enough for conditions affecting transient stability [17, 14].Controllers are included in excitation systems (AVR). The 'Proportional, Integral, Differentiator or PID regulator is the most used regulator. It is employed in the vast majority

of industrial installations due to its simplicity and performance. The usual location of the regulator in a loop is located in the chain of action, just after the comparator. It's important aim is to satisfy performance standards relating to the stability, the accuracy, and the speed such as response time, transient overshoot, stability margins (gain margin or phase), and permanent precision[18].

In first section, the synchronous machine, its parts and functionality have been represented. The second section is devoted to the study of the excitation system. Then, it is followed by a third section that deals with AVR regulators.

2.2 Synchronous machine

The electro-energy system is a power system that covers a large number of customers and many power production plants. The electrical energy produced by power plants transferred through the meshed transmission lines with high and very high voltage levels throughout an area comprising one or more states, before being routed through the medium and low voltage distribution networks, whose tree structure allows it to reach end customers.

The power plant is the source of electrical energy, which consists of many synchronous machines (turbo-alternators) that convert mechanical power into electrical power which in turn is delivered via transmission lines for prospective industrial as well as domestic applications. The utilities are continuously looking for efficient methods to improve output and assure continuity of power supply. The electrical energy users demand a consistent level of service and a reliable power production. The position of a turbo-alternator in a power plant is shown in Figure (1.1). A turbo-alternator consists of a turbine and an alternator, which converts mechanical energy (movement), using steam or gas, into electricity. The majority of alternators are extremely powerful machinery used in power plants. They are composed of two main parts: a *stator*, which is the fixed part, and a *rotor*, which is the rotating element [14]

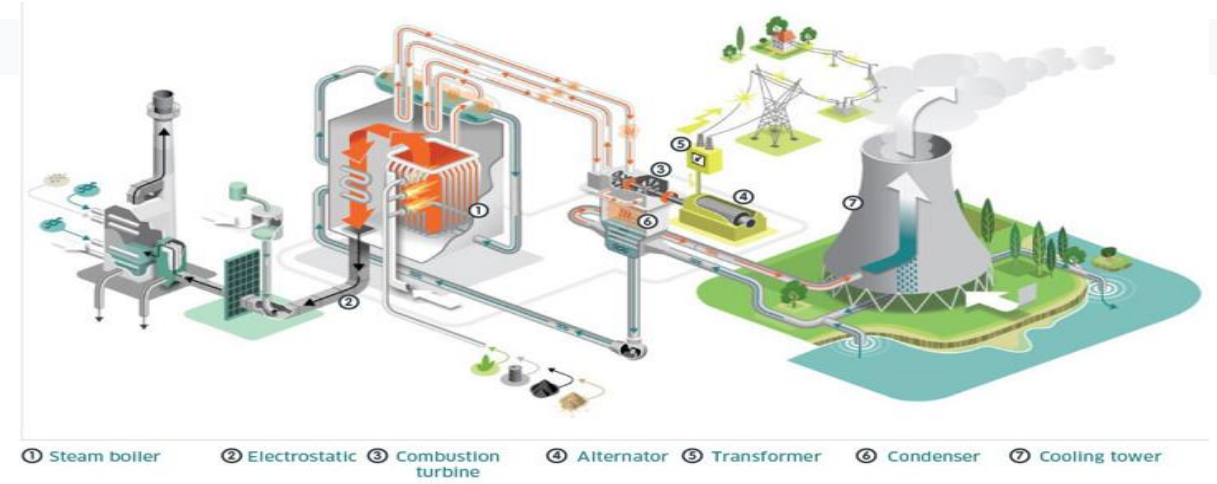

Figure 2.1 The Position of Alternator in a Power Plant [19].

The stator is separated by a small air gap from the rotor. Both the stator and the rotor are made of *a magnetically permeability-rich material core* [20].

2.2.1 Synchronous machine parameters

In power system simulations, lumped parameter circuit models for synchronous generators, which simulate electromagnetic and mechanical phenomena with varying degrees of accuracy, are often utilized. Field-circuit models that use the electromagnetic field equations coupled with the equations of electric circuits of the windings are considered to be the most accurate generator models. Numerical mesh approaches are used to solve such equations, with the finite element method being the most popular [26 - 33].

They can be divided into two categories:

- Models expressed by resistances and inductances of electric circuits (RL models).
- Models expressed by standard parameters, reactances and time constants of subtransient, transient and steady states (XT models). In the models expressed by resistances and inductances of electric circuits (RL models), rotor equivalent circuits with lumped constants of RL type approximate damping circuits with distributed constants. Denoting the type of the generator mathematical model by a pair of numbers (1+nd, nq), where nd, nq determine the number of equivalent damping circuits in the d and q axes of the rotor, there are determined the models of (3,3),(2,2),(2,1)and(1,0)types [34 - 38].

The models expressed by standard parameters (XT models) are approximate models. They are expressed by reactances and time constants of sub-transient, transient and steady states (X_d, X'_d, X''_d, T_{do}, T'_{do}) [34 39 40]. Since the mid-twentieth century, models of this type have been used in investigations of PS system stability and have been implemented i.a. in the PSS/E program, in which they appear under the names GENROU, GENROE, GENSAL, GENSAE. In XT models, the rotor damping circuits with distributed constants are represented by one equivalent damping circuit with lumped constants in the d-axis and two equivalent damping circuits in the q-axis(turbo-generator—GENROU and GENROE models)or one damping circuit in the q-axis(hydro-generator—GENSAE and GENSAL models). The characteristic features of the XT models under consideration are given in Table 2.1.

In XT models, the transformation voltages in the stator are neglected and the saturation of magnetic cores is taken into account. The omission of transformation voltages causes algebraization of the stator equations and reduction of the order of the differential equations of the model. XT models of synchronous machines are often used in simulation investigations of slowly changing electromechanical transient states in power systems to assess, among others, the angular stability of the system. The physical quantities and parameters of the models described in the Park's coordinate system (d, q, 0) are expressed in relative units, when assuming as the reference quantities [34 38 41 42].

2.3 Excitation System for Synchronous Generator

Excitation that is very important in the generator defines its output values: voltage and reactive power. A generator excitation regulation is regulation of generator output energy, which affects the stability of entire electric power system. Excitation current is provided by the excitation system, which, usually consists of autonomic voltage regulator (AVR), exciter, measuring elements, power system stabilizer (PSS) and limitation and protection unit (Figure2.2) [43].

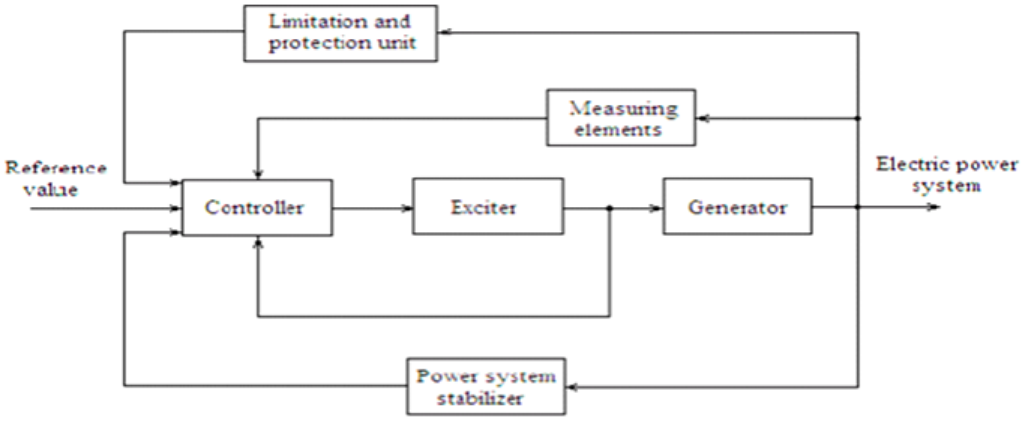

Figure.2.2 Excitation System of Synchronous Generator [44].

Excitation systems comprise machines, devices, and appliances intended to supply the generator field winding by current directly and then this current is regulated. They are also responsible for control and protection of the power system. The excitation system is an important control unit for synchronous generator, and its dynamic performance has immediate impact on a generator stability and reliability.

When the behavior of a synchronous machine is to be simulated accurately for a power system stability case study, the excitation system must be modeled adequately.

The excitation current is the current producing the required magnetic flux in the air gap; it is the field winding current at a particular load (or rated load).

Based on their excitation power gain these are the types of excitation systems [45 46]:

- Independent - exciter unconnected to the grid thus excitation parameters have no direct connection with the grid parameters; turbine mechanical power is used for the excitation.
- Dependent - exciter utilizes the generator power or connects to the grid; in terms of the excitation source these are further classifications of excitation systems: DC, AC Static.

DC excitation systems: define as the systems are providing current to the rotor of the synchronous generator through the slip rings directly; exciter placed on the same shaft or is separately by a motor and self–excited or separately excited, with a permanent magnet.

AC excitation systems describes as the exciter is typically placed on the same shaft as the turbine. The AC is rectified by controlled or non-controlled rectifiers and provides DC to the

generator field winding. The DC output is fed to generator field winding by slip rings at stationary rectifiers. Rotating rectifiers do not need slip rings, brushes and DC is directly fed to generator as the armature of the exciter and rectifiers rotate with the generator field. Such systems are known as *brushless systems* and were developed to avoid problems with the brushes when extremely high field currents of large generators are applied.

Static (ST) excitation systems have stationary status for all elements. Such systems use slip rings which directly provide excitation current to synchronous generator field winding. Rectifiers in ST systems gain generator power through auxiliary windings or step-down transformers. In such systems the generator itself is a power source, i.e., the generator is self-excited. The generator is unable to produce any voltage without excitation voltage, so it must have an auxiliary power source to provide field current and energize itself. Station batteries are the usual additional power source, used in what is termed f*ield flashing.* Different excitation systems have different relative advantages and disadvantages [47].

Table 2.1 Common Classification of Synchronous Generator Excitation System [48].

<table>
<tr><th>Exciter type</th><th>Whether the rectifier controlled</th><th>Whether has pilot exciter</th><th>Bruch/no Bruch</th></tr>
<tr><td>DC</td><td>/</td><td>/</td><td>/</td></tr>
<tr><td rowspan="5">AC</td><td rowspan="3">No</td><td rowspan="3">Yes</td><td>With Bruch</td></tr>
<tr><td>Without Bruch</td></tr>
<tr><td>With Bruch</td></tr>
<tr><td>No</td><td>Without Bruch</td></tr>
<tr><td>Yes</td><td>No</td><td></td></tr>
<tr><td rowspan="3">Static</td><td colspan="3">Self-compound Excitation</td></tr>
<tr><td colspan="3">Self Excitation</td></tr>
<tr><td colspan="3">Constant voltage power supply</td></tr>
</table>

Since the capacity of DC exciter is hard to expand because of commutator restrictions, it is no longer used in the new production generator sets of 100MW and above. Currently, most the new large generator put into operation are using self-shunt excitation system or AC excitation system with pilot exciter (referred to three-machine excitation [48].

2.3.1 Exciter Control Chain Components and protection

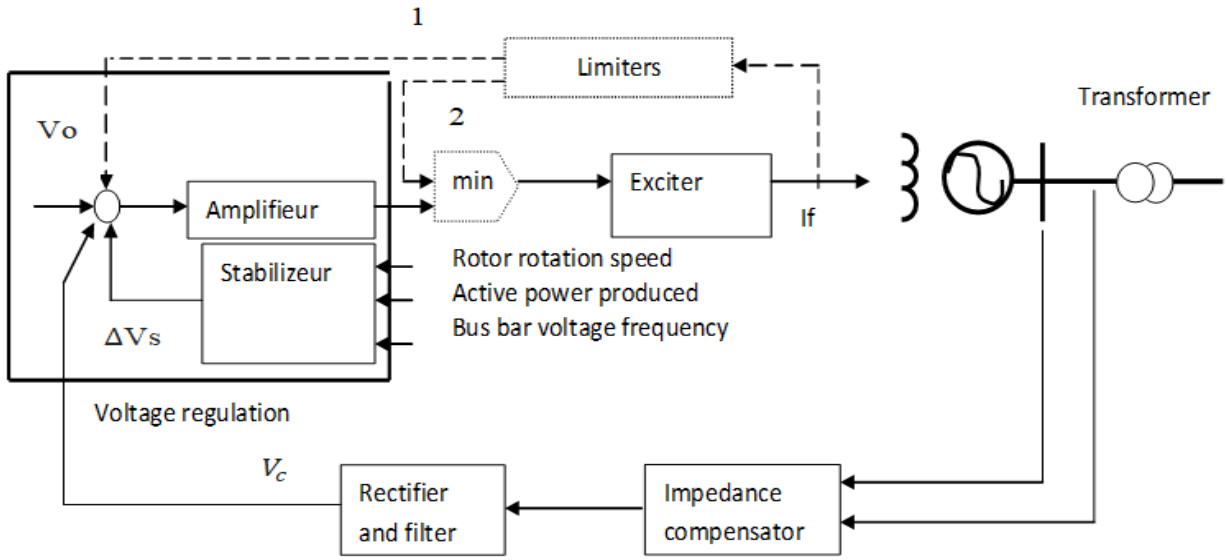

Figure 2.3 Block diagram of synchronous machine excitation system

The voltage V at the generator busbar is measured via a potential transformer then rectified and filtered to give a DC signal Vc, proportional to the rms value of the AC voltage. The voltage regulator compares Vc to the voltage set point V_o, amplifies the difference and puts the result in the form suitable for controlling the exciter. When the terminal voltage V drops or the set point Vo rises, the core idea of this control is to increase the generator's excitation voltage Vf, and vice versa.

The regulator is frequently integrated with a "stabilizer," whose function is to add a transient component ΔVs to the error signal Vo-Vc, increasing the dynamics of the machine in operation on the network. The rotor oscillations are reduced (relative to the uniform motion corresponding to the established perfect regime).

ΔVs can be worked out from one or more measurements, typically the speed of rotation, the frequency of the voltage at the busbar or the active power produced by the generator.

These signals are passed through transfer two chosen functions so that to increase the component of the electromagnetic torque providing you with damping.

The exciter is an auxiliary machine. In steady-state,it supplies a direct current if under a continuous voltage Vf, the power Vf*If being at the level required by the excitation winding of the generator. It must be able to quickly vary Vf and if in response to a variation of the signal supplied by the voltage regulator.

The regulator can also be equipped with an impedance equalizer, combining the current and the voltage measured at the output of the generator to produce a signal corresponding to the phasor:

$$V_c^- = V^- - Z_c I^- \quad (2.1)$$

Zc is the compensation impedance. This signal is rectified and filtered as mentioned above, to obtain:

$$V_c = |V^- - Z_c I^-| \quad (2.2)$$

Taking for Zc a fraction (typically between 50 and 90%) of the serial impedance of the step-up transformer, Vc is the voltage at a fictitious point located between the busbar of the machine and the corresponding network busbar. The voltage drop in the step-up transformer is therefore partially compensated and the grid voltage is better regulated.

A) Rotor current limiter (or over-excitation)

A synchronous machine must operate within certain limits, specified by its capacity curves.In response to a large disturbance, such as a short circuit, it is important to let the voltage regulator and exciter provide high excitation current to sustain the mains voltage.

In such circumstances, the excitation voltage may increase rapidly to a “ceiling” value and the excitation current may reach a value of the order of 2 Ifmax, where Ifmax is the maximum permanently admissible current.

Such a value cannot be tolerated for more than a few seconds, on pain of damaging the excitation winding. However, since the heating is proportional to a ∫i2dt.

After the overload delay has elapsed, the rotor current must be reduced. Two techniques can be used for this purpose; the first (dotted branch 1 in figure 2.3) consists in controlling the exciter by the smallest of the signals provided, respectively, by the voltage regulator and by the limiter. This therefore “opens” the feedback loop of the voltage V;

In the second technique (see Figure 2.3), the limiter injects a correction signal at the summing point of the regulator. Normally, this signal is zero, while when the limiter acts; it is such that the excitation current is brought back to the desired limit.

This can be seen as a decrease in the Vo setpoint such that the excitation current remains at the desired level. With this technique, the protection of the excitation winding still relies on the voltage regulator.

Generally, the voltage regulator automatically resumes control as soon as the operating conditions allow it, for example following an intervention in the network.

B) Stator current limiter

Stator current limiters are not as widespread as rotor limiters. The main reason is the greater thermal inertia of the stator, which allows slower action by the operator in the power plant. The latter will react to a stator overload alarm, either by decreasing the Vo (which reduces the production of reactive power) or by reducing the active power produced.

Some generators are equipped with automatic stator current limiters, which act on the excitation system in the manner described for the rotor [20].

2.3.2 Excitation System with AVR

Synchronous Generators (SGs) with field windings require DC-supplies to excite them, and as they are constant speedy machines for constant frequency supply, the output voltage depends radically on the excitation current. The control of excitation current to maintain constant voltage at the SG output terminals starts with the control of the exciter (Figure 2.4).

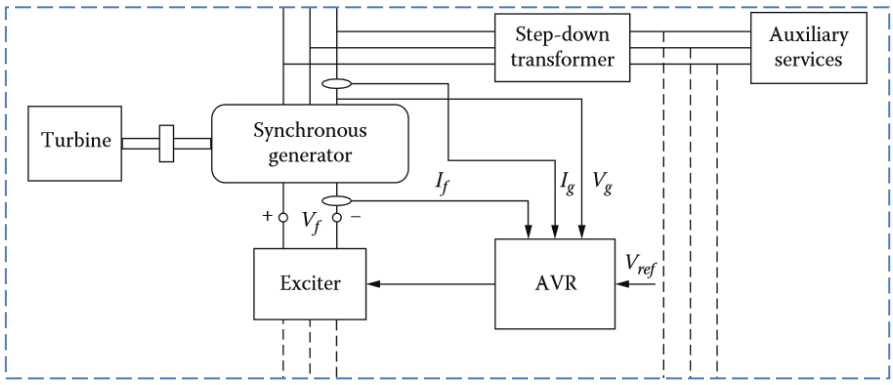

Figure 2.4 Structure of Excitation System with AVR.

The performance requirements of the excitation system are determined by considering the SG. Along supplying and automatically adjusting the field current, the excitation system plays an important role in protection and stability of the machine, it must respond rapidly to disturbances to enhance system robustness.

The aim of this section is to give short review on excitation system used in this work are presented, as well as on different possibilities to regulate those systems.

In this chapter, the structure and the working principle of the excitation system used in this work are presented. The functionality of each part of the excitation system along with the automatic voltage regulator (AVR) are discussed. The controller gains are tuned using the zero/pole cancelation and the particle swarm optimization (PSO) methods.

Chapter 3

Modeling and Parameter Identification of Synchronous Generator with Exciting System

Chapter 3

Modeling and Parameters Identification of Synchronous Generator with Exciting System

3.1 Introduction

A complete synchronous generator (SG) model consists of a combination of a model structure and a set of parameter values. This definition can be broken into two parts. The first part is the construction of the model structure which is the basic form for machine representation. The second part is the evaluation of the model parameters [72].

The model structure can be formed as lumped-parameter equivalent circuit, transfer function, differential equation representation, etc. On the other hand, the model parameters can be evaluated either based on the manufacturers' data, experimental test results, or some other techniques cited in chapter II section 2.2.1 [72].

This chapter contains a general description of the developed methods and tools supporting the measurement process of determining reliable values of mathematical model parameters of generating unit elements, in particular synchronous generators and excitation systems. Special measuring tests are the basis for determining the parameters. They can be carried out under normal operating conditions of generating units.

3.2 Modeling requirements for synchronous machines

In the study of most power system control categories, synchronous machines can be modeled with many details as possible. This contains an adequate representation of the dynamics of the field winding, the excitation system, and the rotor damping circuits (subject to data availability). No need to simplify models for specific areas of research with modern computing tools. Further, experience has shown that the use of simplified models, which are sometimes considered acceptable for a particular type of study, can mask essential problems [74].

Table 3.1 Synchronous Generator XT Models[73]

GENROU	Cylindrical synchronous machine expressed by standard parameters. One damping circuit in d axis and two damping circuits in the q axis. Approximation of the saturation correction by quadratic function
GENROE	Cylindrical synchronous machine expressed by standard parameters. One damping circuit in d axis and two damping circuits in the q axis. Approximation of the saturation correction by exponential function
GENSAL	Salient pole synchronous machine expressed by standard parameters. One damping circuit in d axis and one damping circuits in the q axis. Approximation of the saturation correction by quadraticfunction
GENSAE	Salient pole synchronous machine expressed by standard parameters. One damping circuit in d axis and one damping circuits in the q axis. Approximation of the saturation correction by exponential function

perturbation techniques to separate the fast and slow dynamics and appropriately approximate fast dynamics [74].It is important to recognize the following special requirements when representing synchronous machines for different categories of studies [21].

3.3 Conventional Model Structure

The schematic of three-phase SG is illustrated in Figure 3.1. SGs consist of two essential elements: field and armature. The field winding carries direct current and produces a magnetic field which induces alternating voltage in the armature windings [41].

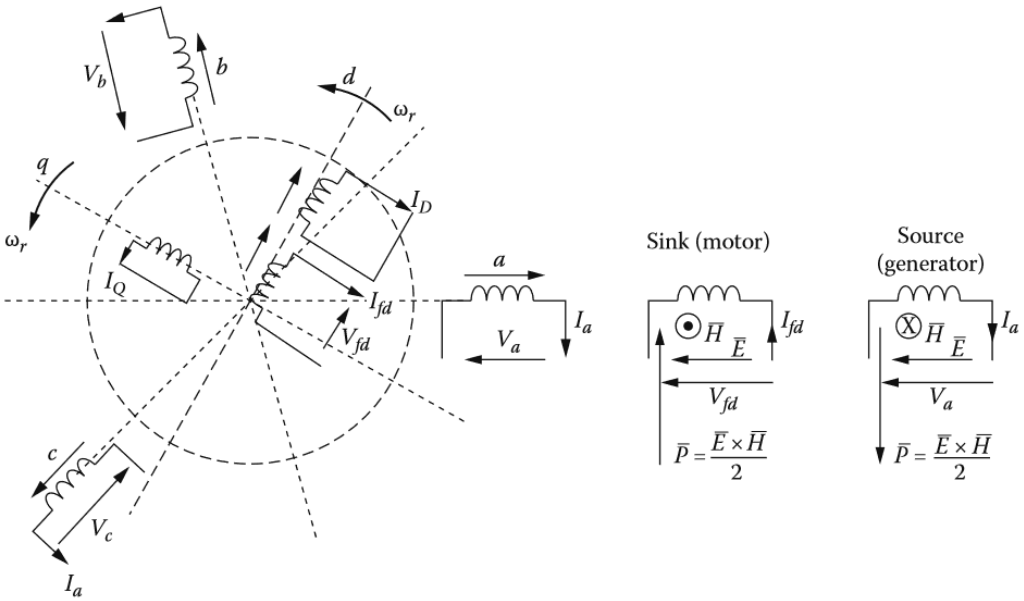

Figure 3.1 Schematic Diagram of Three-Phase Synchronous Generator.

The three-phase windings of the armature (a, b and c) are distributed 120° electrical degrees apart. The rotor structure has an excitation or field winding and one or more

equivalent rotor body windings. The magnetic axis of the machine is defined as the direct-axis (d-axis), and an orthogonal quadratic-axis (q-axis) is located 90° electrical degrees ahead of the d-axis [41].

Before proceeding in developing model for SG some assumptions are made: [41]

- Magnetic saturation effect, temperature effect and magnetic hysteresis are neglected.
- Stator winding currents are assumed to set up a magneto-motive force (mmf) sinusoidal distributed in space around the air gap. Therefore, the effect of space harmonics in the field distribution is neglected.
- The mmf acting along the d-axis produces a sinusoidal distributed flux wave along that axis. The same for the q- component of the mmf.

3.4Mathematical Formulation and dq-Model

The model structure is to be formed as a set of equations that are suitable for system studies and analysis. These equations must completely describe the behaviour of the SG.

3.4.1 SG in Natural-Reference Frame

By applying Maxwell's equation to the configuration shown in Figure 3.1, the generator phase voltage equations, in natural-reference frame are simply: [41, 94]

$$\begin{aligned} I_A R_s + V_a &= \frac{d\psi_A}{dt} \\ I_B R_s + V_b &= \frac{d\psi_B}{dt} \\ I_C R_s + V_c &= \frac{d\psi_C}{dt} \\ I_f R_f - V_f &= -\frac{d\psi_f}{dt} \\ I_D R_D &= -\frac{d\psi_D}{dt} \\ I_Q R_Q &= -\frac{d\psi_Q}{dt} \end{aligned} \tag{3.1}$$

The flux linkage to current relationship in phase (a) winding at any instant is given by:

$$\psi_A = -L_{AA} I_A - L_{AB} I_B - L_{AC} I_C + L_{Af} I_f + L_{AD} I_D + L_{AQ} I_Q \tag{3.2}$$

Similarly, one can write the flux linkage to current relationships in phases (b) and (c). The flux linking the three-phases of the stator winding is a function of θ. i.e., the angular displacement of the d-axis from phase (a) [41].

Equations (3.1) completely describe the electrical behavior of a SG. However, these equations contain inductance terms which vary with angle θ – rotor position – which in turn varies with time. For that, the machine model was further developed by Park who mathematically transformed the three-phase time-varying stator quantities (voltages, currents and flux linkages) into time-invariant d- and q-axes quantities under steady-state conditions [72]

The dq-model should express both stator and rotor equations in rotor coordinates, aligned to rotor d- and q-axes because, at least in the absence of magnetic saturation, there is no coupling between the two orthogonal axes. The rotor windings *f*, *D* and *Q* are already aligned along the d- and q-axes. It is only stator equations that have to be transformed to rotor orthogonal coordinates. The transformation from abc- to dq-variables can be written in the following matrix form: [94]

$$\mathrm{P}(\theta)=\frac{2}{3}\begin{pmatrix}\cos(\theta) & \cos(\theta-\frac{2}{3}\pi) & \cos(\theta+\frac{2}{3}\pi)\\ -\sin(\theta) & -\sin(\theta-\frac{2}{3}\pi) & -\sin(\theta-\frac{2}{3}\pi)\end{pmatrix} \tag{3.3}$$

Therefore:

$$\begin{bmatrix}V_d\\V_q\end{bmatrix}=P(\theta)\begin{bmatrix}V_A\\V_B\\V_C\end{bmatrix}$$
$$\begin{bmatrix}I_d\\I_q\end{bmatrix}=P(\theta)\begin{bmatrix}I_A\\I_B\\I_C\end{bmatrix}$$
$$\begin{bmatrix}\psi_d\\\psi_q\end{bmatrix}=P(\theta)\begin{bmatrix}\psi_A\\\psi_B\\\psi_C\end{bmatrix} \tag{3.4}$$

The analysis of SG equations in terms of dq-variables is considerably simpler than in terms of phase quantities, for the following reasons: [41]

- The dynamic performance equations have constant inductances.
- For balanced conditions, zero sequence quantities disappear.
- For balanced steady-state operations, the stator quantities have constant values.

- The parameters associated with d- and q-axes may be directly measured from terminal tests.

The inverse transformation is: [94]

$$P(\theta)^{-1} = \frac{3}{2} P(\theta)^{T} \tag{3.5}$$

The phase currents I_A, I_B and I_C are recovered from I_d and I_q by:

$$\begin{bmatrix} I_A \\ I_B \\ I_C \end{bmatrix} = P(\theta)^{-1} \begin{bmatrix} I_d \\ I_q \end{bmatrix} \tag{3.6}$$

$$\frac{d\theta}{dt} = \omega_r \tag{3.7}$$

Note:

An alternative Park transformation uses $\sqrt{\frac{2}{3}}$ instead of $\frac{2}{3}$ for direct and inverse transform [41,94]

The dq-transformation can be seen as representing a SG with orthogonal stator axes fixed magnetically to the rotor d- and q-axes (Figure 3.2) [94].

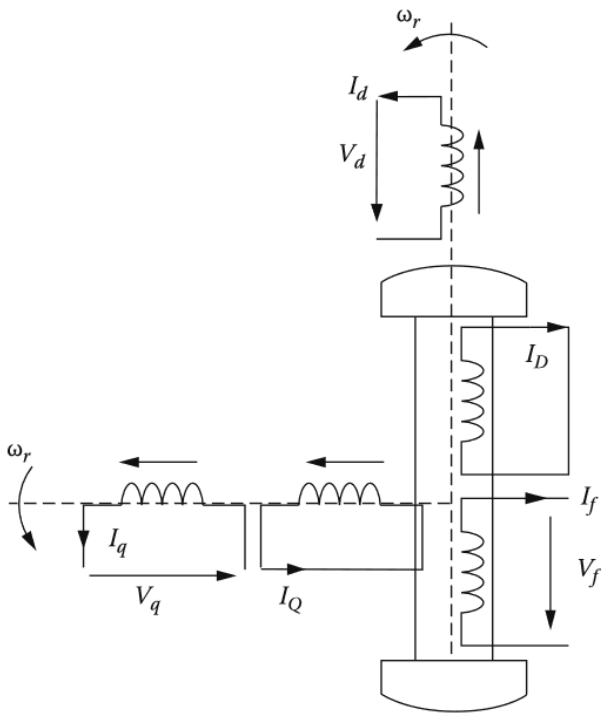

Figure 3.2 The dq-Model of Synchronous Generators.

By applying the dq-transformation the following expressions in terms of transformed components of voltages, flux linkages and currents result: [94]

$$\begin{aligned} I_d R_s + V_d &= \frac{d\psi_d}{dt} - \omega_r \psi_q \\ I_q R_s + V_q &= \frac{d\psi_q}{dt} + \omega_r \psi_d \\ I_f^r R_f^r - V_f^r &= -\frac{d\psi_f^r}{dt} \\ I_D^r R_D^r &= -\frac{d\psi_D^r}{dt} \\ I_Q^r R_Q^r &= -\frac{d\psi_Q^r}{dt} \end{aligned} \tag{3.8}$$

Where:

$$\begin{aligned} \psi_d &= -L_d I_d + M_f I_f^r + M_D I_D^r \\ \psi_q &= -L_q I_q + M_Q I_Q^r \\ \psi_f^r &= (\mathrm{L}_{fl}^r + \mathrm{L}_{fm}) I_f^r - \frac{3}{2} M_f I_d + \frac{3}{2} M_{fD} I_D^r \\ \psi_D^r &= (\mathrm{L}_{Dl}^r + \mathrm{L}_{Dm}) I_D^r - \frac{3}{2} M_D I_d + \frac{3}{2} M_{fD} I_f^r \\ \psi_Q^r &= (\mathrm{L}_{Ql}^r + \mathrm{L}_{Qm}) I_Q^r - \frac{3}{2} M_Q I_q \end{aligned} \tag{3.9}$$

3.4.2 Rotor- to Stator-Reference Frame

Reducing the rotor variable to stator variable is common in order to reduce the number of inductances (Figure 3.3) [94, 95]

$$\begin{aligned} I_d R_s + V_d &= \frac{d\psi_d}{dt} - \omega_r \psi_q \\ I_q R_s + V_q &= \frac{d\psi_q}{dt} + \omega_r \psi_d \\ I_f R_f - V_f &= -\frac{d\psi_f}{dt} \\ I_D R_D &= -\frac{d\psi_D}{dt} \\ I_Q R_Q &= -\frac{d\psi_Q}{dt} \end{aligned} \tag{3.10}$$

Flux-current relations with rotor variables reduced to stator would be:

$$
\begin{aligned}
\psi_d &= -L_{sl} I_d + L_{dm}(-I_d + I_D + I_f) \\
\psi_q &= -L_{sl} I_q + L_{qm}(-I_q + I_Q) \\
\psi_f &= L_{fl} I_f + L_{dm}(-I_d + I_D + I_f) \\
\psi_D &= L_{Dl} I_D + L_{dm}(-I_d + I_D + I_f) \\
\psi_Q &= L_{Ql} I_Q + L_{qm}(-I_q + I_Q)
\end{aligned}
\tag{3.11}
$$

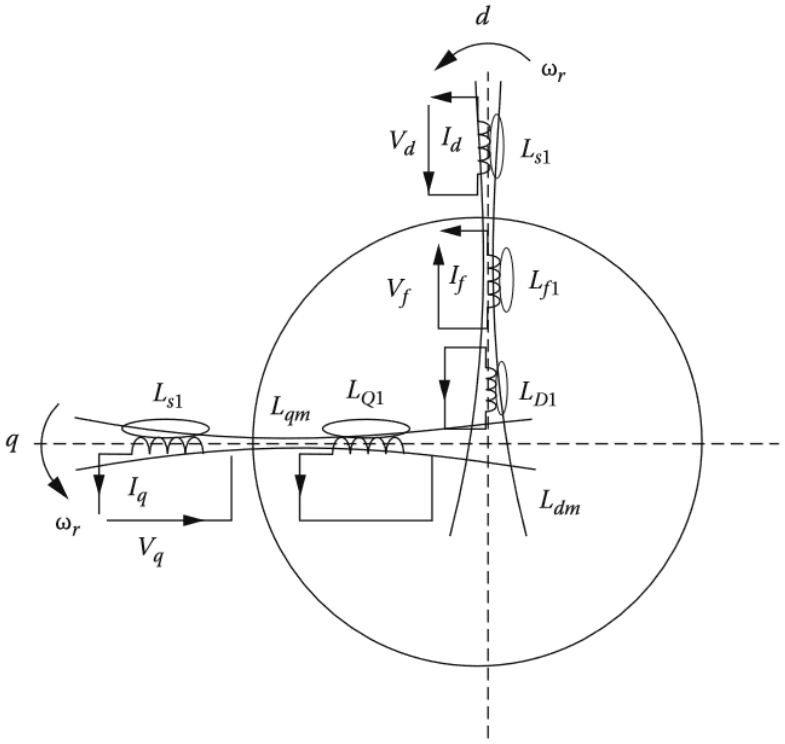

Figure 3.3 The Dq-Model Inductances of Synchronous Generators.

Comparing equations (3.9) and (3.11), the following definitions of current reduction coefficients are considered valid: [94]

$$
I_f = I_f^r K_f \quad I_D = I_D^r K_D \quad I_Q = I_Q^r K_Q \tag{3.12}
$$

Where:

$$
\begin{cases}
K_f = \dfrac{M_f}{L_{dm}} \\
K_D = \dfrac{M_D}{L_{dm}} \\
K_Q = \dfrac{M_Q}{L_{qm}}
\end{cases}
\tag{3.13}
$$

Using coefficients in equation (3.9) gives:

$$\psi_f = \psi_f^r . \frac{2}{3}\frac{1}{K_f} \quad \psi_D = \psi_D^r . \frac{2}{3}\frac{1}{K_D} \quad \psi_Q = \psi_Q^r . \frac{2}{3}\frac{1}{K_Q} \tag{3.14}$$

From equation (3.12) it follows that:

$$L_{fl} = L_{fl}^r . \frac{2}{3}\frac{1}{K_f^2} \quad L_{Dl} = L_{Dl}^r . \frac{2}{3}\frac{1}{K_D^2} \quad L_{Ql} = L_{Ql}^r . \frac{2}{3}\frac{1}{K_Q^2} \tag{3.15}$$

Reducing rotor circuit resistances and field winding voltage to stator quantities results in:

$$\boldsymbol{R_f = R_f^r . \frac{2}{3}\frac{1}{K_f^2}} \quad \boldsymbol{R_D = R_D^r . \frac{2}{3}\frac{1}{K_D^2}} \quad \boldsymbol{R_Q = R_Q^r . \frac{2}{3}\frac{1}{K_Q^2}} \tag{3.16}$$

$$V_f = V_f^r . \frac{2}{3}\frac{1}{K_f} \tag{3.17}$$

Note:

When $\sqrt{\frac{2}{3}}$ is used in Park transformation matrix, the reduction coefficients of equation (3.12) must be multiplied by $\sqrt{\frac{3}{2}}$. However, the factor $\frac{2}{3}$ disappears completely from equations (3.14) through (3.17) [94].

3.5 SG Parameters Determination

Till now, two representations of the SG have been developed. The first representation is given by equations (3.8) and (3.9), it requires the determination of the basic parameters (M_f, M_D, M_Q, M_{fD} ...). The second representation is obtained by reducing rotor-variables to stator-variables and is given by equations (3.10) and (3.11).

3.5.1 Experimental Determination of the Laboratory SG Parameters

In order to perform a valid control on the laboratory 1.5kVA salient-pole Lab-Volt SG, parameters of the machine need to be accurately identified. For this purpose, identification tests held in power-lab are performed. Figure 3.4 shows the test bench of the experiment.

3.5.1.1 Open-Circuit Test

The test is performed on the SG at no-load to obtain the no-load saturation curve or simply the open-circuit characteristic (OCC). This last is used graphically to determine the synchronous reactance. During the test, the SG is first run at rated speed of 1500 rpm with no excitation being applied. The filed current is supplied gradually while measuring both

terminal voltage and current being supplied to obtain I-V curve. The supplied current is increased until the terminal output voltage reaches the saturation condition [96].

The obtained curve (Figure 3.5) is a straight line before the saturation zone. The extension of this line for higher values of excitation current gives the air gap line.

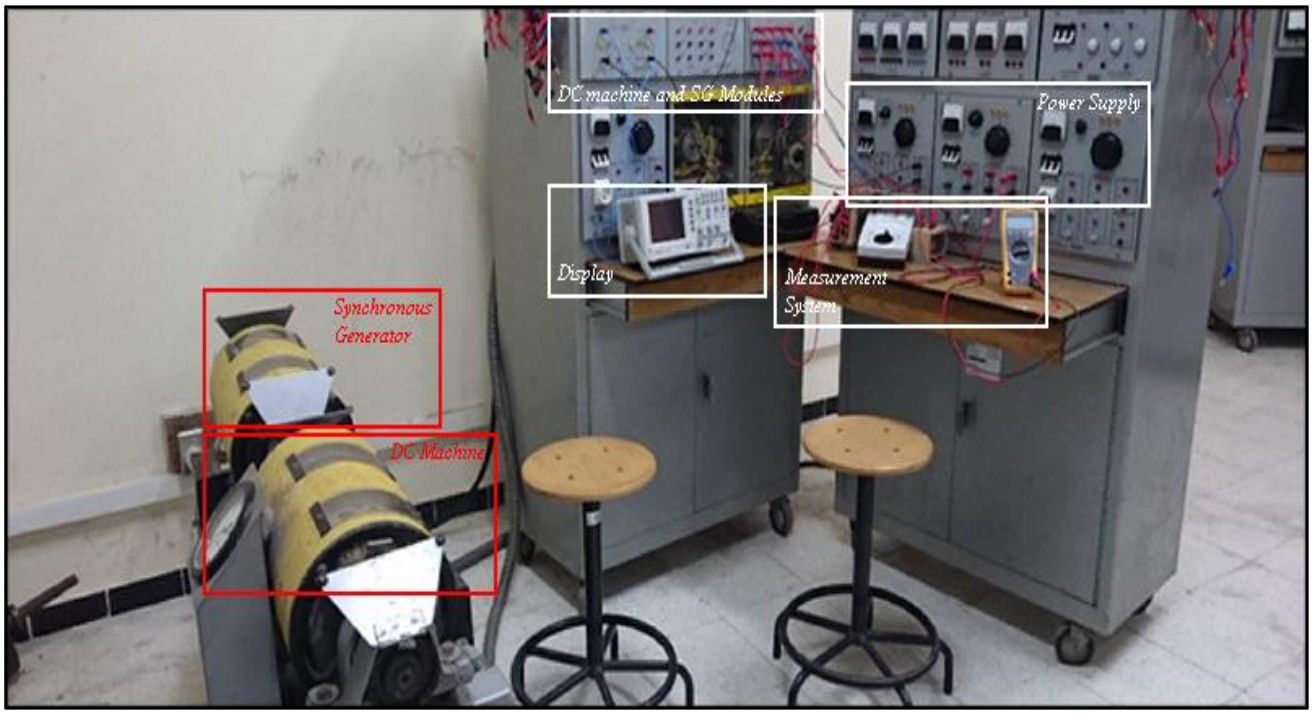

Figure 3.4 Test-Bench of the Experiment.

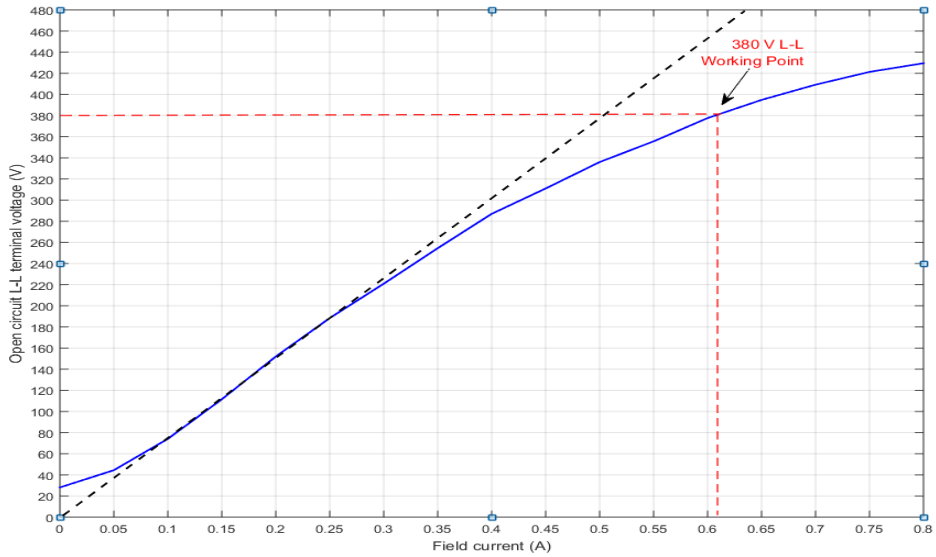

Figure 3.5 Open-circuit Characteristics, Lab-Volt SG.

3.5.1.2 Sustained Short-Circuit Test

The objective of this test is to obtain the short-circuit saturation curve or simply the short-circuit characteristic (SCC) for the SG. This last is used with the previously obtained curve for the same purpose. It is important to keep track of the excitation current value not to exceed the rated value. The field current might exceed the rated value by only a small tolerance to prevent stator windings damage [96].The SG terminals are permanently shorted. The machine is rotating under rated speed of 1500 rpm. The excitation current is injected and increased gradually while measuring the short circuit current flowing in the stator winding. The short-circuit current is plotted versus the excitation current to obtain the SCC. It is convenient to draw both graphs – open- and short-circuit characteristics – on the same figure (see Figure 3.6).

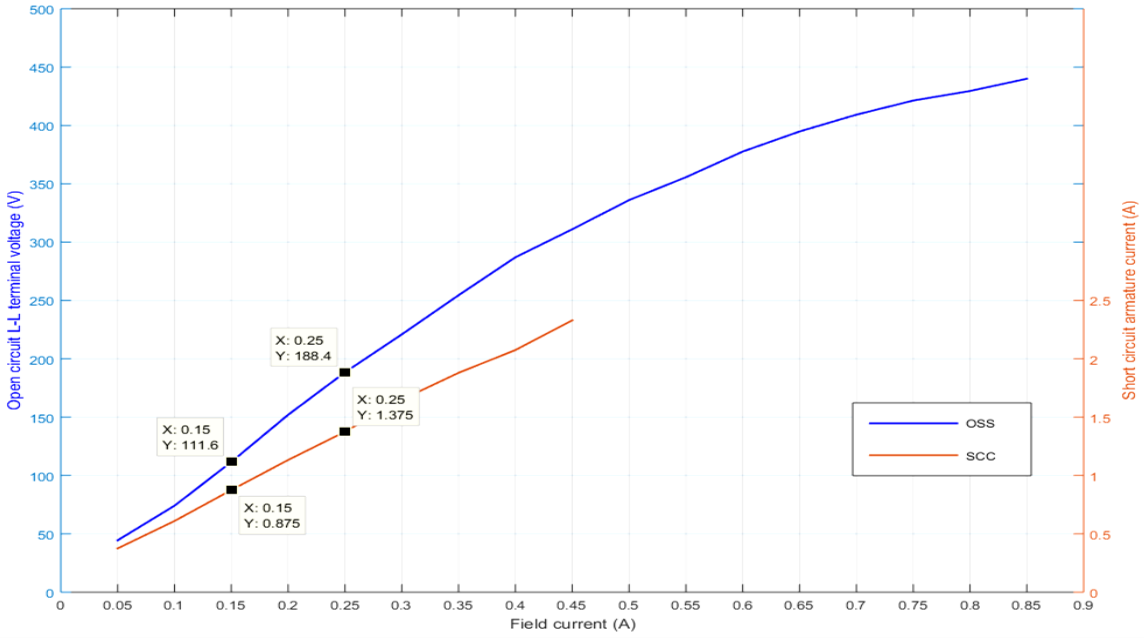

Figure 3.6 Open- and Short-circuit Characteristics, Lab-Volt SG.

The d-axis unsaturated impedance $Z_{d\ (unsat)}$ can be obtained as a quotient of voltage on the OCC taken at a point and the short-current armature current on the SCC corresponding to the field current at that very same point [96]. That is:

$$Z_{d\,(unsat)} = \frac{V_{(\mathrm{L-L})}}{\sqrt{3} I_{SC}} \tag{3.18}$$

The direct-axis unsaturated synchronous reactance $X_{d\ (unsat)}$ is therefore: [4]

$$X_{d(unsat)} = \sqrt{Z_{d(unsat)}^2 - R_s^2} \tag{3.19}$$

Where: R_s is the stator resistance.

3.5.1.3 Slip Test

The aim of the test is to obtain the saliency ratio (X_q/X_d). Using this ratio and the value of X_d obtained from OCC and SCC, X_q is then determined.

The generator during the test is driven at a speed slightly different from the rated speed, about 1% in order to achieve a very small slip. No excitation current is used. A balanced three phase voltage is applied across the SG terminals (about 25% of the rated voltage of the generator) [96].An oscillogram of the stator voltage and current is recorded (Figure 3.7). Stator current is in grey and is shifted up by 1volt. Whereas, stator voltage is in bleu.

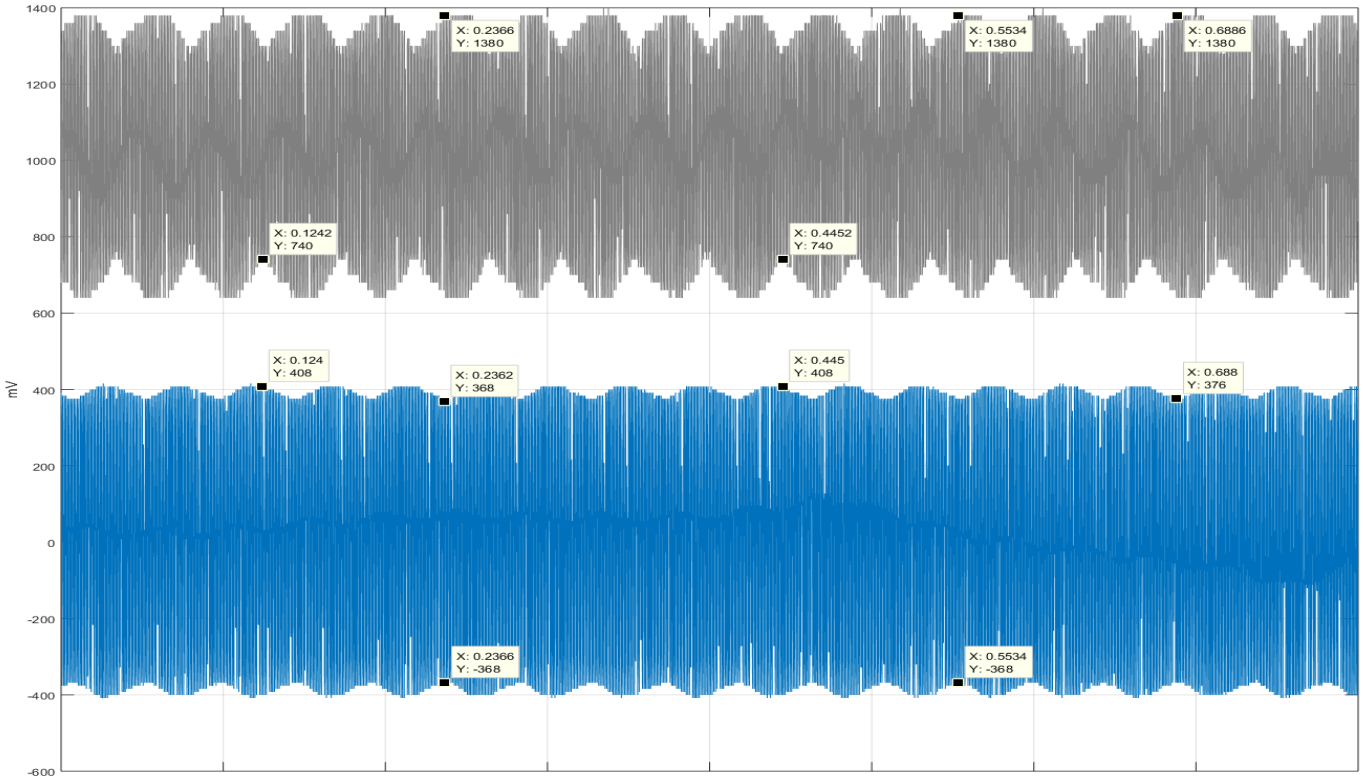

Figure 3.7 Slip test, Lab-Volt SG.

It can be noticed from the figure, at the moment the stator current has its maximum the stator voltage has its minimum and vice-versa. Using the graph, and after calibrating the current as well as the voltage transducers, the following calculations can be made: [96]

$$X_{\mathrm{d(slip)}} = \frac{V_{t(L-L)\max}}{\sqrt{3}I_{\min}}$$
$$X_{q(\mathrm{slip})} = \frac{V_{t(L-L)\min}}{\sqrt{3}I_{\max}} \quad (3.20)$$

The saliency ratio is:

$$\left[\frac{X_q}{X_d}\right]_{slip} = \frac{X_{q(\mathrm{slip})}}{X_{d(\mathrm{slip})}} \quad (3.21)$$

Finally, X_q is obtained:

$$X_q = X_d\left[\frac{X_q}{X_d}\right]_{slip} \quad (3.22)$$

3.5.1.4 Sudden Three-Phase Short Circuit Test

The goal of the test is to visualize the behavior of the SG during dynamic and electric transients when a sudden three phase short circuit is applied. Many of the transient and sub-transient parameters can be computed from a suitable oscillogram recorded during the three phase short circuit. The test aim to calculate direct-axis transient X_d' and sub-transient reactance X_d''.

The SG is driven at the rated speed with no load, and is excited so that the terminal voltage is at the rated value. The next step is to apply a sudden three phase short-circuit. The current at each phase is recorded with time [96]. A typical current waveform is shown below (Figure 3.8).

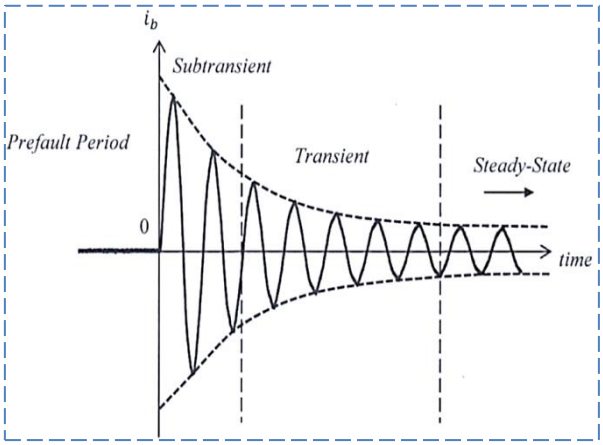

Figure 3.8 Typical phase short-circuit current.

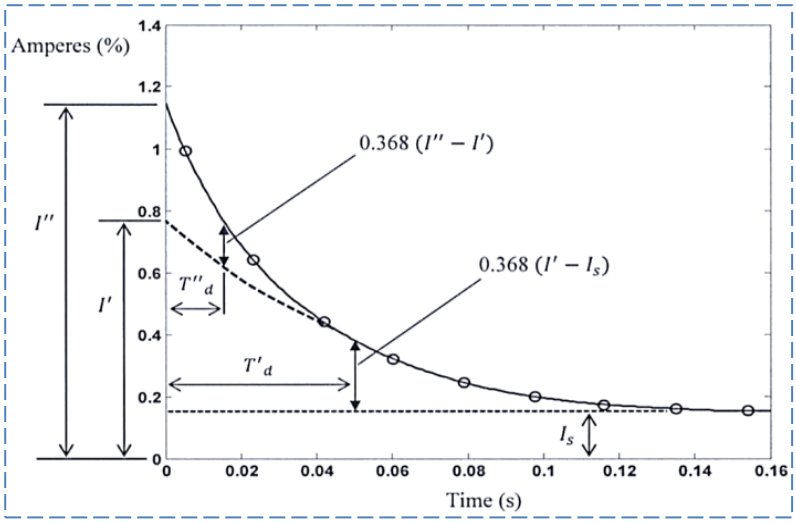

Figure 3.9 Polynomial curve fitting for positive peaks of the phase short-circuit current.

The rms amplitude of the total ac component of the short circuit current in one phase can be expressed as:[96]

$$I_{sc}(t) = \left(I'' - I'\right)e^{\frac{-t}{T_d''}} + \left(I' - I_s\right)e^{\frac{-t}{T_d'}} + I_s \tag{3.23}$$

$$I_{sc}(t) = E_o\left[\left(\frac{1}{X_d''} - \frac{1}{X_d'}\right)e^{\frac{-t}{T_d''}} + \left(\frac{1}{X_d'} - \frac{1}{X_d}\right)e^{\frac{-t}{T_d'}} + \frac{1}{X_d}\right] \tag{3.24}$$

Where E_o is the rms line-to-neutral open circuit pre-fault terminal voltage.

By extrapolating the sub-transient and transient current envelope back to zero-time or the time of the short-circuit occurrence, the sub-transient and transient current components can be evaluated. The value of X_d' and X_d'' can now be calculated: [96]

$$\begin{cases} X_d' = \dfrac{E_o}{I'} \\ X_d'' = \dfrac{E_o}{I''} \end{cases} \tag{3.25}$$

The time constants T_d' and T_d'' as well as the transient and sub-transient short-circuit currents I' and I'' respectively can now be determined (Figure 3.9).

Results of the identification tests performed are finally summarized (Table 3.2).

Table 3.21.5kVA salient-pole Lab-Volt SG parameters.

Nominal power	S_n	*1.5 kVA*
Nominal rms line-to-neutral voltage	U_n	*220 v*
Frequency	f_n	*50 Hz*
Stator resistance	R_s	*2.2* Ω
Rotor resistance	R_f	*127* Ω
Direct-axis synchronous reactance (unsaturated)	X_d	*75.443* Ω
Quadrature-axis synchronousreactance (unsaturated)	X_q	*46.556* Ω
Direct-axis open-circuit time constant	T_{do}'	*0.235 s*
Direct-axis transient reactance	X_d'	*10.309* Ω
Direct-axis transient time constant	T_d'	*0.0776 s*
Direct-axis sub-transient reactance	X_d''	*8.5298* Ω
Quadrature-axis sub-transient reactance	X_q''	*5.2637* Ω
Direct-axis sub-transient time constant	T_d''	*0.0147 s*

In order to simulate the model obtained, leakage inductances must be determined. In this work,the parameters of the SG used are obtained in terms of reactances and time constants (Table 3.2). For that, mathematical relations between these parameters and leakage inductances need to be found.Mathematical relations can be written in the following forms (Table 3.3): [41, 95]

Table 3.3 Mathematical Relations Between Time Constants and Reactances.

$X = Lw_r$	$X_d' = X_{sl} + \frac{X_{dm}X_{fl}}{X_{dm}+X_{fl}}$	$T_d' = \frac{1}{\omega_r R_f}(X_{fl} + \frac{X_{sl}X_{dm}}{X_{sl}+X_{dm}})$	$T_{do}' = \frac{X_{dm}+X_{fl}}{\omega_r R_f}$
$X_d = X_{sl} + X_{dm}$	$X_d'' = X_{sl} + \frac{X_{fl}X_{Dl}}{X_{fl}+X_{Dl}}$	$T_d'' = \frac{1}{\omega_r R_D}(X_{Dl} + \frac{X_{sl}X_{fl}}{X_{sl}+X_{fl}})$	$T_{do}'' = \frac{1}{\omega_r R_D}(X_{Dl} + \frac{X_{fl}X_{dm}}{X_{fl}+X_{dm}})$
$X_q = X_{sl} + X_{qm}$	$X_q'' = X_{sl} + \frac{X_{qm}X_{Ql}}{X_{qm}+X_{Ql}}$	$T_q'' = \frac{1}{\omega_r R_Q}(X_{Ql} + \frac{X_{sl}X_{qm}}{X_{sl}+X_{qm}})$	$T_{qo}'' = \frac{X_{qm}+X_{Ql}}{\omega_r R_Q}$

Based on the expressionsabove, the following result:[95]

Table 3.4 Parameters of the Mathematical Model.

$X_{dm} = \sqrt{T_{do}^{'} w_r R_f (X_d - X_d^{'})}$ $X_{sl} = X_d - X_{dm}$ $X_{qm} = X_q - X_{sl}$	$X_{Dl} = \frac{(X_d^{"} - X_{sl}) X_{fl}}{X_{fl} + X_{sl} - X_d^{"}}$	$R_D = \frac{1}{\omega_r T_{do}^{"}} (X_{Dl} + \frac{X_{dm} X_{fl}}{X_{dm} + X_{fl}})$	$T_{do}^{"} = \frac{X_d^{'}}{X_d^{"}} T_d^{"}$
$X_{fl} = T_{do}^{'} w_r R_f - X_{dm}$	$X_{Ql} = \frac{(X_q^{"} - X_{sl}) X_{qm}}{X_{qm} + X_{sl} - X_q^{"}}$	$R_Q = \frac{X_{qm} + X_{Ql}}{\omega_r T_{qo}^{"}}$	$T_{qo}^{"} = \frac{X_q}{X_q^{"}} T_q^{"}$

3.6 Determination of Reduction Coefficients K_f, K_D and K_Q

The coefficients K_f, K_D and K_Q used in the reduction of rotor-variables to the stator may be calculated through analytical or numerical methods, but they may be also measured [94, 95].

The reduction factor of the excitation $K_f$can be obtained directly from steady-state short-circuit test by taking the average value of the reduction factors obtained at different values of field current. (See figures 3.10 – 3.11)[95].

$$K_f = \frac{I_f}{\sqrt{3} Isc} \tag{3.26}$$

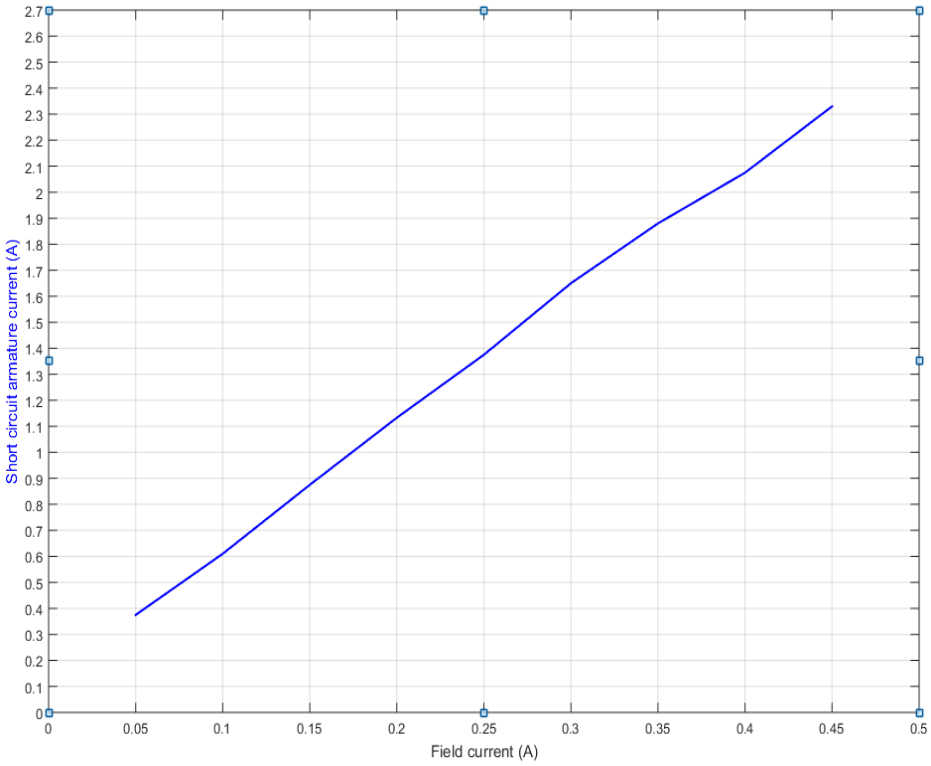

Figure 3.10 Short-circuit characteristics, Lab-Volt SG.

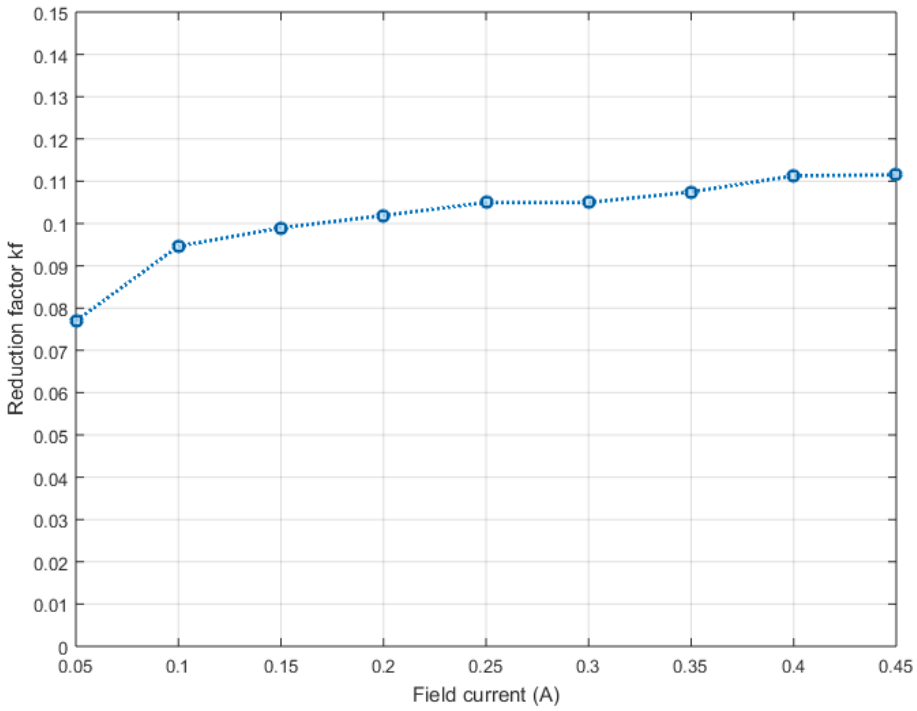

Figure 3.11 Excitation reduction coef .K_f versus field current.

The dampers reduction coefficients K_D and $K_Q$on the other hand are essentially needed to measure damper currents I_D and I_Q. However, these current are not measured practically and since it is possible to see the machine behavior without using these coefficients there is an infinite solution to them.

3.7 Excitation System Modeling

Excitation systems are in fact the power supply that delivers power to the SG field winding. They have taken many forms over the years and can be classified into three types: DC-, AC- and Static-Exciters. The design and types of exciters have been developed through time to meet requirements. The DC- and AC-exciters contain an electric generator coupled on the main shaft and have low power electronics control of their excitation current. The static exciters however take energy from an AC source and convert it into a DC-controlled power which is fed to the field winding of the SG through slip rings and brushes [94].

Modern electric power plants gave way to static exciters (power electronics) where controlled rectifiers supply directly the excitation of the SG. This is due to its fast and good response in voltage and power control and due to its satisfactory steady state stability condition.

In this work, we chose a static excitation system with a voltage source and a regulated rectifier, as shown in (Figure 3.12) where the AC source is the SG output terminals [94].

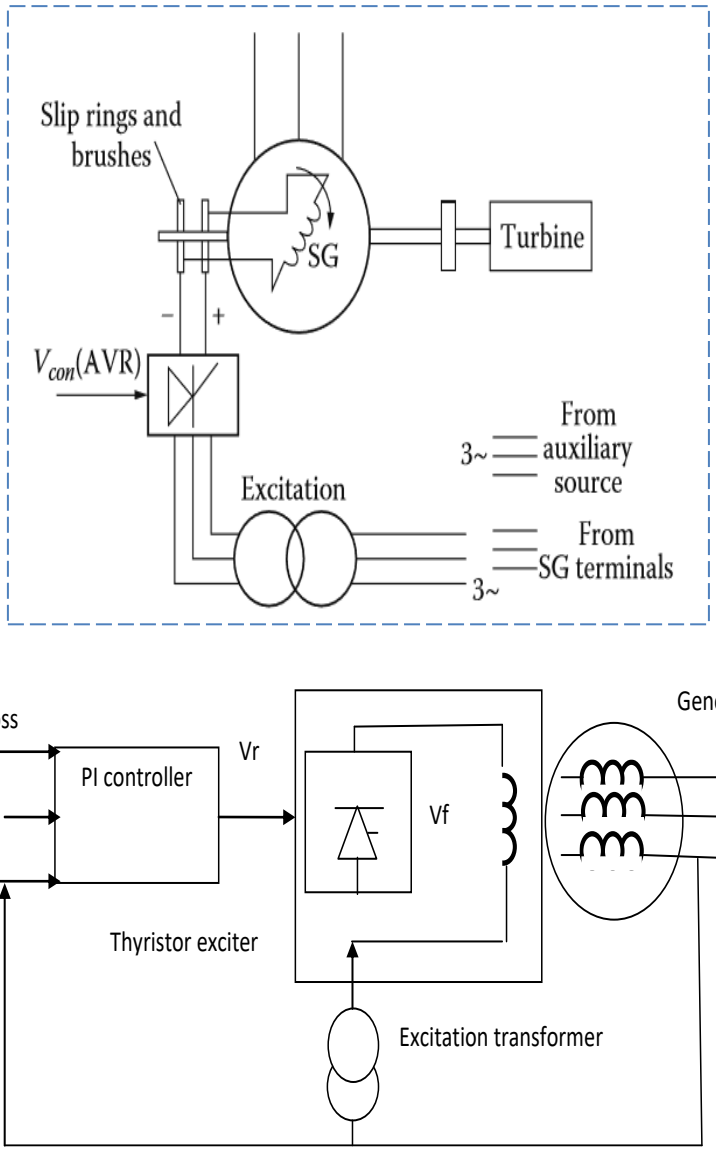

Figure 3.12 Structure of Static Excitation System.

3.7.1 Working Principle of the Excitation System Used

The input voltages to the PI controller block $V_t$and $V_{pss}$are compared for each iteration of the algorithm with the voltage referenceV_{ref}. The output voltage V_r of the PI controller without internal feedback controls the thyristors of the rectifier using a pulse width modulation (PWM) signal. The regulator is supplied by the generator armature circuit via an excitation step down transformer, adjusted to the parameters of the excitation system. The excitation transformer is used to supply the rectifier as well as a galvanic separator of the rotor circuit, as shown in the schematic diagram of the excitation system Figure 3.13, the schema comes from the IEEE Exciter model, type ST1A [97, 20, 98].

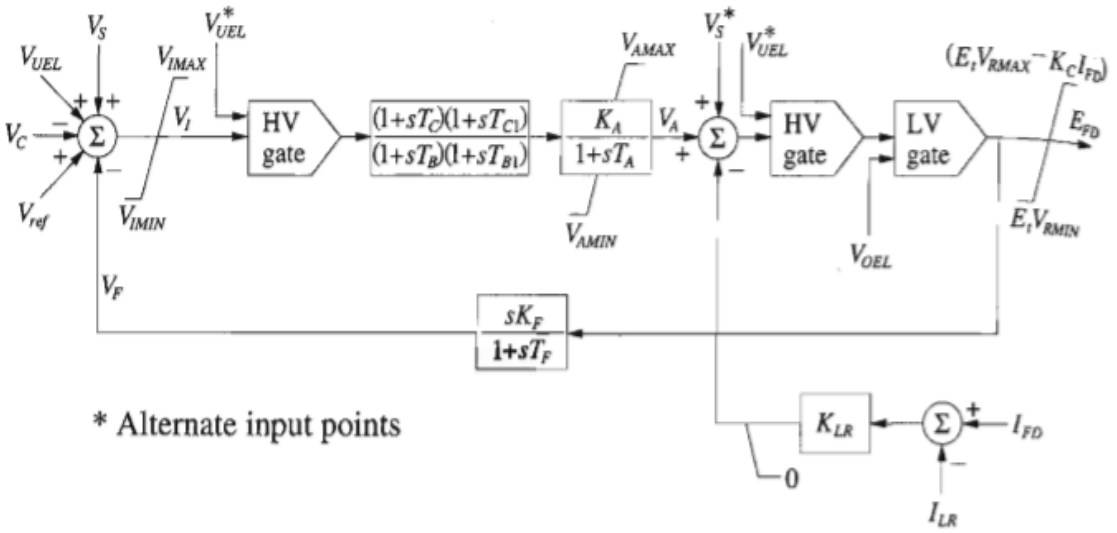

Figure 3.13 Scheme of the Excitation System Used IEEE ST1A 1992.

A) Amplifier model

The static exciter Thyristor Bridge is often modeled by an amplifier while taking into account the stabilization and limitation circuits which resulting. The amplifier can be of magnetic or electronic type, it is characterized by a first-order system including a gain KA and a time constant of TA (Figure 3.14)

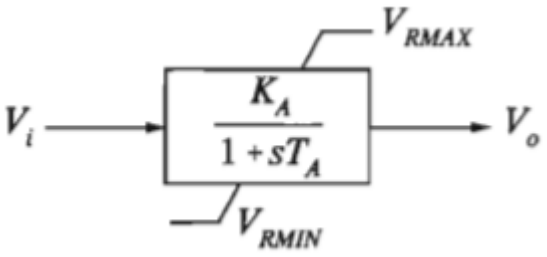

Figure 3.14 Amplifier Model

The amplifier's output voltage is limited by saturation, specified by the terminals VRMAX and VRMIN say the saturation limits.
The amplifier's output voltage limitation often varies depending on the external voltage of the generator (dynamic saturation).

B) Stabilization circuit Model

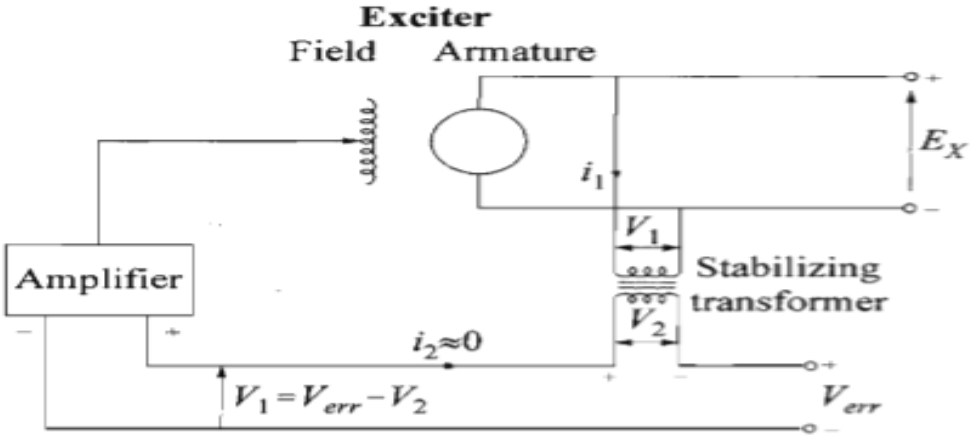

Figure 3.15 Excitation System Stabilizing Transformer

In this type of excitation system, series transformers are the most used as shown in Figure 3.15 above. The equations related to stabilizing transformer are given in the Laplace domain as follows:

$$\begin{cases} V_1 = R_1 * i_1 + sL_1 * i_1 + sMi_2 \\ V_2 = R_2 * i_2 + sL_2 * i_2 + sMi_1 \end{cases} \quad (3.27)$$

The indices 1 and 2 denote the transformer's primary and secondary, respectively, whereas R, L, and M stand for resistance, leakage induction, and mutual induction. Because the transformer's secondary is connected to ahigh impedance circuit, then i2 is neglected, so we will have:

$$\begin{cases} V_1 = (R_1 + sL_1) * i_1 \\ V_2 = sMi_1 \end{cases} \quad (3.28)$$

Thus,

$$\frac{V_2}{V_1} = \frac{sM_1}{R_1 + sL_1} = \frac{sK_F}{1 + sT_F} \quad (3.29)$$

Where: $K_F = \frac{M_1}{R_1}$ and $T_F = \frac{L_1}{R_1}$

- **windup and non-windup limits**

In modeling ST-type excitation systems, limiting circuits play an important role, however it is necessary to distinguish between two kinds, windup and non-windup limits, to do this we illustrate an example of an integration function of the input in each of the two cases, shown in Figure 3.16 below:

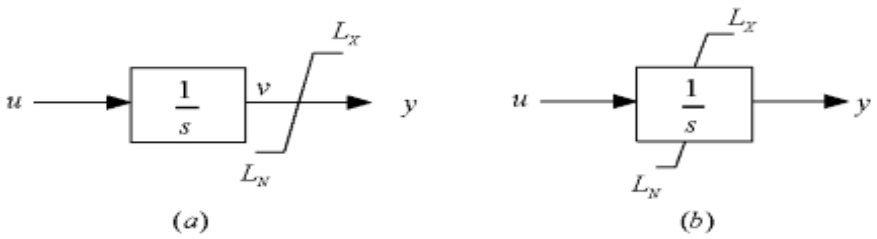

Figure 3.16 Integrator with Windup and Non-windup Limits

From Figure 3.14, we have:

$$\overset{(a)}{\Rightarrow} \frac{dv}{dt} = u \qquad (3.30)$$

The output is calculated there according to the following cases:

If $L_N < v < L_X \Rightarrow y = v$ (3.31)
If $v \geq L_X \Rightarrow y = L_X$ (3.32)
If $v \leq L_N \Rightarrow y = L_N$ (3.33)

$$\overset{(b)}{\Rightarrow} \frac{dy}{dt} = u \qquad (3.34)$$

The output there is calculated as follows:

If $L_N < y < L_X \Rightarrow \frac{dy}{dt} = u$ (3.35)
If $y \geq L_X and \frac{dy}{dt} > 0 \quad \Rightarrow \frac{dy}{dt} = 0\ and y = L_X$ (3.36)
If $y \geq L_N and \frac{dy}{dt} < 0 \quad \Rightarrow \frac{dy}{dt} = 0\ and y = L_N$ (3.37)

For post-block (external) limitations, the variable v is not limited, by consequently the output variable y follows the value of v, until v reaches the Lx and LN terminals. Whereas for block (internal) limitations, the output variable y is limited and takes the value of the bounds as soon as sign changes.
The "Gating" functions:
Auctioneering circuits are often used to control one or two input signals. Figure 3.17 illustrates the Low Value functions (LV gate) and high value (HV gate):

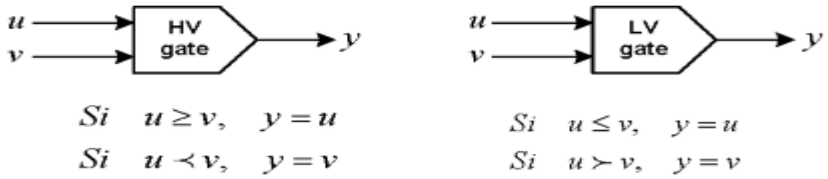

Figure 3.17 Low and High Value Gating Functions

3.7.2 Functionality and System Components

The complete (global) system components and their functionalities can be summarized as follows:

A) Excitation Power and Excitation Transformer

The excitation power is derived from the machine terminals and is conducted via power-electronics into the field winding of the SG. The purpose of the excitation transformer is to adapt the power supply to the converter and to isolate the field winding from the power supply.

The secondary voltage is dimensioned according to the required ceiling voltage, whereas, the current rating of the transformer is determined by the maximum field current of the SG.

B) Power Circuit

A semi-controlled rectifier consisting of thyristors and diodes is to provide power to the field winding and is controlled using a pulse width modulation (PWM) signal.

The power circuit is provided with protection against voltage transients. This is achieved by RC snubber circuits.

C) Measurement System

Measurement of stator voltage is done by means of measurement transformer followed by a full wave rectifier and a precision peak detector. (See Appendix (B))

D) Automatic Voltage Regulator

The AVR control algorithm is to provide closed-loop control of the SG output voltage by keeping it constant. Also, the AVR is required to maintain the stability of the generator in steady-state, as well as during transient disturbances and shall cover all control functions needed for the excitation system.

3.7.3 AVR based PID-Characteristics

The AVR senses the error in SG terminals voltage with respect to the voltage set-point, and causes corrective action – proportional, integral and derivative – to take place. The output is then a control voltage $V_{con\ (AVR)}$[99]

The transfer function of a PID-controller is:

$$G_{PID}(s) = K_P(1 + \frac{1}{sT_I} + sT_D) = K_P(\frac{1 + sT_I + s^2T_IT_D}{sT_I}) \quad (3.38)$$

With: K_P – proportional gain, T_I – integral constant time, T_D – derivative constant time.

For fast and good response in voltage control and rejecting disturbances, the PID-controller need to be tuned. Selecting PID-parameters is called controller tuning, two methods are to be applied in this research work: The conventional Zero/Pole cancelation method and the Particle Swarm Optimization (PSO) method.

Although the AVR is to be implemented digitally, the design of the PID-controller may be done as if it were continuous, because the sampling frequency is more than 20 times the damped frequency of the closed-loop system [94].

3.7.3.1 Zero/Pole Cancelation in Tuning the PID-Controller

The AVR output depends only on the output voltage of the generator. The linearized model of an AVR system with PID-controller is described below (Figure 3.18). The excitation system is of the type IEEE-ST1A [41].The global system can be simplified as illustrated in Fig. 3.19.

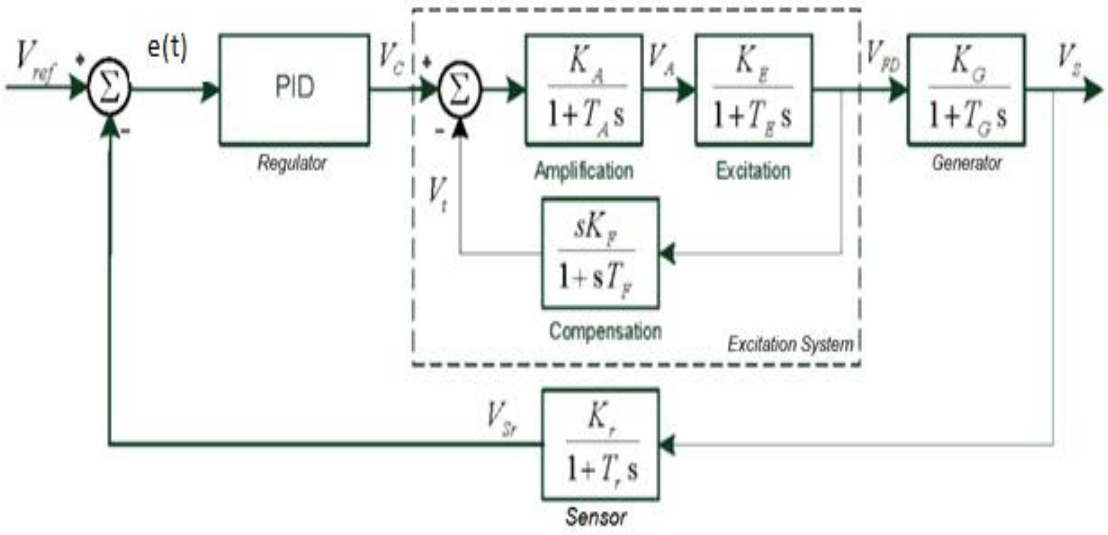

Figure 3.18 Regulation Principle of SG Terminal Voltage.

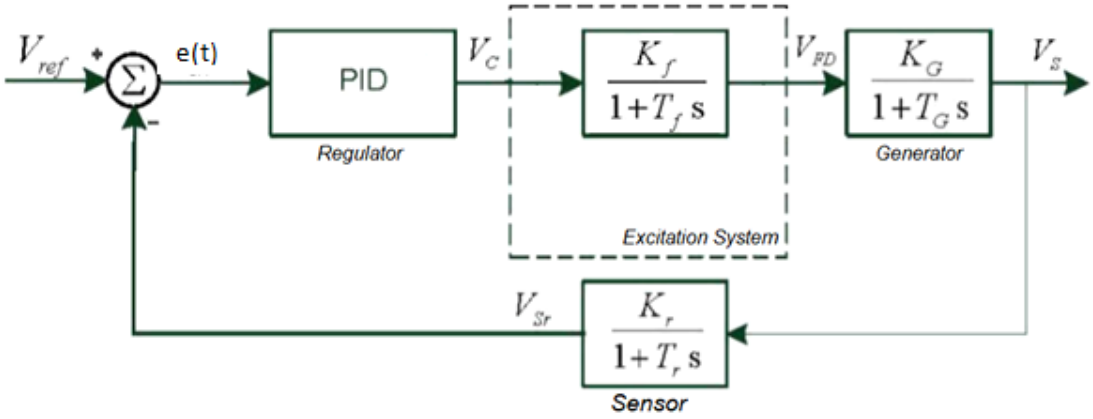

Figure 3.19 Simplified Model of the Voltage Regulation Principle.

The control signal is given by:

$$V_c = K_P\left[e(t) + \frac{1}{T_I}e(t)dt + T_D\frac{de(t)}{dt}\right] \tag{3.39}$$

Where: *e(t)* is the error voltage.

The transfer function of *(excitation system +generator)*is then obtained:

$$G_{EG}(s) = \frac{K_f K_G}{(1+sT_f)(1+sT_G)} = \frac{K_{EG}}{1+s(T_f+T_G)+s^2T_fT_G} \tag{3.40}$$

After applying Zero/Pole cancelation eliminating the poles of equation (3.40) by the zeros of equation (3.38):

$$\begin{cases} T_I = T_f + T_G \\ T_D = \dfrac{T_f T_G}{T_f + T_G} \end{cases} \tag{3.41}$$

The forward-path transfer function is then reduced to:

$$\begin{aligned} G_{FP}(s) &= \frac{K_{FP}}{sT_I} \\ K_{FP} &= K_P K_f K_G \end{aligned} \tag{3.42}$$

Let *H(s)* be the sensor transfer function:

$$H(s) = \frac{K_r}{1+sT_r} \tag{3.43}$$

The closed-loop transfer function of a negative feedback system is given by:

$$G_{cl} = \frac{G_{FP}(s)H(s)}{1+G_{FP}(s)H(s)} \tag{3.44}$$

Replacing equation (3.42) and (3.43) into equation (3.44) yields to the global system transfer function:

$$\begin{aligned} G_{cl} &= \frac{\left(\frac{K_{FP}}{sT_I}\right)\left(\frac{K_r}{1+sT_r}\right)}{1+\left(\frac{K_{FP}}{sT_I}\right)\left(\frac{K_r}{1+sT_r}\right)} \\ &= \frac{1}{1+\left(\frac{sT_I}{K_{FP}}\right)\left(\frac{1+sT_r}{K_r}\right)} \\ &= \frac{1}{1+s\left(\frac{T_I}{K_{FP}K_r}\right)+s^2\left(\frac{T_IT_r}{K_{FP}K_r}\right)} \end{aligned} \tag{3.45}$$

Given the transfer function of a second order system:

$$G(s) = \frac{1}{1+s\left(\frac{2\xi}{\omega_n}\right)+s^2\left(\frac{1}{\omega_n^2}\right)} \tag{3.46}$$

From equations (3.45) and (3.46) and by identification:

$$\begin{cases} \frac{T_I}{K_{FP}K_r} = \frac{2\xi}{\omega_n} \\ \frac{T_IT_r}{K_{FP}K_r} = \frac{1}{\omega_n^2} \end{cases} \tag{3.47}$$

$$\omega_n = \frac{2\xi K_{FP}K_r}{T_I} \tag{3.48}$$

$$K_{FP} = \frac{T_IT_r\omega_n^2}{K_r} \tag{3.49}$$

Replacing equation (3.48) into equation (3.49) yields:

$$K_{FP} = \frac{T_I}{4T_rK_r\xi^2} \tag{3.50}$$

Finally, from equations (3.41), (3.42) and (3.50) we deduce the gains:

$$\begin{cases} K_P = \dfrac{\left(T_f + T_G\right)T_r\omega_n^2}{K_r K_f K_G} \\ or \\ K_P = \dfrac{\left(T_f + T_G\right)}{4K_f K_G T_r K_r \xi^2} \end{cases} \qquad K_I = \frac{1}{T_f + T_G} \quad \& \quad K_D = \frac{T_f T_G}{T_f + T_G} \tag{3.51}$$

3.7.3.2 Calculation of Different TFs Parameters

A) The Simplified SG TF

The simplified transfer function describing the SG is of the form:

$$G(s) = \frac{K_G}{(1 + sT_G)} \tag{3.52}$$

Finding K_G and T_G can be done as follows:

$$\begin{cases} G(s) = K_G \dfrac{1 + sT_{kd}}{\left(1 + sT_{do}^{'}\right)\left(1 + sT_{do}^{''}\right)} \\ K_G = \dfrac{x_{md}}{r_f} \\ T_{do}^{'} = \dfrac{x_{md} + x_f}{r_f} \end{cases} \tag{3.53}$$

With:

$$x_{md} \approx x_f \rightarrow T_G = T_{d\grave{a}}^{'} \approx \frac{x_f}{r_f}$$

T_{kd} and $T_{do}^{''}$ are neglected [3].

B) The exciter TF

The relationship between the generator output voltage and the AC-DC converter output voltage is given by: [3]

$$V_{S_{DC}} = 0.9V_{S_{ab\_eff}} \cos(\alpha) \tag{3.54}$$

$$\begin{cases} V_f = 0.9V_2 \cos(\alpha) = 0.9K_e V_G \cos(\alpha) \\ V_c = V_{tb} \cos(\alpha) = K_{tb} V_G \cos(\alpha) \end{cases} \tag{3.55}$$

Where:

$$\begin{cases} K_e = \dfrac{V_2}{V_G} \\ K_{tb} = \dfrac{V_{tb}}{V_G} \end{cases} \tag{3.56}$$

V_f: is the voltage applied to the field winding.

V_2: is the rms value of the secondary winding of the excitation transformer.

V_{tb}: is the maximum generator output voltage.

The exciter gain can be calculated then:

$$V_f = 0.9 K_e V_G \frac{V_c}{K_{tb} V_G} = K_f V_c \tag{3.57}$$

$$K_f = 0.9 \frac{K_e}{K_{tb}} \tag{3.58}$$

Finally, the time constant T_f is given by:

$$T_f = \frac{T}{2} \tag{3.59}$$

3.7.3.3 Disadvantages of Conventional Tuning Methods

The disadvantages of classical tuning methods are:

- Difficulty to deal with non-linear process.
- Inadequate dynamics of closed loop response.
- Excessive number of rules to set the gains.

It is difficult to find suitable PID-parameters using classical mathematical approaches. For that, alternative and modern heuristics optimization techniques such as Particle Swarm Optimization PSO, Genetic Algorithm GA, Bat algorithm and others have been given much attention due to their ability to find global solution in PID tuning.

Chapter 4

Particle Swarm Optimization Method Applied to PI Parameters Identification

Chapter 4

Particle Swarm Optimization Method Applied to PI Parameters Identification

Several engineering problems necessitate the application of optimization methods in order to achieve the best solution. Although deterministic approaches have answered this demand, the problem of local optima remains a serious roadblock to finding the global optimum. As a result, stochastic methods known as metaheuristics are used to overcome this difficulty and have a high capacity for finding the global optimum [100].

The introduction of a new class of optimization methods known as methaheuristics represents a major shift in the science of optimization. These are applicable to a wide range of combinatorial issues and can even be applied to continuous problems. These methods allow for the discovery of a good quality solution in a generally reasonable amount of time, without ensuring that the solution discovered is optimal.

Several heuristic methods for adjusting PID controllers have been presented over the years. When compared to other algorithms, these approaches have the following advantages: Heuristic algorithms are generally simple to construct; they can be employed effectively in a multiprocessor environment; they do not require a continuous issue definition function; and they can yield optimal or near-optimal solutions. Particle swarm optimization (PSO) is a well-known and effective stochastic technique that has been used to solve a variety of engineering issues.

This chapter presents an improved PID intelligent control algorithm which applies the automatic voltage regulator (AVR) system, the optimization part, where the method and the optimization technique used are defined.

This choice is justified by the need to find the global optimum of an optimization problem which includes continuous or discrete variables, and which is represented in the form of a system (AVR) whose model is nonlinear, non-differentiable, or having complex analytic expressions. The algorithm uses the PSO algorithm to make an adjustment on PID parameters [56, 100].

Research and optimization techniques are generally classified into three categories [105]: enumerative, deterministic and stochastic.

4.1 Principle of Particle Swarm Optimization Technique

The natural world around him is increasingly inspiring man to create algorithms that imitate animal behavior. If the optimum exists, meta-heuristics make it simple and fast to determine the closest solution. We'll learn about one of these methods, called "optimization by swarms of particles," whose main idea is to simulate the collective behavior of birds within a cloud, and evaluate the feasibility of using it to control our AVR system. The problem to be solved can often be expressed as an optimization problem: we define an objective function, or cost function, which we seek to minimize or maximize with respect to all the parameters concerned.

Let's go back to the definition of hard optimization. Two kinds of problems have been studied in the literature, this name, not strictly defined (and linked, in fact, to the state of the art in terms of optimization):

- Certain discrete optimization issues for which an accurate polynomial technique is unknown (i.e. whose computation time is proportional to Nn, where N denotes the number of unknown parameters of the problem, and n is an integer constant). This is true, for example, for "NP-hard" problems, for which it is predicted that there is no constant n such that the resolution time is bounded by a polynomial of degree n.
- Certain continuous-variable optimization problems for which no algorithm exists that can find a global optimum (that is, the best possible solution) with certainty and in a finite number of calculations.

Efforts have long been made, separately, to solve these two types of problems. In the field of continuous optimization, there is thus a large arsenal of classical methods called global optimization [98], but these techniques are often ineffective if the objective function does not have a particular structural property, such as convexity. In the field of discrete optimization, a large number of heuristics, which produce solutions close to the optimum, have been developed; but most of them were designed specifically for a given problem.

The metaheuristic based on the method of particle swarms ("Particle Swarm Optimization", PSO) was developed by Kennedy and Eberhart in 1995. The principle of the method comes analogously with the collective behavior of animals. Particle Swarm Optimization (PSO) is categorized as population-based stochastic optimization techniques. A brief description of the PSO algorithm is presented in the following paragraphs.

Observe a field being plowed in the fall; when the plow share first penetrates the ground, the field is devoid of gulls, and a cloud follows the tractor a few minutes later. At the beginning of the plowing, a bird discovers the food supply, and another soon follows, and so on. What went wrong? The news of a possible feast has travelled quickly among the gulls. The gulls flew in a more or less organized fashion in search of food, and the gathering was facilitated by a (voluntary or not) social exchange of information between members of the same species. One of them found a solution, and the rest adapted by duplicating it, resulting in an adaptive system.

Initially, J. Kennedy and R. Eberhart wanted to imitate birds' abilities to fly in synchrony and quickly change direction while maintaining an ideal formation. After that, they developed a simple and effective optimization algorithm based on the model they suggested. Individuals are the particles, and they move through search hyperspace. There are two rules that govern the search process:

1. Each particle has a memory that permits it to remember the best spot it has already passed through, and it tends to return there.

2. Each particle is notified about the most well-known location in its direct proximity, and it will move toward it.

These two designers, Russel Eberhart and James Kennedy, wanted to replicate social interactions amongst "agents" that had to attain a certain goal in a shared search environment, each with a limited capacity for memorizing and processing data. The primary criterion was that there should be no conductor, or even any knowledge of all information by the agents, and that only local knowledge should be used. After that, a basic model was created.

The collective behavior of these creatures has recalled that of a swarm of real beings, occasionally converging in numerous sub-swarms towards fascinating areas, since the initial simulations. Many other models, specifically inspired by natural systems, exhibit this behavior. The most appropriate metaphor here is arguably that of a swarm of bees, because a bee who has discovered a promising spot knows how to inform some of its sisters and that they will use this information in their next journey. Finally, the model proved to be too simplistic to accurately represent social behavior, but it was extremely useful as an optimization tool.

As we'll see, the PSO's operation can be divided into two categories: iterative approaches (where we gradually approach the answer) and stochastic methods (we use chance). We rediscover a behavior as old as life itself under this fairly technical term: improving one's condition by moving partly randomly and partly according to predetermined criteria.

4.1.1 Terminology

The terminology of particle swarm optimization is borrowed from social studies of animal behavior due to the existing analogy.

1. **Particle**: In PSO terminology, a parameter vector is called particle. All the particles in the swarm act individually under the same principle: accelerate towards the best global place and the best personal place while constantly checking the value of its current place.
2. **Position:**The position of the parameter vector in the search space is the particle position.
3. **The cost function (fitness):** As in all evolutionary techniques of calculation there must be some function or method to evaluate the quality of a position. The cost function should take the position in the search space and return a simple number representing the value of that position. The cost function provides the interface between the physical problem and the optimization algorithm.

4. **The best staff (Pbest)**: is the position discovered by a particle with the highest appropriateness value. The path traveled by each particle determines its personal best.
5. **Global Best (Gbest):**The location of the highest fitness value encountered by all particles up to a certain point in time (iteration) is known as the Global Best. For the entire swarm there is only one Global Best. Each particle has the means of knowing the Global Best discovered by the whole swarm. At each point in time each particle compares the fitness of its current location to that of the Global Best. If a particle is reached at a location of higher fitness, Global Best is replaced by that of the particle's current position

4.1.2 Informal description:

The historical version can easily be described from the point of view of a particle. At the start of the algorithm, a swarm is randomly distributed in the search space, each particle also having a random speed. Then, at each time step: each particle is able to evaluate the quality of its position and to keep in memory its best performance, i.e. the best position it has reached so far (which can in fact sometimes e the current position) and its quality (the value at this position of the function to be optimized).

Each particle is able to interrogate a certain number of its congeners (its informants, including itself) and to obtain from each of them its own best performance (and the related quality).At each time step, each particle chooses the best of the best performances of which it is aware, modifies its speed according to this information and its own data and moves accordingly.

The first point is easily understood, but the other two points require some clarification. Informants are defined once and for all as follows.

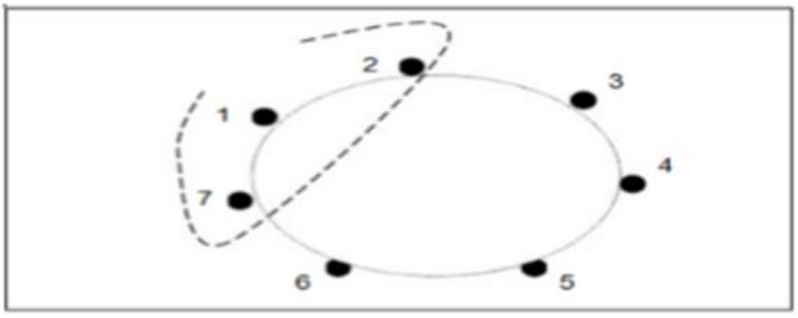

Figure 4.1 the virtual circle for a swarm of seven particles.

The information group of size three of particle 1 is composed of particles 1, 2 and 7. We assume that all the particles are arranged (symbolically) in a circle and, for the particle studied, we progressively include in its informants, first itself, then the nearest ones to its right and left, so as to reach the required total. There are, of course, many variations, including that of selecting informants at random, but this one is both simple and effective. The size three information group of particle 1 is composed of particles 1, 2 and 7. It is assumed that all the particles are arranged (symbolically) in a circle and, for the studied particle, one gradually includes among its informants, first itself, then the closer to its right and to its left, so as to

reach the required total. There are of course many variations, including choosing informants at random, but it is both simple and effective.

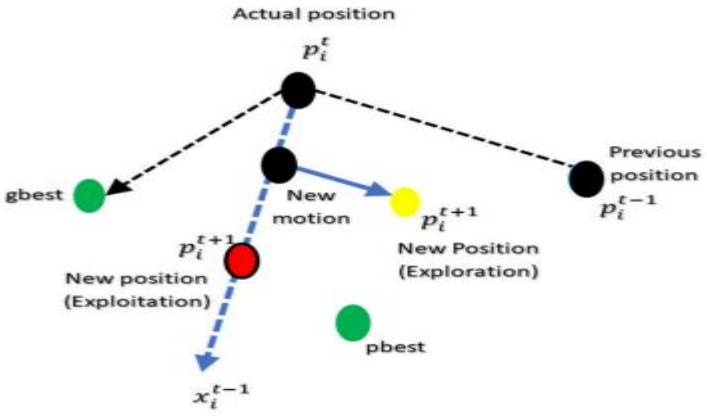

Figure 4.2 Principle diagram of the movement of a particle [106]

To achieve its next move, each particle combines three tendencies: following its own speed, return to its best performance, go to the best performance of its informants.

Once the best informant is detected, changing the speed is a simple linear combination of three trends, using confidence coefficients:

- The "adventurous" tendency, consisting in continuing according to the current speed,
- The "conservative" tendency, bringing more or less towards the best position already found,
- The "panurgi" tendency, orienting approximately towards the best informant.

The terms "more or less" or "approximately" refer to the fact that hazard plays a role, thanks to a limited random modification of the confidence coefficients, which favors exploring the search space.

Naturally, in order to be able to be programmed, all this is formalized in equations of movement. An interesting point is that, unlike many other heuristics that remain purely experimental, there is a mathematical analysis specifying the conditions of convergence and choice of parameters.

4.1.3 The neighborhood:

The neighborhood constitutes the structure of the social network. The particles inside a neighborhood communicate with each other. Different neighborhoods have been studied and are considered in function of the identifiers of the particles and not of the topological information like the Euclidean distances in the search space [107]:

- Star topology (figure 4.3(a)): the social network is complete, each particle is attracted to the best particle rated Gbest and communicates with the others.
- Ring topology (Figure 4.3(b)): each particle communicates with n (n=3) neighbors immediate. Each particle tends to move towards the best in its local neighborhood.

- Ray topology (figure 4.3(c)): a "central" particle is connected to all the others. Only this central particle adjusts its position towards the best, if this causes a improvement the information is disseminated to others.

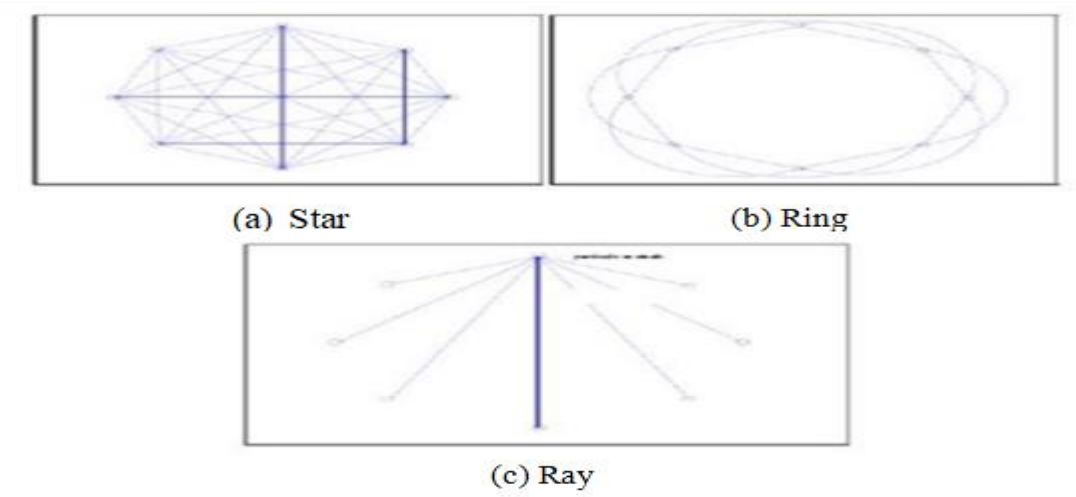

Figure 4.3 the different types of neighborhood (star, ring, and ray)

4.1.4 Main characteristics:

This model has certain interesting properties that make it a useful tool for a variety of optimization problems, particularly severely nonlinear, continuous or mixed issues (some variables are real, while others are integers):

– It is simple to write; in any evolved language, a few lines of code are enough;

– It is robust (bad parameter choices reduce performance but do not prevent finding a solution). We should also mention that there are adaptive versions that eliminate the need for the user to define the parameters (swarm size, number of informant groups, trust coefficients).

Moreover, it should be noted that this heuristic stands out from other evolutionary methods. (typically, genetic algorithms) on two essential points: it emphasizes the cooperation rather than competition and there is no selection (at least in the versions basis), the idea being that even a currently mediocre particle deserves to be kept, because it is perhaps precisely she who will allow future success, precisely because she comes out of the beaten track[1, 108].

4.2 PSO Parameters

The parameters used in the algorithm affect its performance differently. Some parameters have small effects while others have significant effects. Each set of parameters might be valid for a problem but not for another. The choice of parameters depends on the problem in hand and the time the user wants to spend solving it [108].

The main parameters that should be considered are:

- **Swarm Size**: Swarm size or the number of agents (n) in the swarm. A large number generates larger parts covered in the search space, this means less iterations are needed, but also more computation by iteration is needed. Most implementations use n ϵ [20, 60].

- **Iteration Number:** The number the algorithm updates the position of particles (number of steps). A large number may cause additional needless computations while a low number may stop the algorithm before hitting its target.

- **Acceleration parameters c1 & c2:** The values assigned to c1, c2 have been researched. Although a very large number of simulations and many attempts are made, because these two parameters have a large effect on the direction the particle will take at each time step, as we have seen that c1 forces the particle to accelerate towards the best performance already found (Personal Best), and that c 2 forces the particle to accelerate towards the Global Best. Several values are assigned to c1, c 2 but the most used values are given by [Kennedy][110]: c1 = 2, c 2 = 2, consequently it is also advised by several authors to vary c1, c 2 depending on the problem to be optimized.

- **Personal-best and Global-best:**

The algorithm uses a memory to save for each particle its best position visited so far. For each iteration, the actual position is compared with the personal best, if the cost function is decreasing, the actual position is a better fit and the personal best is updated to be the actual. If not, the particle keeps the previous personal best. The global best on the other hand is updated each iteration by taking the minimum of Pbest.

$$Pbest_i^{t+1} = \begin{cases} Pbest_i^t & if \quad f(x_i^{t+1}) > fbest_i^t \\ xbest_i^{t+1} & if \quad fbest_i^t \geq f(x_i^{t+1}) \end{cases} \qquad (4.1)$$
$$Gbest^t = Min(Pbest_1^t, Pbest_2^t, Pbest_3^t, \ldots, Pbest_n^t)$$

- **Velocity and Its Updating Methods:**

The velocity is the rate of change in the particle's position. Represented as a vector and calculated over each iteration as follow:

$$v_i^{t+1} = v_i^t + c_1 r_1 * (Pbest_i^t - x_i^t) + c_2 r_2 * (Gbest^t - x_i^t) \qquad (4.2)$$

Where; c_1, c_2: are two positive constants.

r_1, r_2: are two positive randomly generated numbers less than 1.

- **Constriction Factor Method:**

Clerc and kenedy introduced a new parameter X constriction factor, this last controls the exploration and exploitation tradeoff to ensure convergence behavior [111].

The velocity updated using this method is:

$$v_i^{t+1} = X\left\{v_i^t + c_1 r_1 * (Pbest_i^t - x_i^t) + c_2 r_2 * (Gbest^t - x_i^t)\right\}$$
$$X = \frac{2}{\left|2 - \sqrt{\varphi^2 - 4\varphi} - \varphi\right|} \qquad (4.3)$$
$$\varphi = c_1 + c_2$$

Studies show that: to guarantee quick convergence, φ must be greater than 4, otherwise the system will be slow and might diverge[111].

- **The equation of Movement:**

PSO is basically developed through the simulation of flocking birds in both spatial dimensions.

The position of each agent is represented by the position on the XY axes and the speed is expressed by v_x(the speed of the X axis) and v_y (the speed of the Y axis).

The change in an agent's position shown is defined by the position and speed information.

Each agent knows their best-to-date value (Pbest) and their position (XY).

This information is the analogy of the personal experience of each agent. Additionally, each agent knows the best value so far in the group (Gbest) between Pbests.

This information is analogous to the knowledge of the way in which the other agents which surround have accomplished. Namely, so that each agent can modify its position it is necessary to use the following information:

- itscurrent position (x, y),

- Its current speed (v_x, v_y)

- The distance between its current position and Pbest

- The distance between its current position and Gbest

This modification can be represented by the concept of speed. The speed of each agent can be modified by the following equation :

$$v_i^{t+1} = \omega^t v_i^t + c_1 r_1 * (Pbest_i^t - x_i^t) + c_2 r_2 * (Gbest^t - x_i^t)$$
$$\omega^t = \omega_{\max} - \frac{\omega_{\max} - \omega_{\min}}{t_{\max}} t \qquad (4.4)$$

The inertial weight w decreases from a max value to a min value. Using the above equation, in calculating the speed, which is approximately Pbest and Gbest can be calculated. The current position (search in the space of research) is given by the following equation:

$$x_i^{t+1} = x_i^t + v_i^{t+1} \tag{4.5}$$

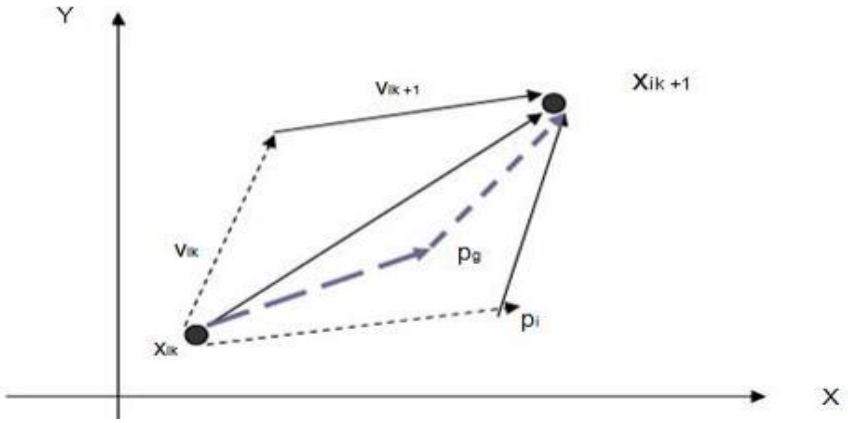

Figure 4.4 Updating a particle with the PSO algorithm.

4.3 The objective function

An optimization problem is one in which we may construct one or more objective functions that allow us to distinguish between excellent and bad solutions. Concretely, these objective functions run through the set of possible solutions of the local search space and are, at each iteration, compared to previously defined optima.

Their equality (or almost equality in the case of a performance guarantee) then leads to the final state; to the solution [112, 113]

The very principle of a metaheuristic is to minimize or maximize these functions in order to reduce the possible solutions and at the same time the execution time.

When a single value is associated with a single objective function, we speak of a single-objective problem. Otherwise, we naturally speak of a multi-objective problem [114].

- **Stopping Rule**

Several stopping criteria are possible for the PSO algorithm:

• A threshold on the cost functions of the best memorized particle.

• A limit in terms of number of iterations or calculation time.

• More improvement of the best particle during a minimum number of iterations fixed at a priori

4.4 Algorithmic description:

The objective of the PSO algorithm is to optimize a function in a given space. In the most cases, the optimization algorithm looks for the global maximum or minimum of the search space. Here is the description of the steps of the PSO algorithm:

Step 0:

Initializing the speed and position of each particle in the swarm.

Step 1:

If the stopping criterion is verified, then the algorithm terminates. If not, a new iteration begins by returning to Step 2 with the first particle (i=1). The stopping criterion usually corresponds to a predefined number of iterations, but one can also specify a stopping criterion based on the best quality value G($Gbest_g$) obtained for all particles.

For all particles in the population, perform Steps 2 through 6

Step 2:

Calculation of quality G ($Pbest_i$) of particle i as a function of G (x_i) and its position vector (x_i).

Step 3:

Establish whether the quality G (x_i) obtained by particle i is superior to the best quality that this particle has obtained previously. if G (x_i) > G ($Pbest_i$) , the present position of the particle x_i is saved as the best position pi obtained to date for the particle i. P_i x_i G ($Pbest_i$) G ($Gbest_g$) V^t_i

Step 4:

Establish whether the quality G (Pbesti) obtained by particle i is greater than the best quality G(Gbestg) obtained for the entire population. If this is the case, the index of the particle having obtained the best quality g takes the value i.

Step 5:

Update Movement Speed Vit+1 of the particle i. This update takes into account the previous velocity of the particle Vi, from its present position xit, from the position of the best quality

pi obtained by this particle as well as the position of the best quality global Pg obtained by the population. Once this speed has been updated, it is necessary to check whether the new speed Vit+1 of the particle i is contained within the authorized limits Vi (- Vmax +Vmax). If this is not the case, the new speed is reduced to the nearest terminal.

Step 6:

Update position xi t+1 of the particle i. This update takes into account the position previous particle xit as well as new speed Vi t+1 calculated in step 5. Once the position of the particle i updated, it is necessary to check if the new position xi t+1 is contained in the search space specified by xi (xmin ,xmax). If this is not the case, the new position is brought back to the most terminal close.

The algorithm below presents a summary of the PSO algorithm.

Algorithm: Optimization by particle swarms
Parameter initialization x_i, V_i,x_{min}, x_{max}, V_{max},
for t = 1 at maximum iteration
for i = 1 to the number of particles
if $G(x_i)>G(pbest_i)$ //G()assess the quality
p i = xi // $pbest_i$ best position
End If g=i // arbitrary
for j = particle neighbor index i
if $G(pbest_i)>G(Gbest_g)$ then g=j // index of the best particle
globale
next j

$$v_i^{t+1} = \omega^t v_i^t + c_1 r_1 * (Pbest_i^t - x_i^t) + c_2 r_2 * (Gbest^t - x_i^t)$$

$$\omega^t = \omega_{max} - \frac{\omega_{max} - \omega_{min}}{t_{max}} t$$

$$x_i^{t+1} = x_i^t + v_i^{t+1}$$

next i
next t
Until the stopping criterion is reached

Figure 4.5 Pseudo code of the algorithm

4.4 Areas of research and applications:

The method appealed to a wide range of issues due to its simplicity of implementation and fast convergence. It was intended to control the parameters of a neural network [106, 115].The results are comparable to, if not better than, the standard back-propagation algorithm.

In general, the PSO provides excellent results for nonlinear continuous problems, often outperforming other approaches in terms of computation time and optimal quality. Mixed issues (to continuous and discrete variables) have also yielded excellent results [116].

Furthermore, the system's fast convergence makes it perfectly adapted to dynamic optimization (where parameters vary over time).

The use of PSO on purely discrete problems has been tried with more mixed results. It is the same when the space is strongly constrained [98]: the variables can only take on a limited number of values and the particles cannot therefore not freely roam in space.

4.5 PSO in Tuning the PI-Controller

4.5.1 PSOBased PI-Controller Algorithm

The flowchart of the code implemented in this work is shown in Fig.4.6. The velocity update is set to be inertia weight based. The performance criteria used in designing the PI-controller is the Integrated of Time weight Square Error (ITSE).

$$ITSE = \int t.e(t)^2 \tag{4.6}$$

The advantage of ITSE over other integral performance criteria, say Integrated Square Error (ISE) and Integrated Absolute Error (IAE) is that ITSE can overcome the disadvantage these last two may face. ISE and IAE minimizations can result in response with small overshoot but a long settling time because they weight all error equally independent of time.

The PSO algorithm is used to determine the parameters of the PI regulator (Kp and Ki) where all the particles in this algorithm are decoded in two dimensions Kp and Ki [1, 108].

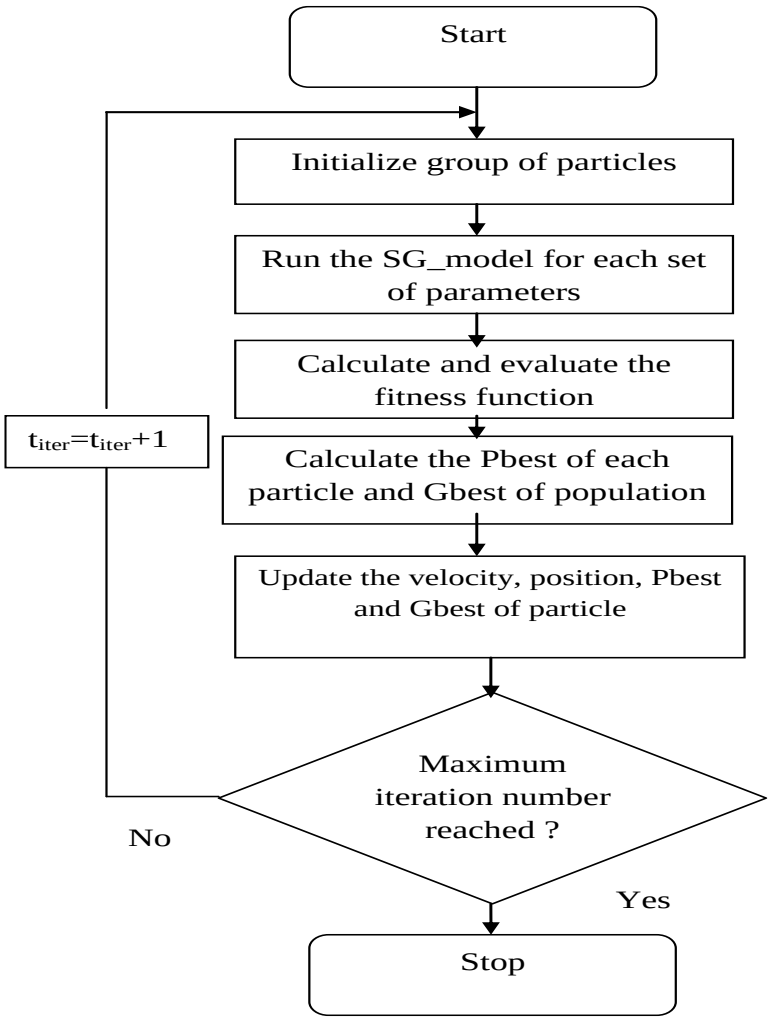

Figure 4.6 Flowchart for the PSO based PI-controller.

4.5.2 PSO base PI controller Tuning Results

The PSO algorithm allows calculating the error and the dynamic characteristics of the system at each position and each particle for each iteration (See Figure 4.6). The PSO parameters are given in table 4.1.

The idea is to have the best solutions for Kp and Ki with PSO convergence characteristics for different parameters, population size and number of iterations. The obtained results are shown in figures 4.7and 4.8.

Table 4.1 PSO parameters settings

Number of variables (Dimension of the problem)	2 (K_p, K_i)
c1	2
c2	2
Velocity updating method	Inertia weight
Wmax	0.9
Wmin	0.4
Correction factor	2.0
Lower bound	[-5.12 -5.12]
Upperbound	[5.12 5.12]
population size	n
number of iterations	t
Fitness function	ITSE

Running the PSO algorithm for several tries and for different parameters of population size and number of iterations, the obtained results are displayed and are in terms of best solution for K_P and K_I along with PSO convergence characteristics (see Figure 4.8).

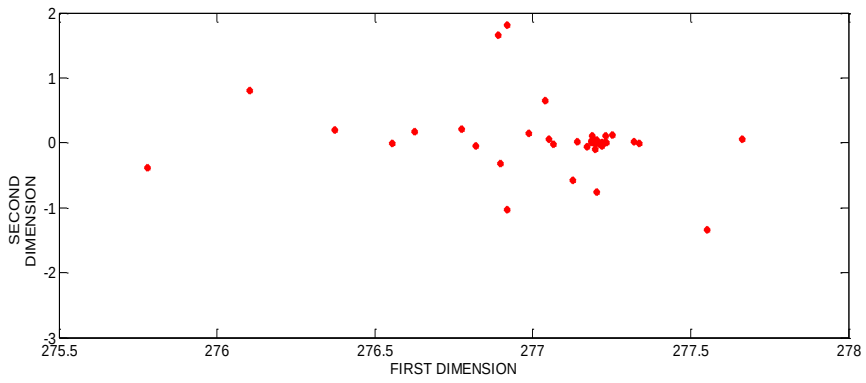

Figure 4.7 Population repartition.

Figure 4.7 presents the population repartition in the space research. The latter is an evolutionary algorithm which uses a population of candidate solutions to develop an optimal solution to the problem in question the parameters Kp and Ki.

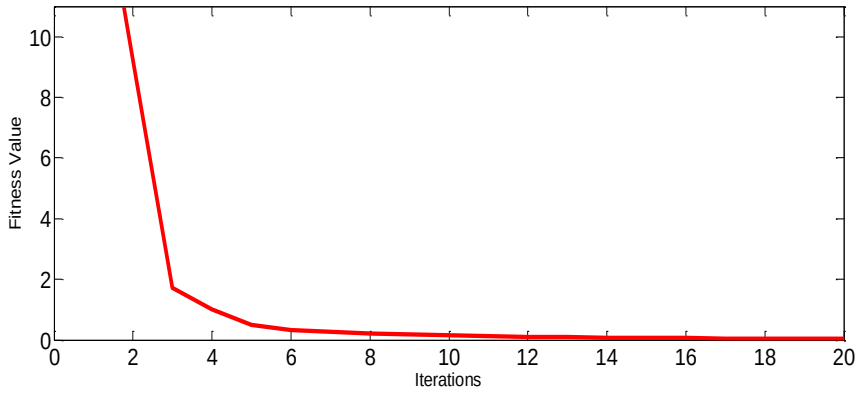

First try: K_p =277.1937, K_i=0.0149 n=10, t=50

Figure 4.8 PSO convergence characteristics and best solutions

Figure 4.8 represents the convergence of the fitness function for many population swarms n and iterations t. The evolution of the objective function towards the global optimum for different populations and iterations

The growth of the cost function and the values of the regulator parameters are depicted in Fig.4.8 The cost function show a quick, then slow, descent, and finally stagnation. After ten iterations, convergence is ensured.

4.6 Microcontroller Based AVR Implementation

4.6.1 PID Algorithm Implementation:

PID algorithm has been implemented within the Arduino software using C++ programming language.

The PID program is shown in Figure 4.9

```
float  PID_compute(float setPoint, float measured, float timeStep )
{
  // Calculate error terms
 float  error = setPoint - measured ;
 float  errorIntegral += (error + errorPrevious) / 2 * timeStep ;
 float  errorDerivative = (error - errorPrevious) / timeStep ;

 // save the current error to the next step
 float  errorPrevious = error;

  // Calculate the PID output
  float  PID_out = Kp * error + Ki * errorIntegral + Kd * errorDerivative;

return PID_out;
  }
```

Figure 4.9 The implemented PID algorithm (PID program)

4.6.2 Schematic diagram:

The schematic diagram consists of two parts, the generator and the microcontroller. The output voltage of the generator is reduced and converted to DC through a step-down transformer and a full wave rectifier and a capacitor, a Zener diode is added in parallel with the capacitor to protect the Arduino from a higher voltage than 5V. The obtained DC voltage will be supplied to the Arduino ADC to be converted into a 10-bit digital value, then; it will be processed by the microcontroller program in order to control the generator excitation voltage.

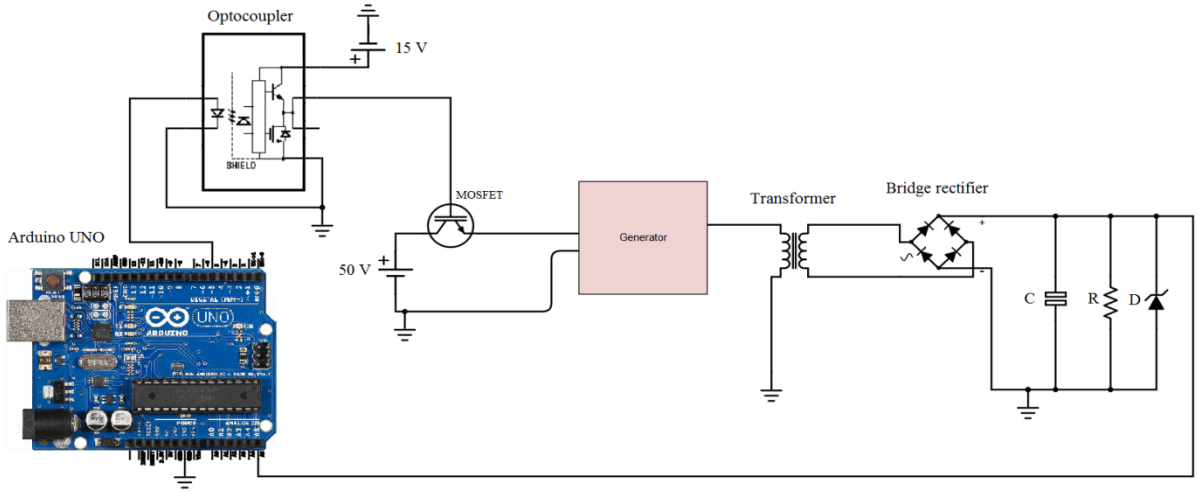

Figure 4.10 Schematic diagram

The microcontroller generates a PWM signal to the gate driver of the MOSFET which controls the excitation voltage fed from a DC power supply; by changing the PWM duty cycle, which in turn increases or decreases the output voltage of the synchronous generator.

4.6.3 Results and discussion:

The schematic diagram shown in figure 4.10 has been implemented successfully as shown in figures 4.11 and 4.12

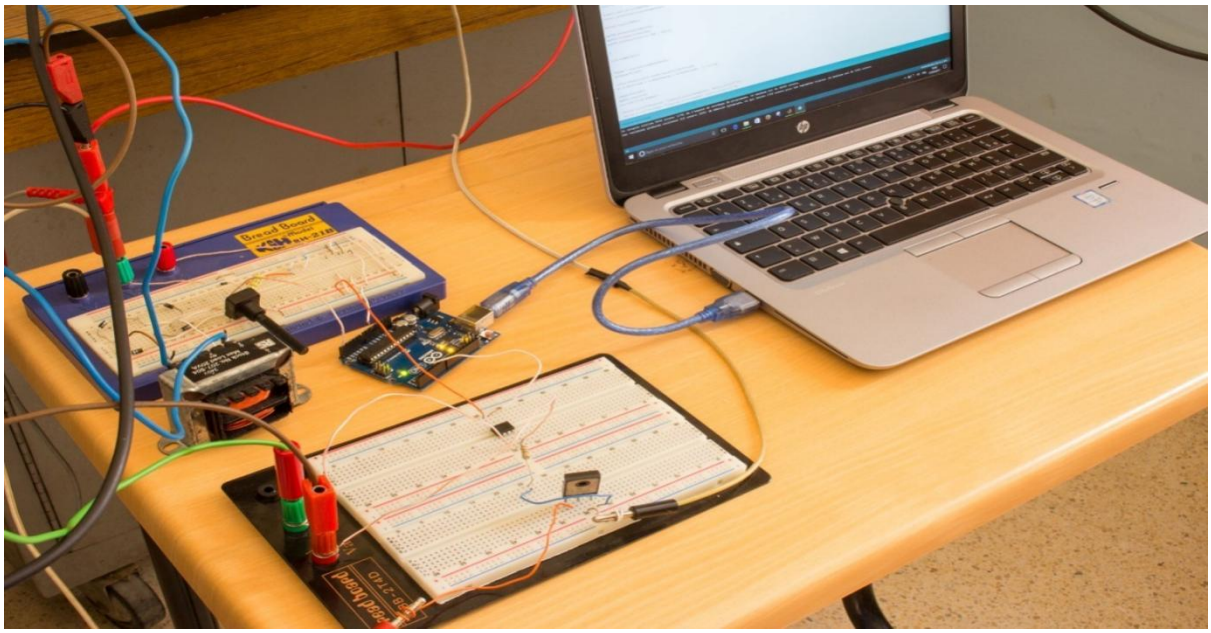

Figure 4.11 The implemented circuit

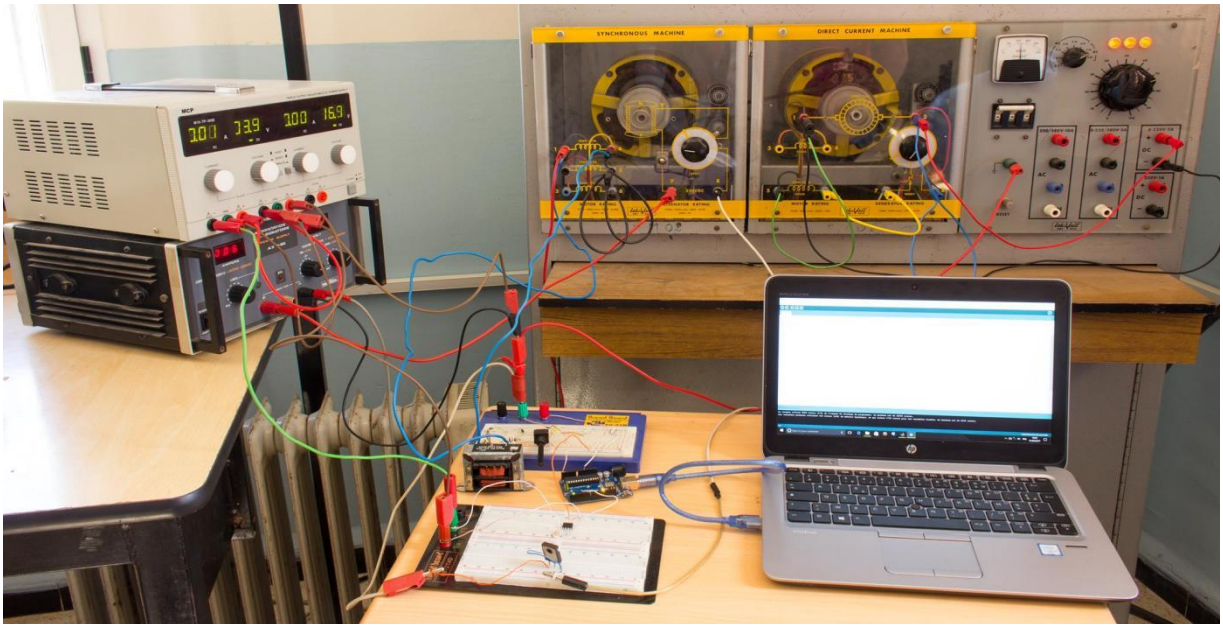

Figure 4.12 The implemented circuit with the synchronous generator

The system has been run with and without the PID controller in order to compare the obtained results, the serial plotter provided with Arduino software has been used to plot the measured data as shown in figures 4.13 and 4.14

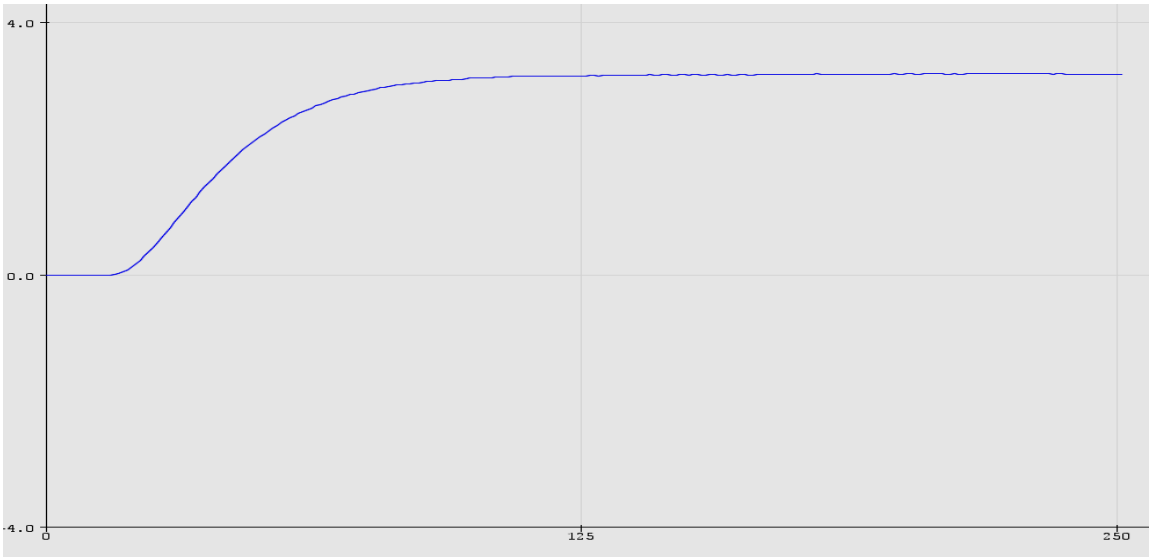

Figure 4.13 The system recorded data without PID

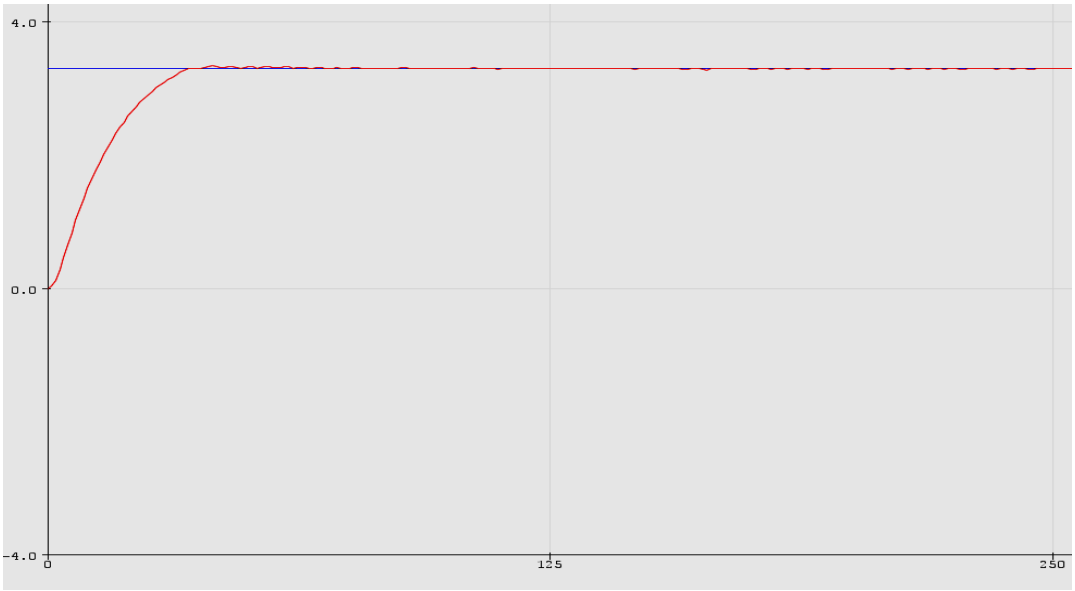

Figure 4.14 Closed loop system data with PID

One can notice clearly that the two systems are stable but the one with PID controller has a better time response. In order to compare the two plots precisely and get the system time domain characteristics the data has been transferred to MATLAB, and plotted in figure 4.15

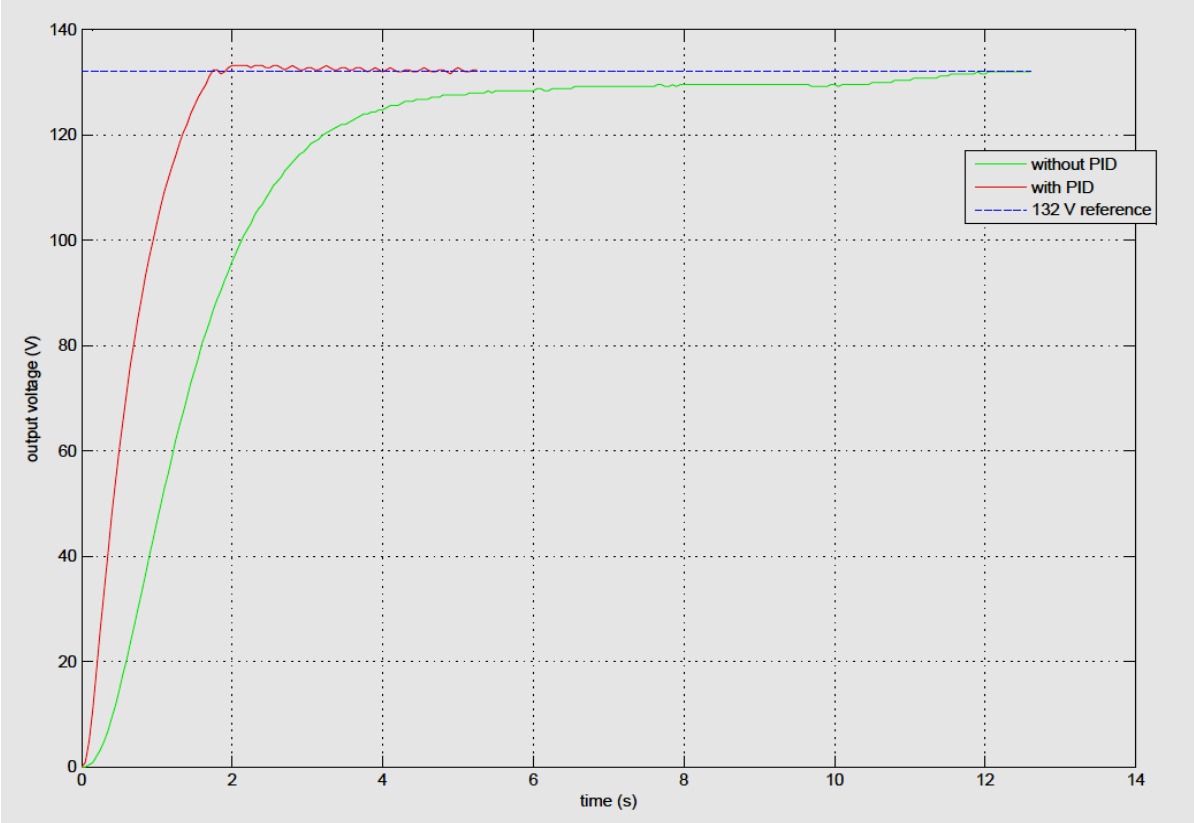

Figure 4.15 Output voltage with and without PID controller

The open loop transfer function has been identified:

Third order estimation: $$G2(s) = \frac{4.51}{s^3+4.662\,s^2+8.424s+4.579} \quad (4.7)$$

A 3rd order model controlled with PID gives a closed loop transfer function with 2 zeros and 4 poles, so the implemented model has been estimated using the identification toolbox with 2 zeros and 4 poles given the following transfer function

$$G(s) = \frac{10.48\,s^2 + 27.93\,s + 160.2}{s^4 + 9.26\,s^3 + 49.34\,s^2 + 132.1\,s + 159.7} \quad (4.8)$$

With a step response and time domain characteristics compared to the open loop system in figure 4.16 and table 4.2

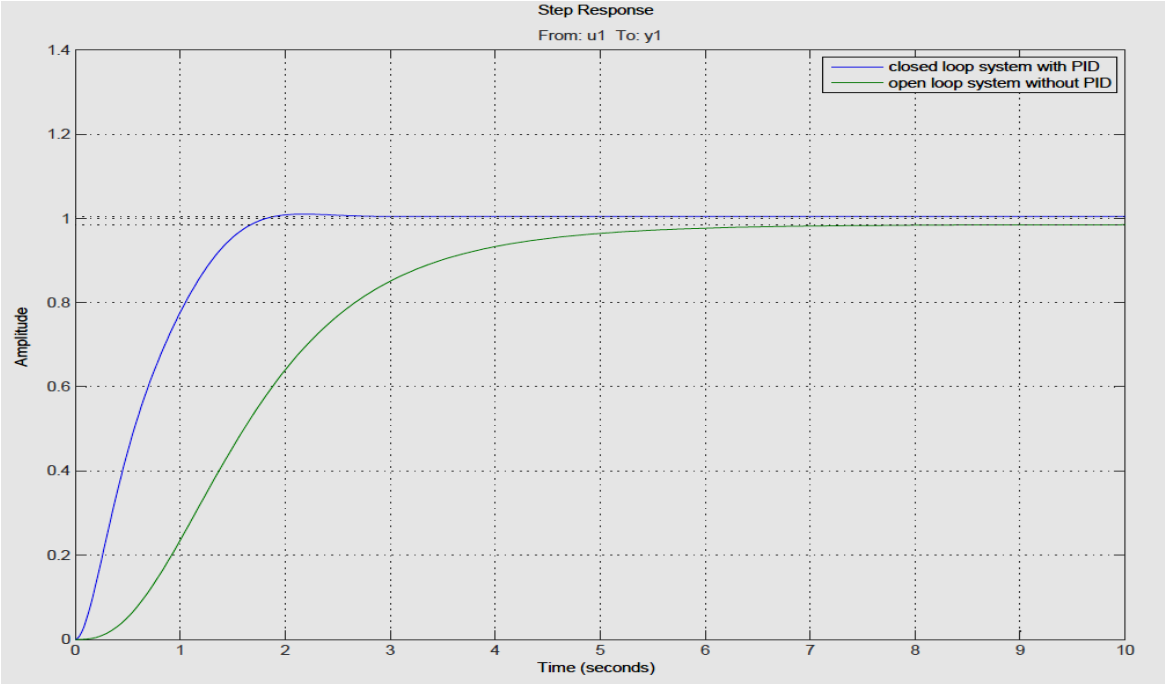

Figure 4.16 open loop vs closed loop with PID step responses

Table 4.2: The time domain characteristics of open loop vs closed loop with PID:

	Rising time (s)	Settling time (s)	Overshoot (%)	SteadyState error %
Open loop	3.57	5.06	0	1.59
Closed loop with PID	1,38	1.66	0.72	0

The results were approximately as expected, the AVR PID controller really gives a good result, and to confirm that a last step is needed which is the comparison of the simulated PID with the implemented PID as illustrated in figure 4.17 and given in table 4.2.

It is necessary to identify the controlled closed loop transfer function obtained from the implementation and compare it with the closed loop 3rdorder model obtained from the simulation.

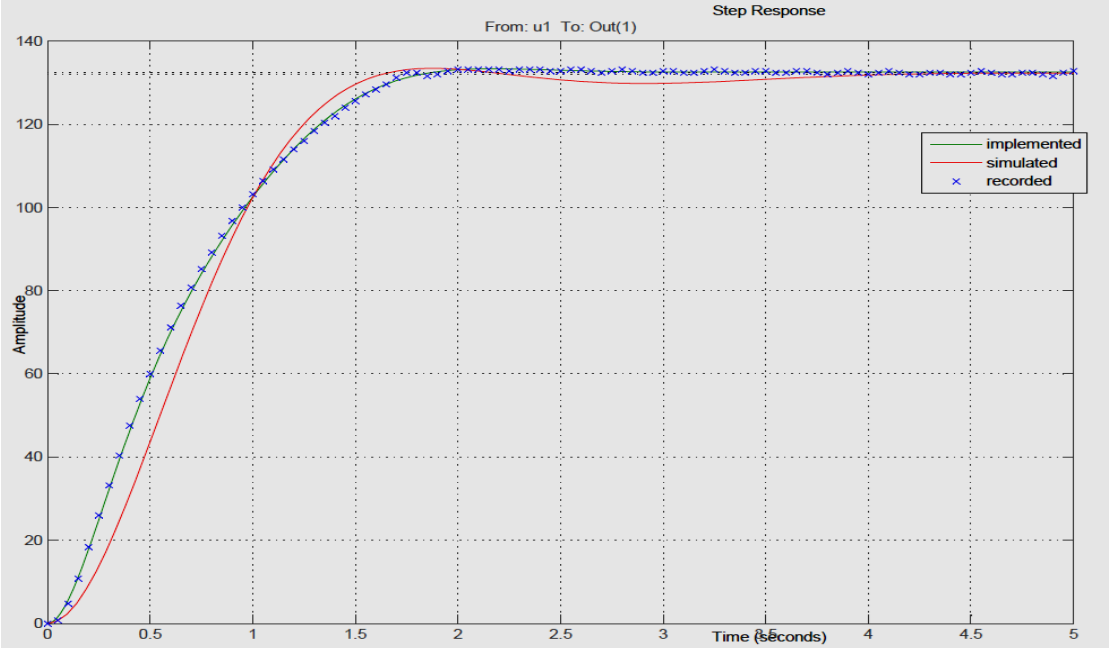

Figure 4.17 Comparison between the simulated and implemented PID systems.

Table 4.3 comparison between the simulated and implemented PID systems

	Rising time (s)	Settling time (s)	Overshoot (%)	SteadyState error %
simulated	0.98	1.49	0.96	0
implemented	1,38	1.66	0.72	0

As shown in figure 4.17 the output of the implemented system is not exactly the same as the simulated one but they are close enough, the data from table 4.3 approves it with a difference of 0.4 seconds in the rising time, and a 0.17 second in the settling time, and 0.24% in the overshoot, and that difference is because of the absence of disturbance and noise in the simulation within MATLAB.

Finally, it was impossible to plot the AC output voltage of the synchronous generator using the scope, because the scope available in the lab can display a maximum of 10 volts per

division which means 50V peak value; however, using a multimeter the RMS voltage has been measured giving values between 133V and 131V which means 132V ± 0.75%.

And the stepped down voltage of the transformer was plotted instead, as shown in figure 4.18

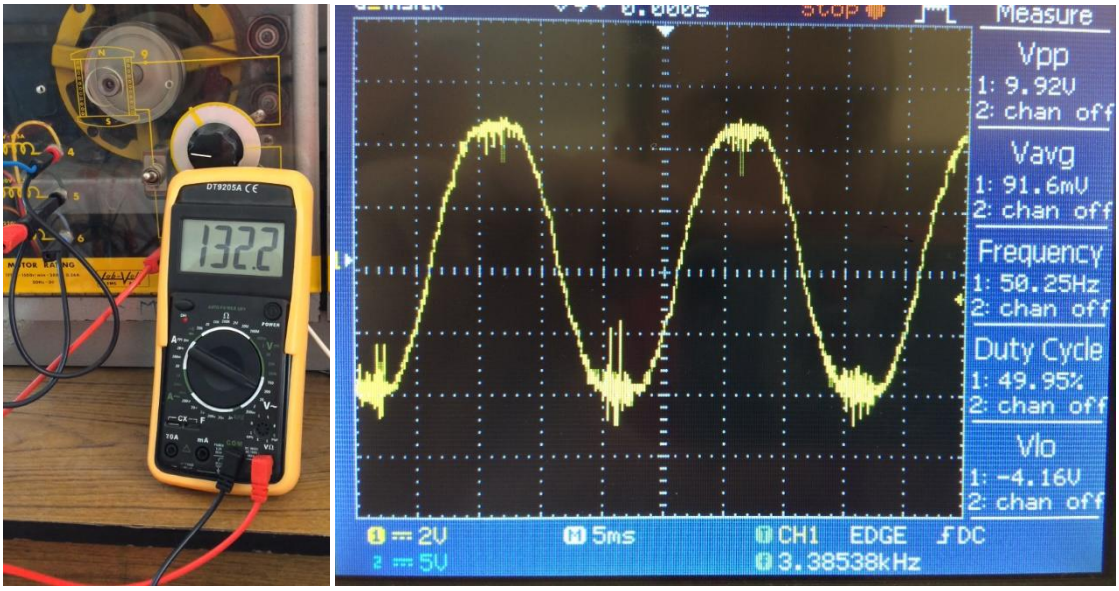

Figure 4.18 The measured RMS and the stepped down AC voltage

As expected the AC voltage frequency of the generator is approximately 50 HZ, and it is noticeable that the AC voltage was not a perfect sinusoidal but a bit noisy, that is because of the disturbance and the old materials used in the implementation

4.7 Conclusion:

One of the advantages of Meta-heuristics methods allows the absence of particular hypotheses on the regularity of the objective function. However, one of the difficulties with swarm particle optimization is parameter choice.

The results obtained by PSO are very satisfactory and confirm the validity of the algorithm.

The advantage of these approaches over traditional techniques is robustness and flexibility[114, 117].

In the implementation of AVR in synchronous generator using microcontroller within the Arduino software using C++ programming language, several problems has been faced, as the burning of H-Bridges that were used before using the MOSFET because of the current overshoot provided by the power supply. Even the later has not been sufficient to reach 220V from the generator, but this was not a big problem because the objective of this project was

not to reach a 220V but regulating the output voltage to a stable value, 132V was chosen randomly within the ability of the power supply. Besides the faced problems, the implementation of the project has been done with positive results. In this project, the objective of design and implementation of an automatic voltage regulator of an engine generator using an Arduino microcontroller has been reached successfully.

Chapter 5

ADRC Control Method

Chapter 5

ADRC Control Method

5.1 Introduction

The birth and large-scale deployments of the powerful yet primitive proportional–integral–derivative (PID) control law dates back to the period of the 1920s–1940s in the last century, in response to the pressing demands of industrial automation before, during, and particularly after World War II. Its role in the explosive growth in the postwar manufacturing industry is unmistakable; its dominance is evident even today across various sectors of the entire industry.

It appears that, as any technology, PID will eventually outlive its usefulness, if it has not already done so. The question is: what will replace this hugely successful control mechanism in the 21st century, retaining its basic soundness and, at the same time, shedding its limitations? It is doubtful that such question was even entertained systematically, let alone answered, in the past. We believe that the answer lies in our understanding of both the characteristics of PID and the challenges it faces. It is such understanding that will lead us to propose further developments in the PID framework and, perhaps, even a drastic innovation toward a new generation of digital control solutions.

Active disturbance rejection control (ADRC) can be summarized as follows: it inherits from proportional–integral– derivative (PID) the quality that makes it such a success: the error driven, rather than model-based, control law; it takes from modern control theory its best offering: the state observer; it embraces the power of nonlinear feedback and puts it to full use; it is a useful digital control technology developed out of an experimental platform rooted in computer simulations. ADRC is made possible only when control is taken as an experimental science, instead of a mathematical one. It is motivated by the ever increasing demands from industry that requires the control technology to move beyond PID, which has dominated the practice for over 80 years. Specifically, there are four areas of weakness in PID that we strive to address: 1) the error computation; 2) noise degradation in the derivative control; 3) oversimplification and the loss of performance in the control law in the form of a linear weighted sum; and 4) complications brought by the integral control. Correspondingly, we propose four distinct measures: 1) a simple differential equation as a transient trajectory generator; 2) a noise-tolerant tracking differentiator; 3) the nonlinear control laws; and finally 4) the concept and method of total disturbance estimation and rejection. All together, they form a new set of tools and a new way of control design. Times and again in experiments and on factory floors, ADRC proves to be a capable replacement of PID with unmistakable advantage in performance and practicality, providing solutions to pressing engineering

problems of today. With the new outlook and possibilities that ADRC represents, we further believe that control engineering may very well break the hold of classical PID and enter a new era, an era that brings back the spirit of innovations.

ADRC has been a work in progress for almost two decades [118, 119],with its ideas and applications appearing in the English literature, amid some questions and confusions, sporadically only in recent years; see, for example [120, 121]. In ADRC, we see a paradigmatic change in feedback control that was first systematically introduced in English in 2001 [120]. The conception of active disturbance rejection was s further elaborated in [122]. However, even though much success has been achieved in practical applications of ADRC, it appears that this new paradigm has not been well understood and there is a need for a paper that provides a full account of ADRC to the English audience [123]. Such need is unmistakable in the recently proposed terminologies such as equivalent input disturbance [121] and disturbance input decoupling [124], all of which can be seen as a special case of ADRC where only the external disturbance was considered. It is primarily for this reason that this paper is written[12].

5.2 Description and Principle of ADRC Method

Active disturbance rejection control (ADRC) is a new generation of digital control solutions, which may replace the efficient conventional controller PID in the 21st century, keeping the same advantages, but trying to reduce its disadvantages [12].

ADRC has been proposed by J. Han [12] and simplified by Z. Gao [120, 122]. In order to understand the idea behind this control law, it is necessary to follow the reasoning of J. Han. [12] (Han, 2009) who noticed that the right idea is to understand the two characteristics of PID and its faced challenges. For this reason, all most innovative control methods that have been developed such as adaptive and robust control, aim to have better control performance even with uncertainties. In this mind, J. Han began the process that ultimately led to the ADRC [125, 126].

In fact, to replace PID control, a control method should have the following properties: 1) a fixed control structure, and the structure should be easy to be implemented in practice; 2) few tuning parameters, and the parameters are directly related to the performance of the closed-loop system, and the tuning is easy to understand by control engineers; 3) can predict or estimate the error between the output and the set-point in real time so that better control performance can be achieved. It is clear that few control methods possess these properties in the development of advanced control theory; this is why PID control is still dominant [127].

Mathematical modeling causes obvious gaps which leads to smart implementation and terrible performance. Academic research, so active in automation, sometimes called "modern" for more than fifty years, finds much of its motivation there [128].

Many systems face disturbance phenomena that reduce the precision, the quality of service or even the age of the processes. Control laws that may be developed must take into

account the need to improve the performance of new components, machines or complex systems such as energy systems and hence the reduction of the effect on the environment.

This research work aims to improve the precision and robustness of processes in energy production by trying to cancel the influence of disturbances on the behavior of the complete system by designing a controller / observer, using an integrated approach [129].

During the period 1980-1990, Jingquin Han published several papers on a new unconventional control method (Han, 1988, 1995a, b, 2009, 1989) [126].

The central idea is to treat the internal uncertainties and external disturbances as a "generalized disturbance," and try to estimate in real time by an extended state observer (ESO), and then it can be used in the feedback with the aim to compensate the disturbance quickly. ADRC configuration is shown in Figure 5.1, where b contains the gain information of the controlled plant; TD is a tracking differentiator that is used to get the desired response for the reference; ESO is the extended state observer that is used to estimate the generalized disturbance and the plant output (including its derivatives of various order); NLSEF is a nonlinear state error feedback that utilizes the error and its derivatives of various order in a nonlinear fashion to achieve good control performance. An important character of ADRC is that the estimated disturbance ˆf is combined with the nonlinear state error feedback so that the final control u can reject the disturbance. The structure is not hard to implement with the modern digital computer technology and is shown to be able to achieve good control performance. However, the structure is still complex and needs to tune a bunch of parameters, which makes it difficult to use in practice. To overcome the difficulty, [130] and [122] consider the "linear" version of ADRC (LADRC), where liner ESO and linear state feedback are used. Furthermore, the number of parameters for the LADRC is reduced to two, the controller bandwidth ωc, and the observer bandwidth ωo, and these two parameters are closely related to the performance of the closed-loop system, thus LADRC possesses all the properties listed above for replacing PID [127].

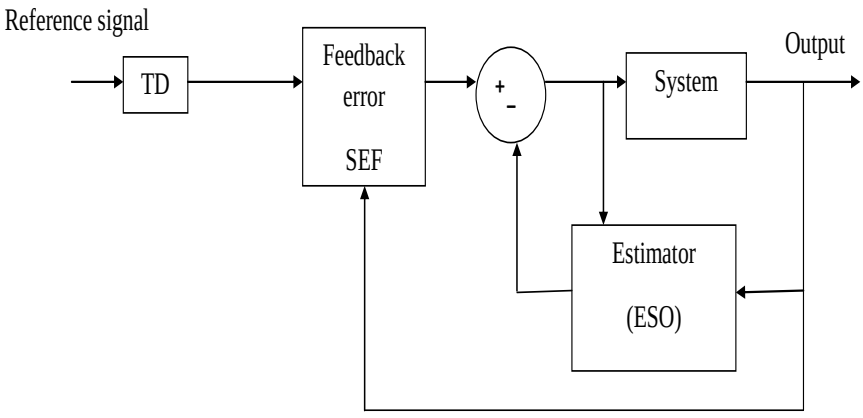

Figure 5.1 ADRC functional block diagram.

The significant difference between the ADRC and other control methods is that the ADRC not only estimates plant uncertainties and external disturbances in the ESO, but also actively compensates for them in the SEF. Therefore, the ADRC becomes a potential candidate for controlling dynamic systems with plant uncertainties and external disturbances [131].

Many ADRC applications have been reported in the literature, e.g., gyroscopes [132], load frequency control [133], gasified [134], two-mass drive [135], tank gun control [136], robotic-enhanced limb rehabilitation trainings[137], under-actuated systems [138], diesel engines [139], and flywheel energy storage system [140]. To advance the study on ADRC, two special issues were published in ISA Transactions in 2014 and Control Theory & Applications in 2013, which greatly propagates the ADRC idea. Though ADRC has made much progress, it has not attracted much attention in the control area, partly because few theoretical results are available to verify the method, among which the most important are frequency analysis for LADRC [141], stability analysis of LADRC [142], verification and performance analysis of ESO [143], frequency analysis of nonlinear ADRC by describing function method [144], convergence of nonlinear ADRC [145], singular perturbation analysis of ADRC [146], adaptive Lyapunov methods for ADRC [147]. Interested readers may refer to [148] for a recent survey on ADRC. It is noted that ADRC only needs to know the relative order of the process and the corresponding gain. This is the advantage of the method, but it is also the target of criticism: 1) Is such little information enough for a good control?

2) If more plant information is available, can such information be used to improve control performance?

3) How can extra information be incorporated in ADRC [127]?

However, owing to the usage of nonlinear functions in all three parts of the ADRC, the complicated controller structure and a large number of tuning parameters pose challenges in practical applications. To simplify the structure of the ADRC, a linear ADRC was proposed in, where the TD is removed and the nonlinear functions used in the ESO and SEF are replaced by linear functions. To date, the application of the linear ADRC has been widely extended to many different fields.

5.3 Stability Analysis of ADRC System

Generally, when a closed-loop control system is linear, the stability can be easily analyzed by determining the Eigen values of the control system. All the Eigen values that have negative real parts indicate that the control system is stable. When the control system is nonlinear, Lyapunov second method is the most general method to study the stability. In [148], the stabilities of the nonlinear ESO and the ADRC system were analyzed based on Lyapunov second method. It was shown that: 1) there exist appropriate observer gains, the estimation errors between the ESO and the system states are convergent; 2) there exist proper gains of the SEF, the ADRC system is stable, i.e., the estimation errors between the transient profiles and the system outputs are convergent. Similarly, the stability analyses of the linear ESO and the ADRC system based on Lyapunov's second method were presented in [132,

142]. It was shown that there exist appropriate gains of the linear ESO and the linear weighted sum, the linear ESO and the ADRC system are stable, and the estimation errors are bounded. The aforementioned stability analyses based on Lyapunov's second method are the generalized justifications of the convergences of the ADRC systems, where the models of the controlled systems are not required. However, for a specific controlled system, these generalized justifications are unable to determine whether a set of gains of the ADRC controller can stabilize the controlled system. The main reason why there is no stability justification of the ADRC for a specific, controlled system can be attributed to the fact that constructing the Lyapunov functions for nonlinear and complex dynamic systems is very challenging, because no constructive rule exists in the Lyapunov stability theory. Therefore, to address this challenge, an alternative means to study the stability of the ADRC system is desirable. In this thesis, the concept of Lyapunov exponents, as a powerful tool for the stability analyses of complicated and nonlinear dynamic systems, is introduced to investigate the stability of the ADRC system consisting of a nonlinear vehicle model. The Lyapunov exponents describe the long-term evolution of a dynamic system with an initial condition[149]. The signs of the Lyapunov exponents describe the stability property of the dynamic system [150]. Compared to Lyapunov's second method, the methods for calculating the Lyapunov exponents are constructive either based on a model of the dynamic system or a time series. The concept of Lyapunov exponents has been applied to the stability analyses of the PD control for a biped [151, 152] and a nonlinear vehicle model in plane motion [153].

5.4 Tuning of ADRC

The linearization of the nonlinear ADRC generates a simple control structure and reduces the number of tuning parameters. Within the framework of the linear ADRC, the number of tuning parameters nt is proportional to the order of the dynamic system n: nt=2n+1 [127]. That is, for a second-order dynamic system, the number of tuning parameters is five. To further facilitate the tuning process, a bandwidth tuning method was proposed to reduce the number of tuning parameters to two, i.e., the observer bandwidth and the controller bandwidth [130]. This is realized by expressing all parameters of the linear ESO as functions of the observer bandwidth and expressing all parameters of the linear weighted sum as functions of the controller bandwidth. Most applications of the ADRC mentioned above were based on this tuning method. The bandwidth tuning method ensures the stability of the ADRC system and works well for tuning the ADRC for controlled systems described by first- and second-order mathematical models [130]. However, it is found to be conservative in tuning the ADRC for controlling hydraulic actuators described by fourth- and fifth-order systems, because a large number of tuning parameters determined by only two bandwidths cannot meet the desired tracking performance [127]. There has been little research on tuning the ADRC. In [127], a tuning method similar to the bandwidth tuning method was proposed. In [127], a method was proposed by incorporating the known system dynamics into the ADRC. This method works for systems for which accurate models are available but not for complicated systems with plant uncertainties and faults [131].

5.4.1. State representation of Model

Consider a system of n order written in the standard form proposed by Han;

$$y^{(n)}(t) = bu(t) + f(t) \tag{5.1}$$

Its output quantity is y (t), the control quantity u (t) and f (t) the quantity defining the total disturbances which will be estimated and rejected after that.

The perturbation rejection is done according to the ADRC as follows:

$$u(t) = \frac{1}{b}(-f_0(t) + u_0(t)) \tag{5.2}$$

Where,

$f_0(t)$ is estimate of the total disturbance f(t),

$u_0(t)$ is the new control input that will be used to reach the objective.

Substituting equation (5.1) in equation (2), we obtain:

$$y^{(n)}(t) = b[\frac{1}{b}\left(-f_0(t) + u_0(t)\right)] + f(t) \tag{5.3}$$

If f(t) is well estimated by$f_0(t)$, we will have$f_0(t) = f(t)$, then, equation (5.3) can be simplified to:

$$y^{(n)}(t) = u_0(t) \tag{5.4}$$

It can be concluded that if the total disturbance is well estimated, the ADRC control does not require knowledge of any system parameters (without model) to follow the reference value.

This estimation of the total disturbance f(t)is provided by the extended state observer (ESO).

The equation (5.5) summarizes the mathematical model of a linear system in state representation

$$\begin{cases} \dot{x}(t) = A\,x(t) + Bu(t) + Eq(t) \\ y(t) = Cx(t) + Du(t) \end{cases} \tag{5.5}$$

Where: x(t) is the state vector with the matrix A which characterizes the internal dynamics of states, u(t) is the control inputs vector with the matrix B which characterizes the way in which the control inputs modify the states of the system, q(t) is the disturbance vector with the matrix E characterizes.

The way in which measurable disturbances act on the system states; where y(t) is the output vector. Matrix C characterizes the evolution of outputs as a function of the states of the system; it is called the output matrix.

The matrix D characterizes the direct influence of the control quantities on the system outputs; it is a direct connection matrix. When the system is causal the matrix D is null. The

function $h(t)$ is set at an unknown function which represents the derivative of the function $f(t)$. This function exists because $f(t)$depends on the unmodeled dynamics of the system, so it accepts a dynamic that is necessarily differentiable.

Moreover, the function $h(t)$ is introduced just for the needs of state representation; it will not be used in the further development.

The equation (5.5) becomes:

$$\begin{cases} \dot{x}(t) = A\,x(t) + Bu(t) + Eh(t) \\ y(t) = Cx(t) \end{cases} \qquad (5.6)$$

Where, $A = \begin{bmatrix} 0 & 1 & 0 & 0 & \dots & 0 \\ 0 & 0 & 1 & 0 & \dots & 0 \\ \vdots & \vdots & \vdots & \ddots & \dots & \vdots \\ 0 & 0 & 0 & 0 & \dots & 1 \\ 0 & 0 & 0 & 0 & \dots & 0 \end{bmatrix}$, $B = [0 \quad 0 \quad \dots \quad b \quad 0]^T$,

$C = [1 \quad 0 \quad \dots \quad 0 \quad 0]$,

$E = [0 \quad 0 \quad \dots \quad 0 \quad 1]^T$.

It can be concluded that only the term b added by the designer takes place in the control structure [127]. The disturbance rejection control is based on the idea of formulating a robust control strategy. It aims to compensate for dynamics and disturbances in real time. This approach accurately and quickly estimates disturbances using an extended and compensated non-linear state observer (ESO) during each sampling period to meet the performance requirements of these systems and improve their efficiency [12].

5.4.2. Extended State Observer

Knowing that the inputs to ESO are the system output y and the control signal u, and the output of ESO provides the important information about F. Now we move to the structuring of the observer.

We have chosen one of the most famous observers in the state feedback controls is the Luenberger observer. It allows reconstructing the state of the system under observation when all or part of the state vector cannot be measured. It can also estimate the variable or unknown parameters of a system.

A full order Luenberger state-observer can be designed as follows:

$$\begin{cases} \hat{\dot{x}}(t) = A\,\hat{x}(t) + Bu(t) + L(y(t) - \hat{y}(t)) \\ \hat{y}(t) = C\hat{x}(t) \end{cases} \qquad (5.7)$$

$\hat{\dot{x}}(t)$ and $\hat{y}(t)$ respectively the dynamics and the output of ESO, L Correction gain matrix or the observer.

It must emphasize on the term $L(y(t) - \hat{y}(t))$ which defines the error between the real system and that given by the observer. It can be noted that the good choice of the matrix L makes it possible to modify the dynamics of the observer which helps us to cancel the error and to converge estimating system to the real one.

5.4.3. Sizing of the observer gain L

A well-dimensioned estimator gives a zero error between real system and observable, these results in:

$$(y(t) - \hat{y}(t) = 0 \equiv C\big(x(t) - \hat{x}(t)\big) = 0 \quad (5.8)$$

The error $\varepsilon(t)$ is the difference between the internal states of the system and the estimated ones,

$$\varepsilon(t) = x(t) - \hat{x}(t) \quad (5.9)$$

The derivation of this error gives the difference between the two dynamics describing the two systems:

$$\dot{\varepsilon}(t) = \dot{x}(t) - \dot{\hat{x}}(t) \quad (5.10)$$

The substitution of equations (4.6) and (4.7) in (4.10), gives:

$$\dot{\varepsilon}(t) = A\big(x(t) - \hat{x}(t)\big) - L(y(t) - \hat{y}(t)) \quad (5.11)$$

Using equations (5.8) and (5.9) in (5.11), we obtain:

$$\dot{\varepsilon}(t) = (A - LC)\varepsilon(t) \quad (5.12)$$

Hence, the error is given by the following expression:

$$\varepsilon(t) = e^{(A-LC)t}\varepsilon(0) \quad (5.13)$$

In order the estimation error tends towards 0 when t increases, it is necessary to choose L so that the Eigen values of the matrix $(A - LC)$ have strictly negative real parts.

$$VP(A - LC) = (p + \omega_0)^{n+1} \quad (5.14)$$

Where, ω_0 is the observer's bandwidth.

And,

$$H(s) = \frac{K_r}{1+sT_r} \quad (5.15)$$

Determination of the matrix L helps to find out the observer poles.

All elements of the matrix L depend on a single parameterω_0. Therefore, the adjustment of the observer is conditioned by the choice of its own pulsation $\omega_0$with$(\omega_0 > 0)$.

The combination of this observer with the control law leads to this final structure of the ADRC control [154].

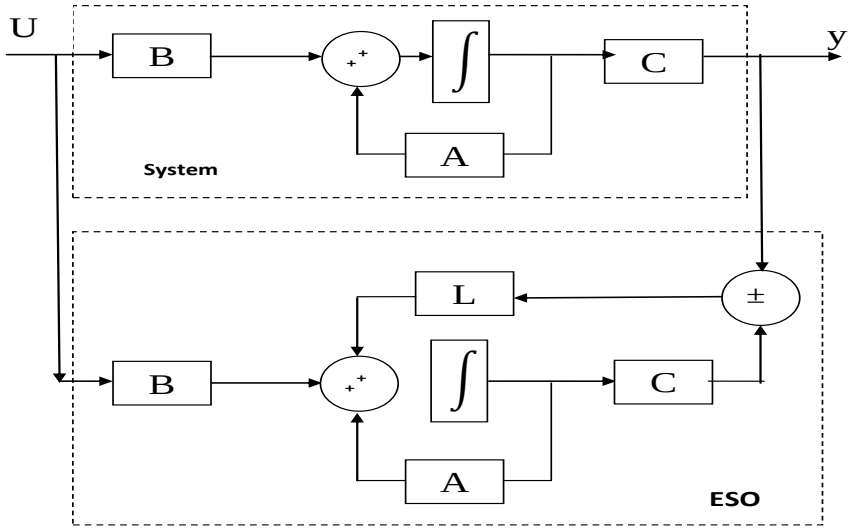

Figure 5.2ADRC control structure

5.5. Illustration of the LADRC command on a nonlinear system

Referring [130, 155], the aim of this section is to present the linear example of ADRC in a stand-alone manner.

Due to the important practice, the first-order case will be treated first and explicitly, even though the fact that there are numerous systems - although technically they are all first-order. Non linear and higher-order, in which, at least at some operating points, exhibit first-order-like dominant behavior.

The justification for the second-order order will be established later (case of our systems).

5.5.1. First-Order ADRC

Consider a simple first-order process, P(s), with a DC gain, K, and a time constant, T:

$$p(s) = \frac{y(s)}{u(s)} = \frac{K}{Ts+1} \rightarrow T.\dot{y}(t) + y(t) = Ku(t) \qquad (5.16)$$

We add an input disturbance, d(t), to the process, abbreviate b = K/ T and rearrange:

$$\dot{y}(t) = -\frac{1}{T}.y(t) + \frac{1}{T}d(t) + \frac{K}{T}.u(t) = -\frac{1}{T}.y(t) + \frac{1}{T}d(t) + b.u(t) \qquad (5.17)$$

As our last modelling step, we substitute$b = b_0 + \Delta b$, where b0 shall represent the known part of $b = \frac{K}{T}$ and Δb, an (unknown) modeling error, and, finally, obtain Equation (4.18). We will see soon that all that we need to know about our first-order process to design an ADRC is $b0 \approx b$, i.e., an approximate value of $\frac{K}{T}$. Modeling errors or varying process parameters are represented by Δb and will be handled internally.

$$\dot{y}(t) = \underbrace{\left(-\frac{1}{T}\,.\,y(t) + \frac{1}{T}\,d(t) + b.\,u(t)\right)}_{\text{Generalized disturbance f(t)}} + b_0 u(t) = f(t) + b_0 u(t) \qquad (5.18)$$

By combining$-\frac{1}{T}\,.\,y(t)$, the disturbance d(t), and the unknown part $\Delta b \cdot u(t)$ to a so-called generalized disturbance, f (t), the model for our process changed from a first-order low-pass type to an integrator. The fundamental idea of ADRC is to implement an extended state observer (ESO) that provides an estimate, $\hat{f}(t)$, such that we can compensate the impact of f(t) on our process (model) by means of disturbance rejection. All that remains to be handled by the actual controller will then be a process with approximately integrating behavior, which can easily be done, e.g. by means of a simple proportional controller. In order to derive the estimator, a state space description of the disturbed process in Equation (5.18) is necessary:

$$\begin{pmatrix}\dot{x}_1(t)\\ \dot{x}_2(t)\end{pmatrix} = \underbrace{\begin{pmatrix}0 & 1\\ 0 & 0\end{pmatrix}}_{A}.\begin{pmatrix}x_1(t)\\ x_2(t)\end{pmatrix} + \underbrace{\begin{pmatrix}b_0\\ 0\end{pmatrix}}_{B} u(t) + \begin{pmatrix}0\\ 1\end{pmatrix}\dot{f}(t) \qquad (5.19)$$

$$y(t) = \underbrace{(1 \quad 0)}_{C}\begin{pmatrix}x_1(t)\\ x_2(t)\end{pmatrix}$$

Since the "virtual" input, $\dot{f}(t)$, cannot be measured, a state observer for this kind of process can, of course, only be built using the input, u(t), and output, y(t), of the process. An estimated state,$\dot{x_2}(t)$, however, will provide an approximate value of f (t), i.e., $\hat{f}(t)$, if the actual generalized disturbance, f(t), can be considered piecewise constant. The equations for the extended state observer (integrator process extended by a generalized disturbance) are given in Equation (5.20). Note that for linear ADRC, a Luenberger observer is being used, while in the original case of ADRC, a nonlinear observer was employed [122].

$$\begin{pmatrix}\dot{\hat{x}}_1(t)\\ \dot{\hat{x}}_2(t)\end{pmatrix} = \begin{pmatrix}0 & 1\\ 0 & 0\end{pmatrix}.\begin{pmatrix}\hat{x}_1(t)\\ \hat{x}_2(t)\end{pmatrix} + \begin{pmatrix}b_0\\ 0\end{pmatrix} u(t) + \begin{pmatrix}l_1\\ l_2\end{pmatrix}.(y(t) - \hat{x}_1(t))$$

$$= \underbrace{\begin{pmatrix}-l_1 & 1\\ -l_2 & 0\end{pmatrix}}_{A\text{-}LC}.\begin{pmatrix}\hat{x}_1(t)\\ \hat{x}_2(t)\end{pmatrix} + \underbrace{\begin{pmatrix}b_0\\ 0\end{pmatrix}}_{B} u(t) + \underbrace{\begin{pmatrix}l_1\\ l_2\end{pmatrix}}_{L}.y(t) \qquad (5.20)$$

One can now use the estimated variables, $\widehat{x_1}(t) = \hat{y}(t)$ and $\widehat{x_2}(t) = \hat{f}(t)$, to implement the disturbance rejection and the actual controller.

$$u(t) = \frac{u_0(t) - \hat{f}(t)}{b_0} \tag{5.21}$$

with $u_0(t) = K_p.(r(t) - \hat{y}(t)$

According the structure of the control loop, it is presented in Figure 5.3. Since KP acts on $\hat{y}(t)$, rather than the actual output y(t), we can have a estimation-based state feedback controller, but the resemblance to a classical proportional controller is striking to practitioners. In equation (5.21), $u_0(t)$represents the output of a linear proportional Controller.

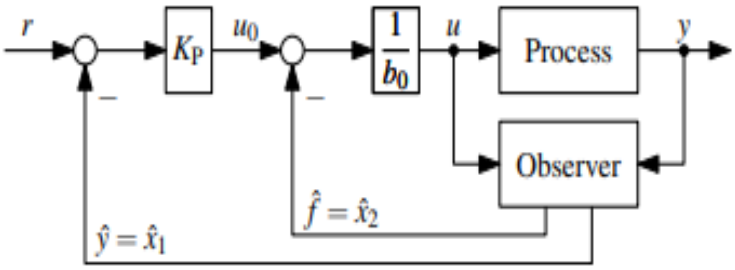

Figure 5.3 Control loop structure with ADRC for a first-order process.

The remainder of the control law in u(t) is chosen such that the linear controller acts on a normalized integrator process if $\hat{f}(t) \approx f(t)$ holds. The effect can be seen by putting Equation (5.21) in Equation (5.18):

$$\dot{y}(t) = f(t) + b_0.\frac{u_0(t) - \hat{f}(t)}{b_0} = \left(f(t) - \hat{f}(t)\right) + u_0(t) \approx u_0(t) = K_p.(r(t) - \hat{y}(t))$$

If $\hat{y}(t) \approx y(t)$ holds, we obtain a first-order closed loop behavior with a pole, $s^{CL} = -K_p$:

$$\frac{1}{K_p}\dot{y}(t) + \hat{y}(t) \approx \frac{1}{K_p}\dot{y}(t) + y(t) \approx r(t)$$

If the state estimator and disturbance rejection work properly, one has to design a proportional controller only one single time to obtain the same closed loop behavior, regardless of the parameters of the actual process. For example, one can calculate K_p from a desired first-order system with 2%-settling time:

$$K_p \approx \frac{4}{T_{settle}} \tag{5.22}$$

In order to work properly, observer parameters,l_1 and l_2, in Equation (5.4) still have to be determined. Since the observer dynamics must be fast enough, the observer poles, $s_{1/2}^{ESO}$,

must be placed left of the closed loop pole,s^{CL}. A simple rule of thumb suggests for both poles:

$$s_{1/2}^{ESO} = s^{ESO} \approx (3 \dots 10).\, s^{CL} \text{with} s^{CL} = -K_p \approx -\frac{4}{T_{settle}} \tag{5.23}$$

Placing all observer poles at one location is also known as "bandwidth parameterization" [130]. Since the matrix (A − LC) determines the error dynamics of the observer, we can compute the necessary observer gains for the common pole location,s^{ESO}, from its characteristic polynomial:

$$\det\big(sI - (A - LC)\big) = s^2 + l_1.s + l_2 = (s - s^{ESO})^2 = s^2 - 2s^{ESO}.\, s(s^{ESO})^2 \tag{5.24}$$

From equation (5.24), the solutions forl_1 and l_2 can immediately be read off:

$$l_1 = -2s^{ESO} \text{ and } l_2 = (s^{ESO})^2 \tag{5.25}$$

To summarize, in order to implement a linear ADRC for a first-order system, four steps are necessary:

1. Modeling: For a process with (dominating) first-order behavior, $p(s) = \frac{K}{Ts+1}$, all that needs to be known is an estimate $b_0 \approx \frac{K}{T}$.

2. Control structure: Implement a proportional controller with disturbance rejection and an extended state observer, as given in equations (5.20) and (5.21):

$$\begin{pmatrix} \dot{\hat{x}_1}(t) \\ \dot{\hat{x}_2}(t) \end{pmatrix} = \begin{pmatrix} -l_1 & 1 \\ -l_2 & 0 \end{pmatrix}.\begin{pmatrix} \hat{x_1}(t) \\ \hat{x_2}(t) \end{pmatrix} + \begin{pmatrix} b_0 \\ 0 \end{pmatrix} u(t) + \begin{pmatrix} l_1 \\ l_2 \end{pmatrix}.y(t)$$

$$u(t) = \frac{K_p.\big(r(t) - \hat{y}(t)\big) - \hat{f}(t)}{b_0} = \frac{K_p.\big(r(t) - \hat{x_1}(t)\big) - \hat{x_2}(t)}{b_0}$$

3. Closed loop dynamics: Choose K_p, e.g. according to a desired settling time equation (5.22):

$$K_p \approx \frac{4}{T_{settle}}$$

4. Observer dynamics: Place the observer poles left of the closed loop pole via equations (5.23) and (5.25):

$l_1 = -2\ s^{ESO}$, $l_2 = (s^{ESO})^2$ with $s^{ESO} \approx (3 \dots 10).\, s^{CL}$and $s^{CL} = -K_p$

It should be noted that the same control structure can be applied to a first-order integrating process:

$$p(s) = \frac{y(s)}{u(s)} = \frac{K_I}{s} \rightarrow y(t) = K_I u(t) \tag{5.26}$$

With an input disturbance, $d(t)$, and a substitution, $K_I = b = b_0 + \Delta b$, with Δb representing the unknown part of K_I , we can model the process in an identical manner as equation (5.18), with all differences hidden in the generalized disturbance, $f(t)$:

$$\dot{y}(t) = \underbrace{\left(-\frac{1}{T}.y(t) + \frac{1}{T}\,d(t) + b.u(t)\right)}_{\text{Generalized disturbance } f(t)} + b_0 u(t) = f(t) + b_0 u(t) \qquad (5.27)$$

Therefore, the design of the ADRC for a first-order integrating process can follow the same four design steps given previously, with the only distinction that b_0 must be set to $b_0 \approx K_I$ in step 1.

5.5.2. Second-Order ADRC

Following the previous section, we now consider a second-order process, $p(s)$, with a DC gain, K, damping factor, D, and a time constant, T.

$$p(s) = \frac{y(s)}{u(s)} = \frac{K}{T^2 s^2 + 2DTs + 1} \rightarrow T^2 \ddot{y}(t) + 2DT\dot{y}(t) = Ku(t) \qquad (5.28)$$

As for the first-order case, we add an input disturbance, $d(t)$, abbreviate $b = \frac{K}{T^2}$ and split b into a known and unknown part, $b = b_0 + \Delta b$:

$$\ddot{y}(t) = \underbrace{\left(-\frac{2D}{T}.\dot{y}(t) - \frac{1}{T^2}d(t) + \Delta b.u(t)\right)}_{\text{Generalized disturbance } f(t)} + b_0.u(t) \qquad (5.29)$$

With everything else combined into the generalized disturbance $f(t)$, all that remains of the process model is a double integrator. The state space representation of the disturbed double integrator is:

$$\begin{pmatrix} \dot{x_1}(t) \\ \dot{x_2}(t) \\ \dot{x_3}(t) \end{pmatrix} = \underbrace{\begin{pmatrix} 0 & 1 & 0 \\ 0 & 0 & 1 \\ 0 & 0 & 0 \end{pmatrix}.\begin{pmatrix} x_1(t) \\ x_2(t) \\ x_3(t) \end{pmatrix}}_{A} + \begin{pmatrix} 0 \\ b_0 \\ 0 \end{pmatrix}.u(t) + \underbrace{\begin{pmatrix} 0 \\ 0 \\ 1 \end{pmatrix}}_{B}.\dot{f}(t) \qquad (5.30)$$

$$y(t) = \underbrace{(1 \quad 0 \quad 0)}_{C}.\begin{pmatrix} x_1(t) \\ x_2(t) \\ x_3(t) \end{pmatrix}$$

In order to employ a control law similar to the first-order case, an extended state observer is needed to provide estimation, $\widehat{x_1}(t) = \hat{y}(t)$, $\widehat{x_2}(t) = \dot{y}(t)$ and $\widehat{x_3}(t) = \hat{f}(t)$:

$$\begin{pmatrix}\dot{\widehat{x_1}}(t)\\ \dot{\widehat{x_2}}(t)\\ \dot{\widehat{x_3}}(t)\end{pmatrix}=\begin{pmatrix}0 & 1 & 0\\ 0 & 0 & 1\\ 0 & 0 & 0\end{pmatrix}.\begin{pmatrix}\widehat{x_1}(t)\\ \widehat{x_2}(t)\\ \widehat{x_3}(t)\end{pmatrix}+\begin{pmatrix}0\\ b_0\\ 0\end{pmatrix}.u(t)+\begin{pmatrix}l_1\\ l_2\\ l_3\end{pmatrix}.(y(t)-\widehat{x_1}(t))$$

$$=\underbrace{\begin{pmatrix}-l_1 & 1 & 0\\ -l_2 & 0 & 1\\ -l_3 & 0 & 0\end{pmatrix}}.\begin{pmatrix}\widehat{x_1}(t)\\ \widehat{x_2}(t)\\ \widehat{x_3}(t)\end{pmatrix}+\begin{pmatrix}0\\ b_0\\ 0\end{pmatrix}.u(t)+\begin{pmatrix}l_1\\ l_2\\ l_3\end{pmatrix}.(y(t) \quad (5.31)$$

A-LC

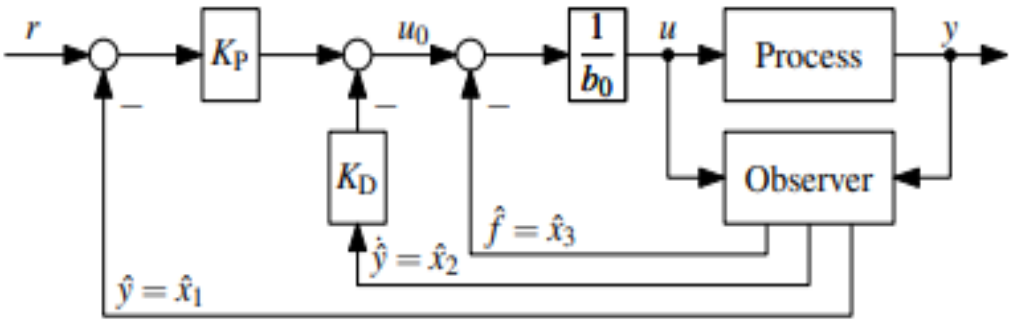

Figure 5.4 Control loop structure with active disturbance rejection control (ADRC) for a second-order process.

Using the estimated variables, one can implement the disturbance rejection and a linear controller for the remaining double integrator behavior, as shown in Figure 5.4 A modified PD controller (without the derivative part for the reference value r(t)) will lead to a second-order closed loop behavior with adjustable dynamics. Again, this actually is an estimation-based state feedback controller.

$$u(t)=\frac{u_0(t)-\hat{f}(t)}{b_0} \text{ with } u_0(t)=K_p.\left(r(t)-\hat{y}(t)\right)-K_D.\dot{\hat{y}}\,(t) \quad (5.32)$$

Provided the estimator delivers good estimates, $\widehat{x_1}(t)=\hat{y}(t)\approx y(t), \widehat{x_2}(t)=\dot{\hat{y}}\,(t)\approx \dot{y}(t)$ and $\widehat{x_3}(t)=\hat{f}(t)\approx f(t)$, one obtains after inserting Equation (5.31) into Equation (5.32):

$$\ddot{y}(t)=\left(f(t)-\hat{f}(t)\right)+u_0(t)\approx u_0(t)\approx K_p.\left(r(t)-y(t)\right)-K_D.\dot{y}\,(t) \quad (5.33)$$

Under ideal conditions, this leads to:

$$\frac{1}{K_p}\ddot{y}(t)+\frac{K_D}{K_p}\dot{y}(t)+y(t)=r(t) \quad (5.34)$$

While any second-order dynamics can be set using K_p and K_D, one practical approach is to tune the closed loop to a critically damped behavior and a desired 2% settling time T_{settle}, i.e., choose K_p and K_D to get a negative-real double pole, $s_{1/2}^{CL} = s^{CL}$:

$$K_p = (s^{CL})^2 \text{ and } K_D = -2.s^{CL} \text{ with } s^{CL} \approx -\frac{6}{T_{settle}} \quad (5.35)$$

Similar to the first order case, the placement of the observer poles can follow a common rule of thumb:

$$s_{1/2/3}^{ESO} = s^{ESO} \approx (3 \dots 10).s^{CL} \text{ with } s^{CL} \approx -\frac{6}{T_{settle}} \quad (5.36)$$

Once the pole locations are chosen in this manner, the observer gains are computed from the characteristic polynomial of (A − LC):

$$\begin{aligned}\det\big(sI - (A - LC)\big) &= s^3 + l_1.s^2 + l_2.s + l_3 = (s - s^{ESO})^3 \\ &= s^3 - 3s^{ESO}.s^2 + 3.(s^{ESO})^2.s - (s^{ESO})^3\end{aligned}$$

The respective solutions for l_1, l_2 and l_3 are:

$$l_1 = -3s^{ESO},\ l_2 = 3.(s^{ESO})^2 \text{ and } l_3 = -(s^{ESO})^3 \quad (5.37)$$

To summarize, ADRC for a second-order system is designed and implemented as follows:

1. Modeling: For a process with (dominating) second-order behavior,$p(s) = \frac{K}{T^2s^2+2DTs+1}$one only needs to know an approximate value$b_0 \approx \frac{K}{T^2}$
2. Control structure: Implement a proportional controller with disturbance rejection and an extended state observer, as given in equations (5.30) and (5.31):

$$\begin{pmatrix}\dot{\widehat{x_1}}(t)\\ \dot{\widehat{x_2}}(t)\\ \dot{\widehat{x_3}}(t)\end{pmatrix} = \begin{pmatrix}-l_1 & 1 & 0\\ -l_2 & 0 & 1\\ -l_3 & 0 & 0\end{pmatrix}.\begin{pmatrix}\widehat{x_1}(t)\\ \widehat{x_2}(t)\\ \widehat{x_3}(t)\end{pmatrix} + \begin{pmatrix}0\\ b_0\\ 0\end{pmatrix}.u(t) + \begin{pmatrix}l_1\\ l_2\\ l_3\end{pmatrix}.(y(t)$$

$$u(t) = \frac{K_p.\big(r(t) - \hat{y}(t)\big) - K_D.\dot{\hat{y}}(t) - \hat{f}(t)}{b_0} = \frac{(K_p.\big(r(t) - \widehat{x_1}(t)\big) - K_D.\widehat{x_2}(t)) - \widehat{x_3}(t)}{b_0}$$

3. Closed loop dynamics: Choose (K_p and K_D, e.g. according to a desired settling time as given in equation (5.32):

$$K_p = (s^{CL})^2 \text{ and } K_D = -2.s^{CL} \text{ with } s^{CL} \approx -\frac{6}{T_{settle}}$$

4. Observer dynamics: Place the observer poles left of the closed loop poles via Equations (5.33) and (5.34):

$l_1 = -3s^{ESO},\ l_2 = 3.(s^{ESO})^2$ and $l_3 = -(s^{ESO})^3$with $s^{ESO} \approx (3 \dots 10).s^{CL}$[156].

5.6LADRC Robustness

Since the nonlinear system is usually much more complex than the linear system, the linearization methods, which are invented based on the exact model information, cannot avoid the computation burden. More seriously, since uncertainties widely exist in practical systems, the model-based control design met great challenges in engineering practice, especially the problem of robustness.

The high level of robustness and the superior transient performance are the most valuable characteristics of ADRC to make it be an appealing solution in dealing with real world control problems. Next, the main results of [144, 157], which can explain these characteristics from the views of the frequency-domain and the time-domain, respectively.

In [158], the capability of LADRC for linear time-invariant SISO minimum-phase systems with unknown but bounded relative degrees, and unknown input disturbances, was analyzed. The result explains why one ADRC with fixed parameters can be applied to a group of plants of different orders, relative degrees, and parameters. In [141, 144], the analysis results in the frequency domain were shown. In [141], the loop gain frequency response was analyzed for a second-order linear time-invariant plant. The result showed that the LADRC based control system possesses a high level of robustness. The bandwidth and stability margins, in particular, are nearly unchanged as the plant parameters vary significantly; so is the sensitivity to the input disturbance. Such characteristics explain why LADRC is an appealing solution in dealing with real world control problems where uncertainties abound. Xue and Huang [144] further investigated the frequency properties of LADRC with the reduced-order LESO for a typical class of n-th order linear time-invariant uncertain system. It was shown that the phase margin and crossover frequency are almost unchanged in the presence of some uncertain parameters. And moreover, different kinds of uncertain parameters have various influences on the robustness of the ADRC based control system, t will be shown that the phase margin and crossover frequency are almost unchanged in the presence of some uncertain parameters. And moreover, different kinds of uncertain parameters have various influences on the robustness of the LADRC based control system [144, 148].

To make the system more robust without changing the setpoint-tracking performance, two options are possible. 1) Increase the time constant λd of the disturbance-rejection filter (i.e., decrease the observer bandwidth ωo). 2) Increase the gain b.

The first option is natural since the robustness of the system is directly related to λd. The larger λd is, the more robust the system will be. The second option may seem strange. Deviating b from its nominal value introduces more model error in the system, which leads more difficulty in controller design. Nevertheless, if the controller design method can provide a controller with more robustness, then it is worth the risk of allowing more uncertainties in the model, as long as the nominal performance does not degrade. Moreover, the ESO of the LADRC can estimate the uncertainty and compensate it quickly, so for LADRC tuning, it is a good practice to increase b to achieve better robustness. That is why sometimes in some

literature, LADRC has three tuning parameters instead of two, partly due to unknown information on b and partly due to robustness requirement [127].

In [127]To increase robustness of the system against uncertainty in the time delay, two sets of parameters are considered:

1) Decrease ωo

2) Increase b

The system becomes unstable for the first set of parameters, while it is still stable for the second. So increasing b may achieve better robustness than decreasing ωc for LADRC.

b is the high-frequency gain of the system. The exact value of b is not necessary for a satisfactory control of LADRC. Its effect can be compensated with choice of ωc and ωo. Choice of b influences the robustness of the closed-loop system. However, detuning of the control loop using parameter b may be a compensation for the poor choice of the closed-loop poles. If more plant information is incorporated, or different poles are chosen in LADRC design, then the parameter b should not be a tuning parameter. Instead, the gain K_o and L_o should be designed for LADRC

5.7 Conclusion

This section focuses on the nature of industrial control problems: obtaining reliable performance in processes full of uncertainties, the solution of which cannot be easily found in a model-based control theory. The essential in such problems is disturbance rejection, and how the disturbance is mitigated, in view of new principles methods, algorithms, and rigorous justifications.

After ADRC has been introduced, which becomes a widely used method. Unlike PID, ADRC not only tracks the disturbance using ESO, but it illuminates the disturbance as well making the system stabilize at the equilibrium point. Additionally, ADRC has been proven to have a high accuracy and efficiency than PID.

LADRC obtains a good performance of robustness against the internal parameter perturbations and the external load variations, and it does not need an exact machine model.

Chapter 6

Designed AVRs Validation

Chapter 6

Designed AVRs Validation

Validation tests of both approachesare investigated using simulation of the designed complete system behavior. With the help of SimPowerSystem library provided by Matlab/Simulink, the previously explained system has been implemented. In the first test, the output voltage is regulated by acting on the excitation voltage for a synchronous machine with salient pole of power 1.5 KVA by adopting a static excitation. For the control purpose, two control methods are used. The first method is a conventional method the PSO to optimize the parameters of the PI regulator; however, the second one is a digital ADRC method. In the second test, same control methods are applied to a self-excited synchronous machine with a power of 187 MVA. The results obtained by the ADRC are compared with the PSO-PI method results. Validation of the designed automatic voltage regulators has been presented in this chapter.

6.1 SG Simulink Model

The simulation of the model obtained in the 3rd chapter is performed using Matlab/Simulink. The system of equations (3.10) and (3.11) can be rewritten as:

$$\begin{cases} V_d = -R_s I_d + (\mathrm{L}_{sl} + \mathrm{L}_{qm})\omega_r I_q - L_{qm}\omega_r I_Q - (\mathrm{L}_{sl} + \mathrm{L}_{dm})\dfrac{dI_d}{dt} + L_{dm}\dfrac{dI_f}{dt} + L_{dm}\dfrac{dI_D}{dt} \\ V_q = -R_s I_q - (\mathrm{L}_{sl} + \mathrm{L}_{dm})\omega_r I_d + L_{dm}\omega_r I_f + L_{dm}\omega_r I_D - (\mathrm{L}_{sl} + \mathrm{L}_{qm})\dfrac{dI_q}{dt} + L_{dm}\dfrac{dI_Q}{dt} \\ V_f = R_f I_f + (\mathrm{L}_{fl} + \mathrm{L}_{dm})\omega_r I_d - L_{dm}\dfrac{dI_d}{dt} + L_{dm}\dfrac{dI_D}{dt} \\ 0 = R_D I_D + (\mathrm{L}_{Dl} + \mathrm{L}_{dm})\dfrac{dI_D}{dt} + L_{dm}\dfrac{dI_f}{dt} - L_{dm}\dfrac{dI_d}{dt} \\ 0 = R_Q I_Q + (\mathrm{L}_{Ql} + \mathrm{L}_{qm})\dfrac{dI_Q}{dt} - L_{qm}\dfrac{dI_q}{dt} \end{cases} \quad (6.1)$$

In matrix form,

$$\begin{bmatrix} V_d \\ V_q \\ V_f \\ 0 \\ 0 \end{bmatrix} = Z \begin{bmatrix} I_d \\ I_q \\ I_f \\ I_D \\ I_Q \end{bmatrix} + L\frac{d}{dt}\begin{bmatrix} I_d \\ I_q \\ I_f \\ I_D \\ I_Q \end{bmatrix} \quad (6.2)$$

With

$$Z = \begin{pmatrix} -R_s & (L_{sl}+L_{qm})\omega_r & 0 & 0 & -L_{qm}\omega_r \\ -(L_{sl}+L_{dm})\omega_r & -R_s & L_{dm}\omega_r & L_{dm}\omega_r & 0 \\ 0 & 0 & R_f & 0 & 0 \\ 0 & 0 & 0 & R_D & 0 \\ 0 & 0 & 0 & 0 & R_Q \end{pmatrix} \quad (6.3)$$

$$L = \begin{pmatrix} -(L_{sl}+L_{dm}) & 0 & L_{dm} & L_{dm} & 0 \\ 0 & -(L_{sl}+L_{qm}) & 0 & 0 & L_{qm} \\ -L_{dm} & 0 & (L_{fl}+L_{dm}) & L_{dm} & 0 \\ -L_{dm} & 0 & L_{dm} & (L_{Dl}+L_{dm}) & 0 \\ 0 & -L_{qm} & 0 & 0 & (L_{Ql}+L_{dm}) \end{pmatrix} \quad (6.4)$$

Then, it is possible to write the system in state-space (SS) representation as follows:

$$\begin{cases} \dfrac{dX}{dt} = AX + BU \\ Y = CX \end{cases} \quad (6.5)$$

Where,

$$A = -L^{-1}Z,\ B = L^{-1},\ U = \left[V_d, V_q, V_f, 0, 0\right]^T \qquad X = \left[I_d, I_q, I_f, I_D, I_Q\right]^T$$

In order to create terminals *A*, *B* and *C* and to generate and measure three-phase voltage, star-connected resistances r_{exc} of 10^4 Ω are used. The implementation scheme of this model in Matlab-Simulink software is shown in Figure 6.1.

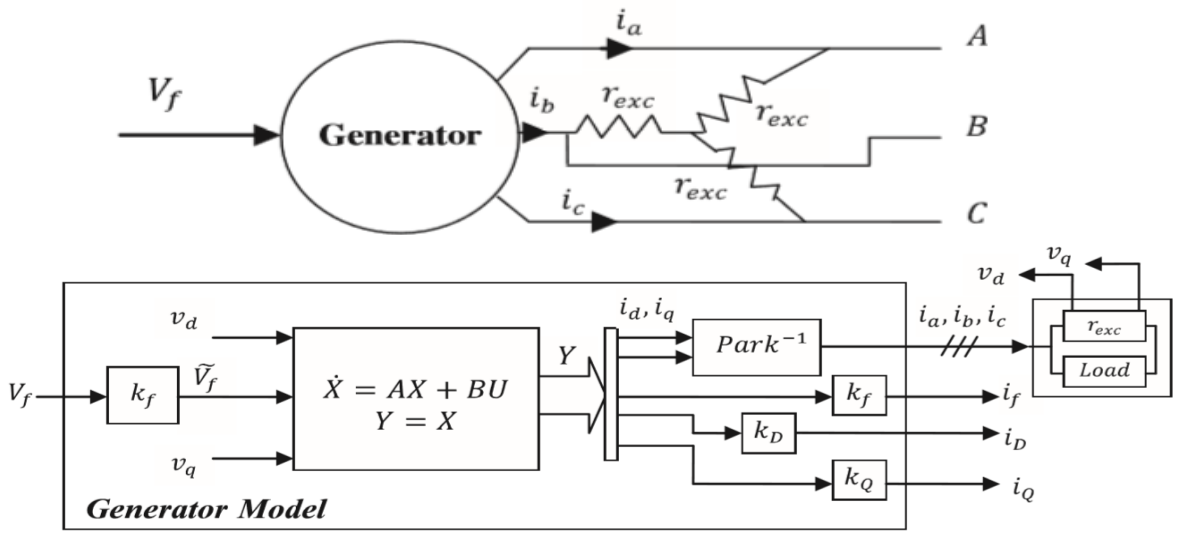

Figure 6.1 SG Simulink representations.

ω_r can be considered as a constant parameter in matrix Z, since speed variation is neglected.

6.2 Validation of the SG-Model

To check the fitness of the model developed, a three-phase short-circuit is applied across the SG, which represents a high load impact on the machine.

The three-phase short-circuit is applied at 55% rated voltage. The field current as well as the armature current obtained by experimental tests and those obtained by simulation are plotted in same graphs (see figures 6.2 – 6.3).

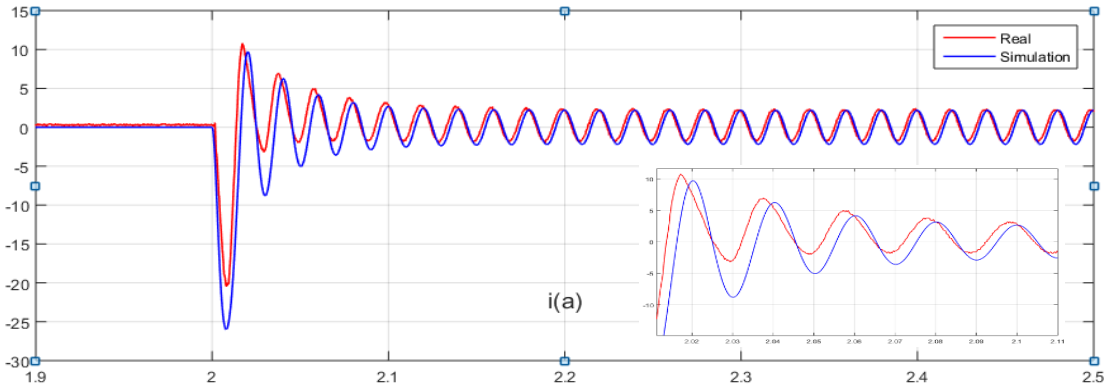

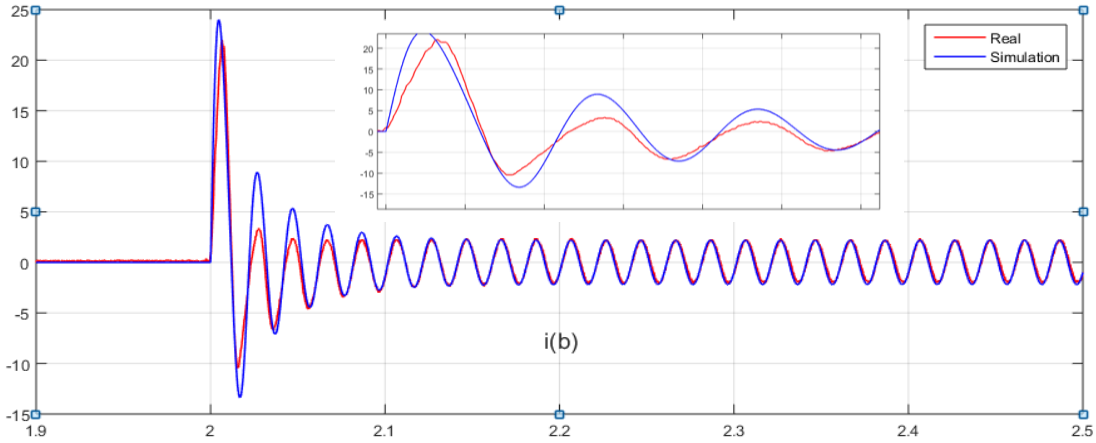

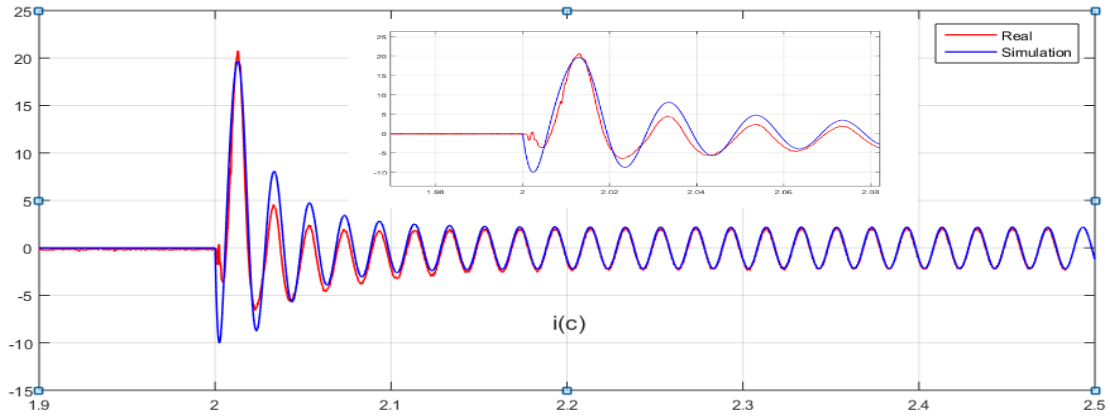

Figure 6.2 Real and simulation armature current of sudden three-phase short-circuit, at 55% rated voltage.

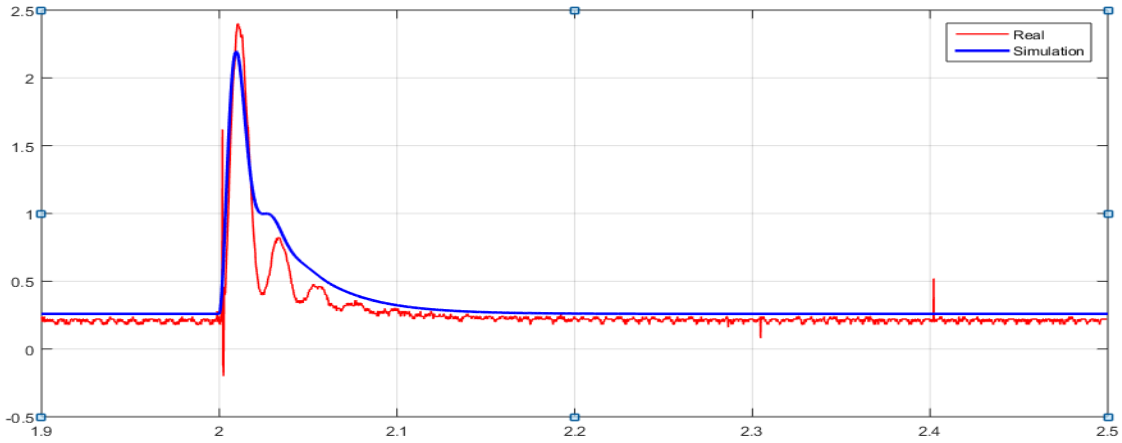

Figure 6.3 Real and simulation armature currentof sudden three-phase short-circuit, at 55% rated voltage.

As shown in figure 6.3, the real and simulation current quantities have approximately the same waveforms. The calculated quantities have very similar shapes to the real ones. The difference is due to the approximation made in the obtained model (the effects of saturation and hysteresis are neglected), and due to measurement errors performing during the identification tests.

6.3 System Closed-Loop Performance

The purpose of this experiment is to maintain constant voltage at the Lab-Volt SG terminals regardless to the variation of loads connected to it. For that reason, the complete system has been implemented in Simulink and is considered to be closest as possible to the real one. The response of the system to loads variation (resistive loads are modelled as pure resistances in series with small valued inductances, whereas, inductive loads are modelled as pure inductances in series to small valued resistances) has been discussed.

SG is first run at no load in its rated conditions. Then, at t=1s, a load is connected to the machine.

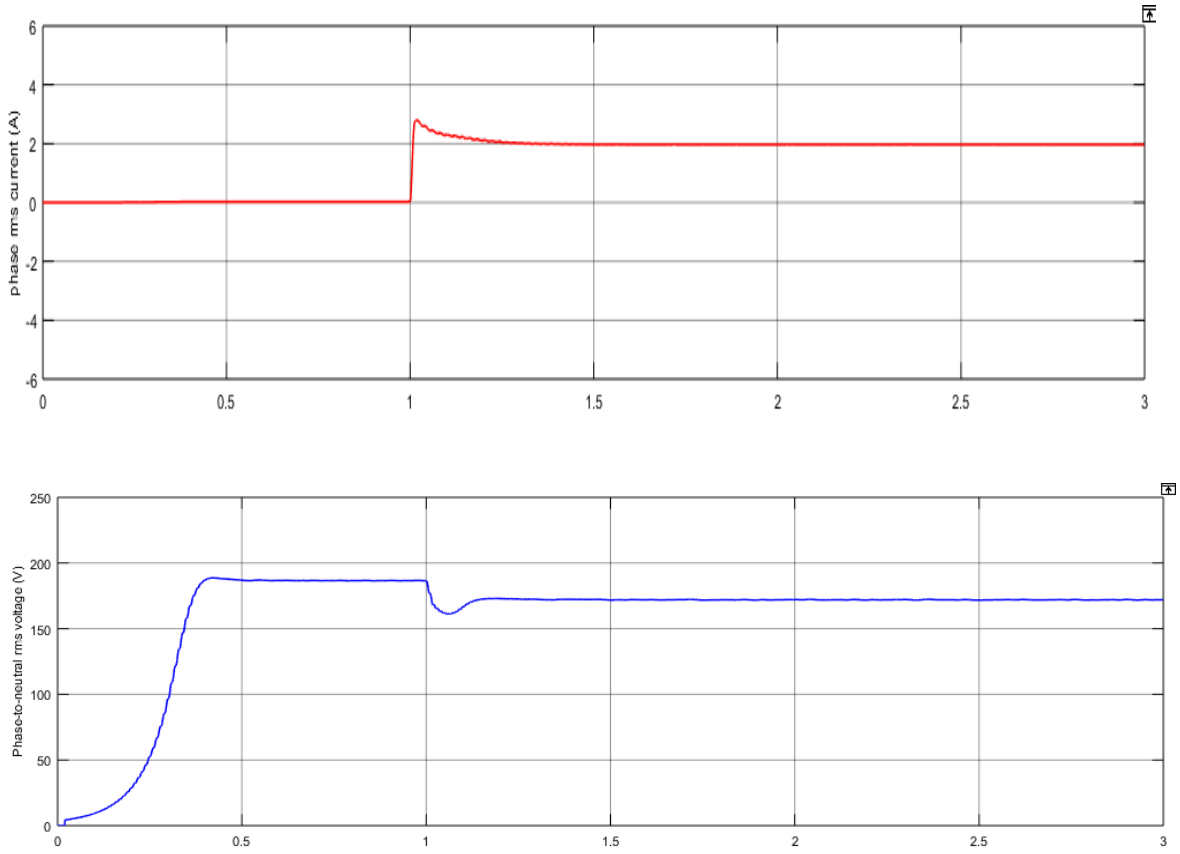

Figure 6.4 Phase-to-neutral rms voltage and rms current.

It can be seen that a steady state error voltage is presented before connecting the load. However, after load connection a decay of voltage is captured, which is due to load current rise (see figure 6.4).

The system with unity control is not able to reach the reference voltage and to reject the effect of connecting loads. In this case, loads are considered disturbance to the system. For better performance in closed-loop system, PI-controller may be introduced.

6.3.1 PSO tuning results of the first generator tested for different types and loads values

Setting the PI-parameters obtained previously in chapter 3 (see Table 3.1). The AVR based PI-controller functionality is tested for different valued loads connecting at different times of operation. The machine is set to work at its rated values, at t=1s a load is suddenly connected. Table 5.1 summarizes the different types and values of loads to be connected to the SG terminals.

Table 6.1 Used loads during disturbance tests.

	P (Watt)	*Q (VAR)*	*pf*
1st case	270	130.7	0.9
2nd case	675	326.92	0.9
3rd case	90	286.19	0.3
4th case	270 then +90	130.7 then +286.19	0.3

In order to better see the response of the system, the phase-to-neutral RMS voltage is presented. Before introducing disturbance to the system (load connection), the SG is set to operate at rated conditions, the phase-to-neutral RMS voltage is set at 220 volts.

At t=1s, a 270Watts and 130.7 VARs load is suddenly connected (1st case). As shown in figure 6.7, a drop in voltage followed by a rise in current is observed. The AVR senses this drop causing corrective actions to take place giving rise to field voltage, hence, field current in figure 6.8. It is also remarkable that the load has small influence on the SG terminal voltage and that the performance of the PI-controller before and after applying disturbance is considered valid.

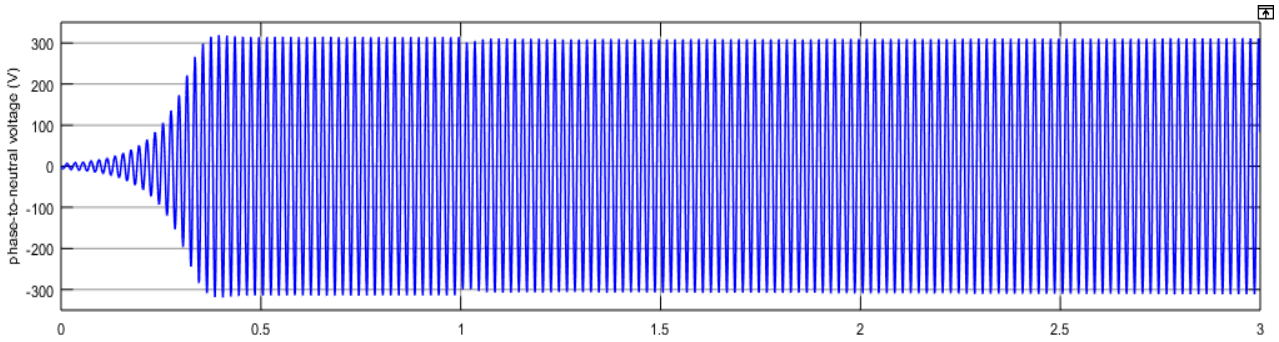

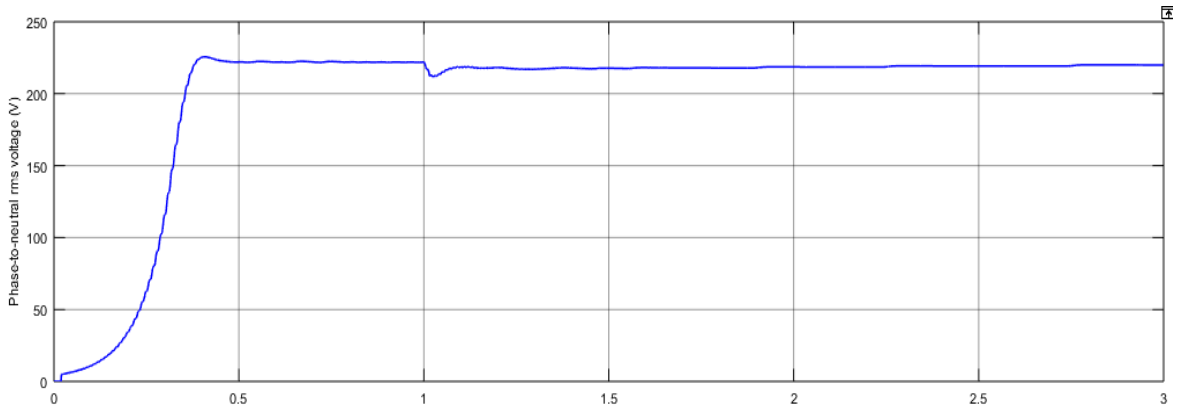

Figure 6.5 Phase-to-neutral and phase-to-neutral rms output voltage. 1st case.

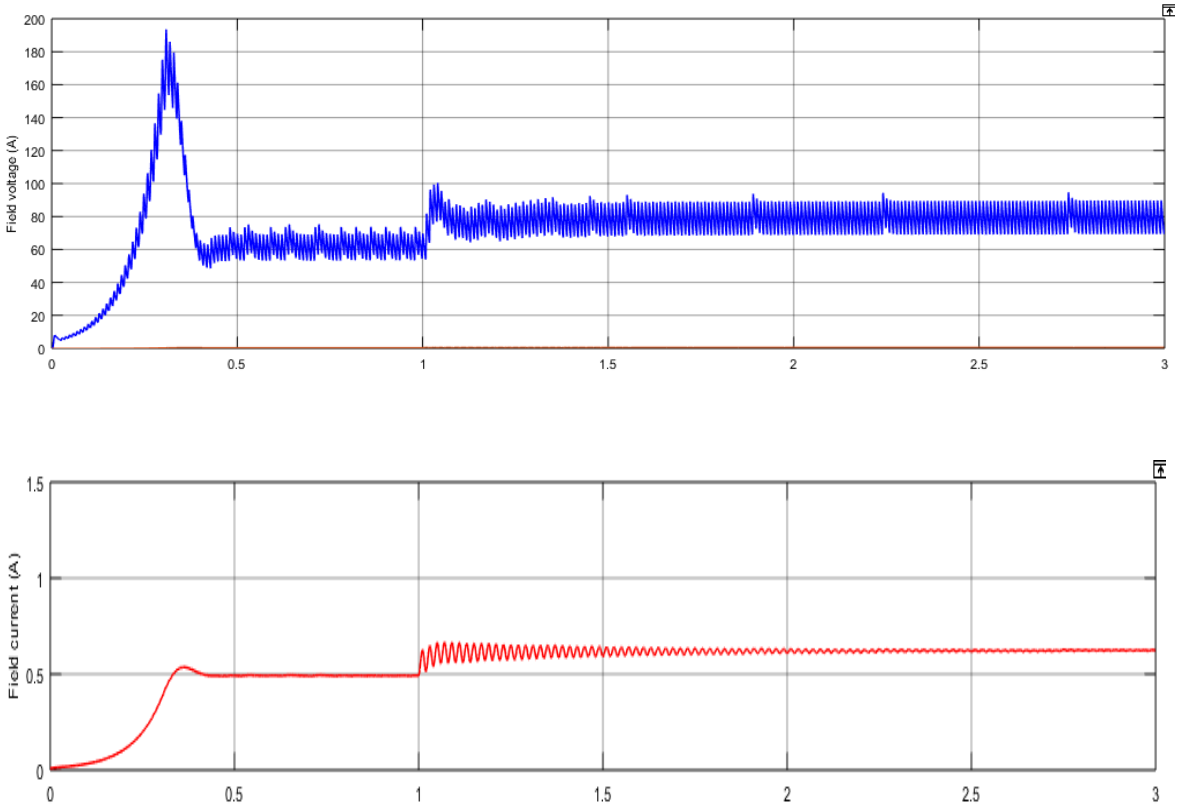

Figure 6.6 Field voltage and field current. 1st case.

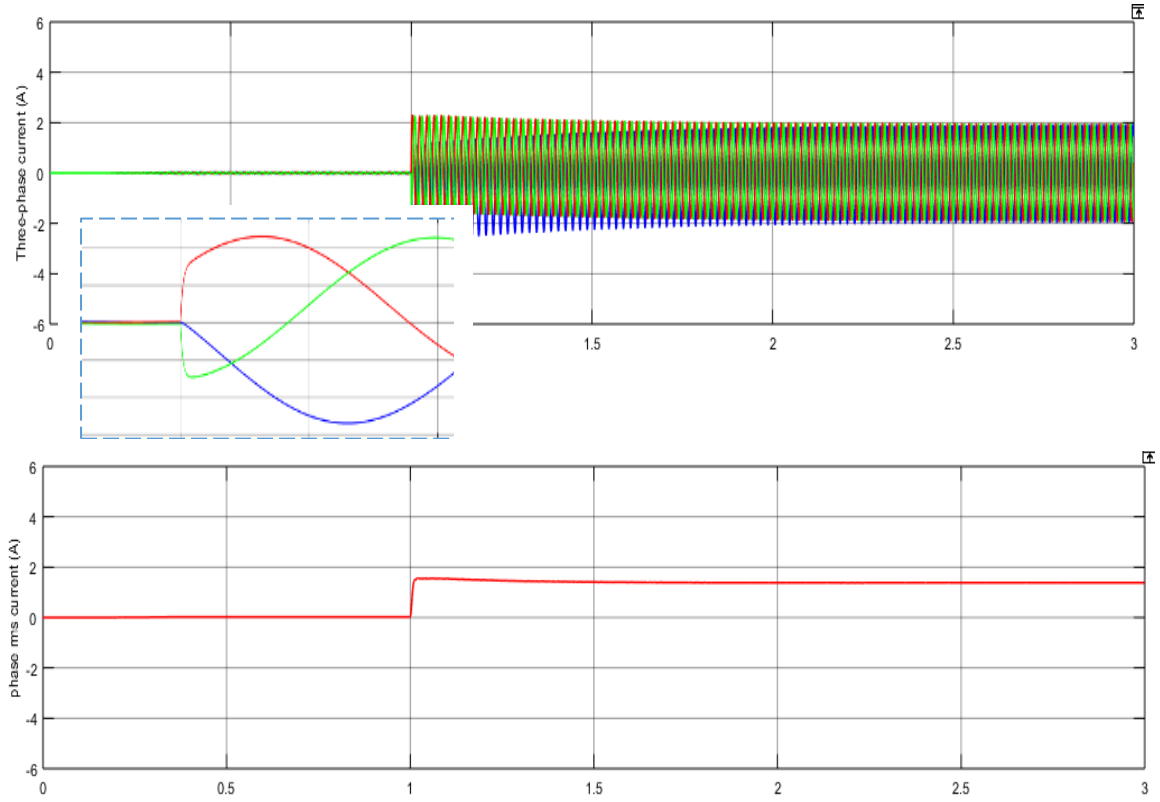

Figure 6.7 Three-phase current and single-phase rms current 1st case.

The 2ndcase disturbance is done by connecting a higher valued load to the SG terminals. A load consumes half of the nominal apparent power with a 0.9 power factor (675Watts and 326.92 VARs). The influence of this 2nd case is greater comparing to the 1st one. The field current rises considerably to compensate the drop in voltage (see figure 6.9 b). Also, the system takes longer time to reach stability again.

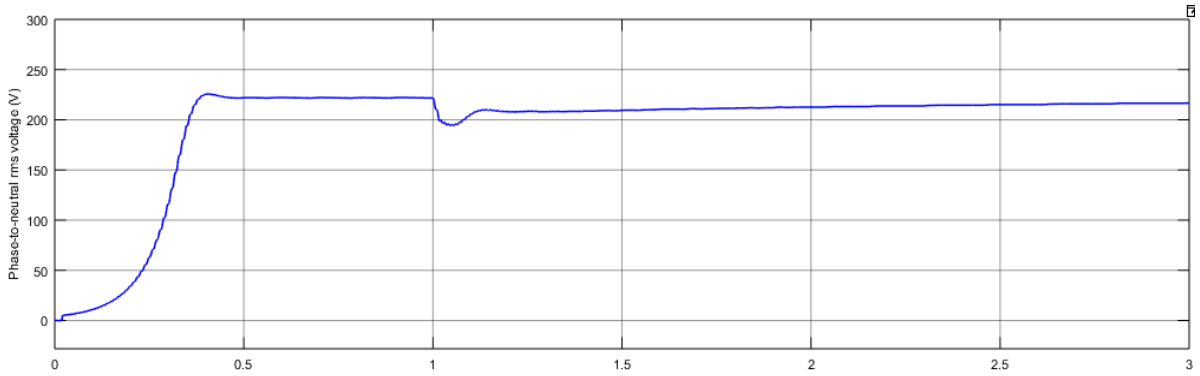

Figure 6.8 Phase-to-neutral rms output voltage 2nd case.

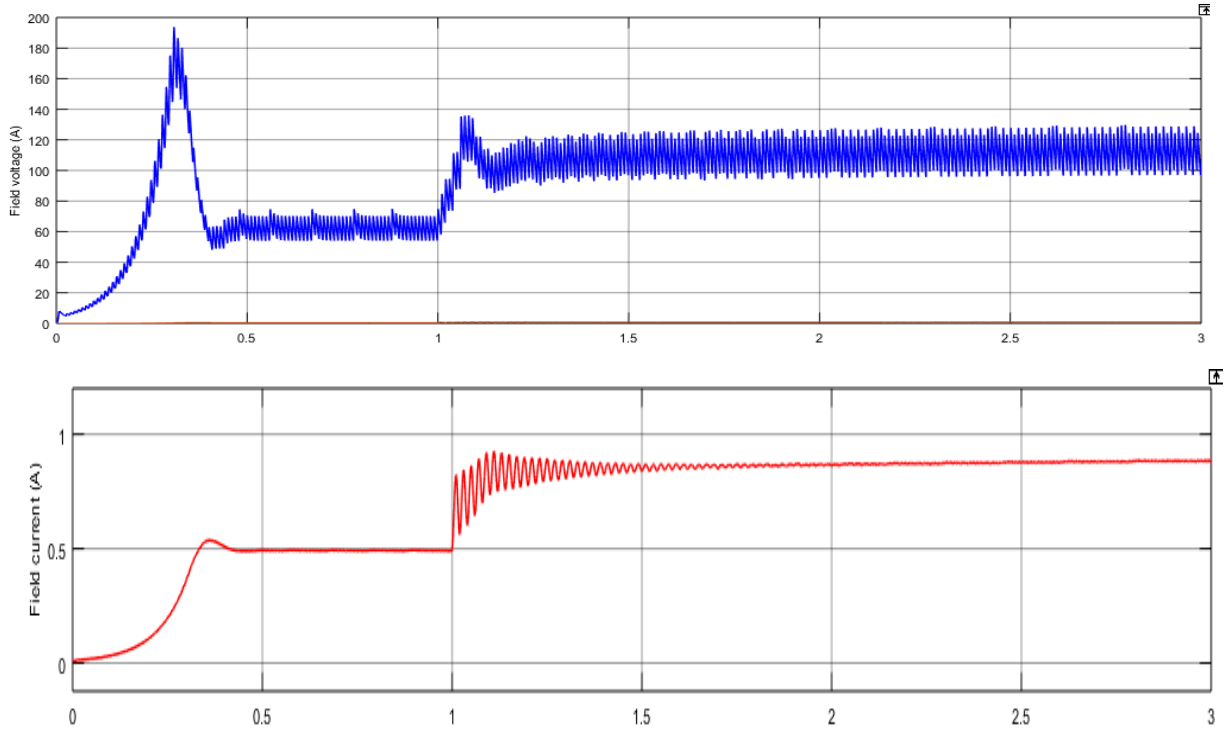

Figure 6.9 Field voltage and field current 2nd case.

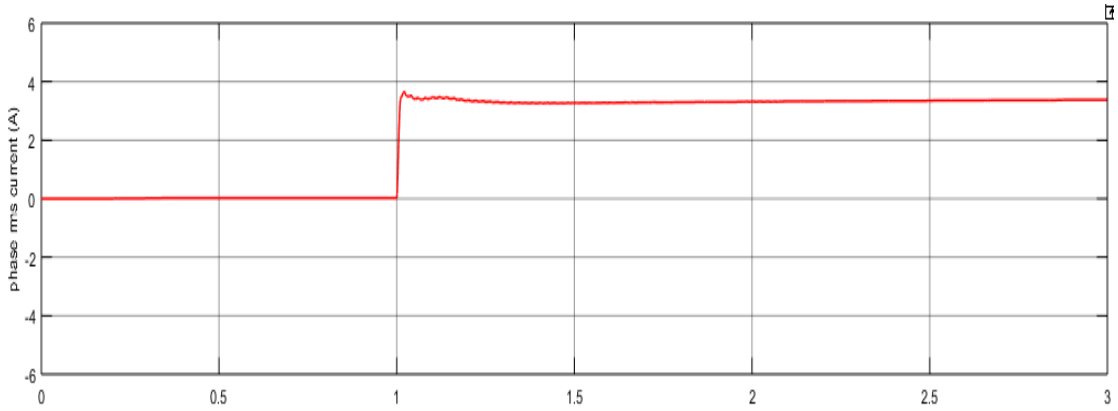

Figure 6.10 single-phase rms current 2nd case.

In the other hand, the 3rd case disturbance deals with a 0.3 power factor load. Even though the load is of another type (reactive), the AVR does not have any effect on the system.

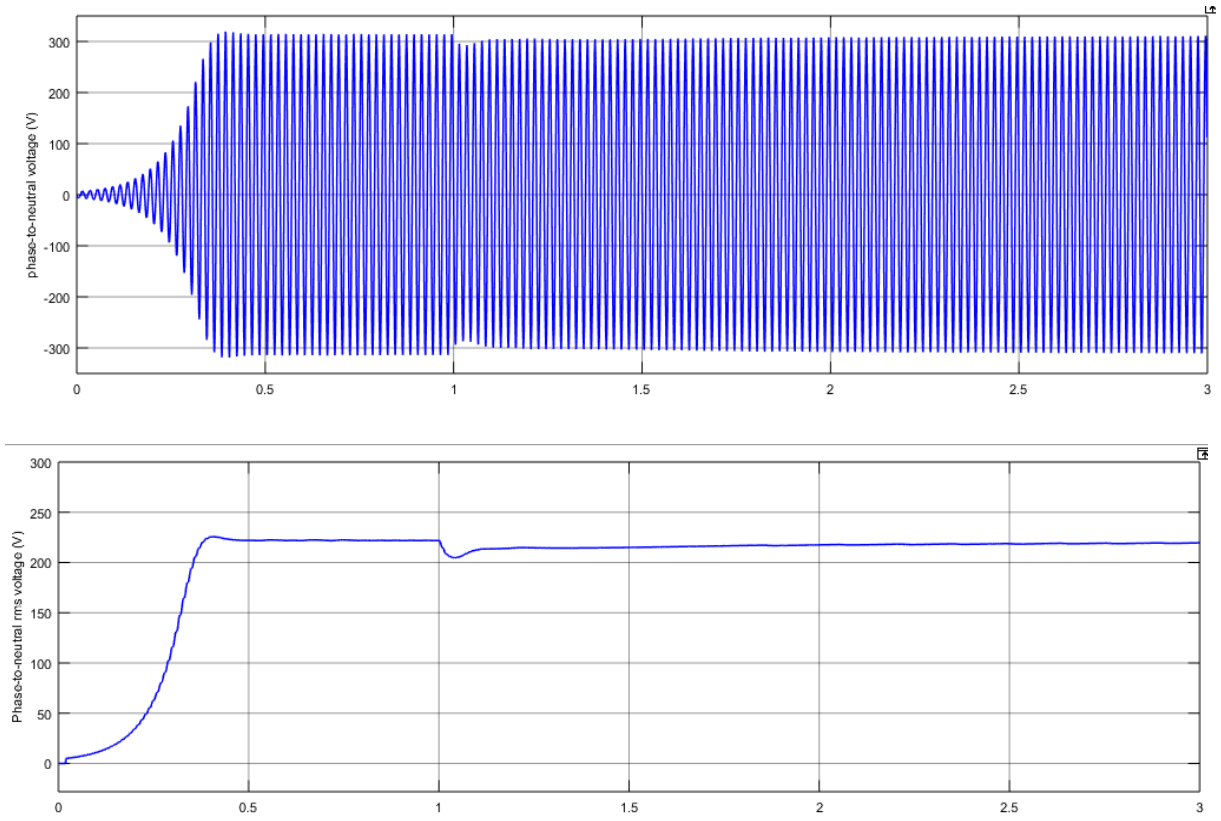

Figure 6.11 Phase-to-neutral and phase-to-neutral rms output voltage3rd case

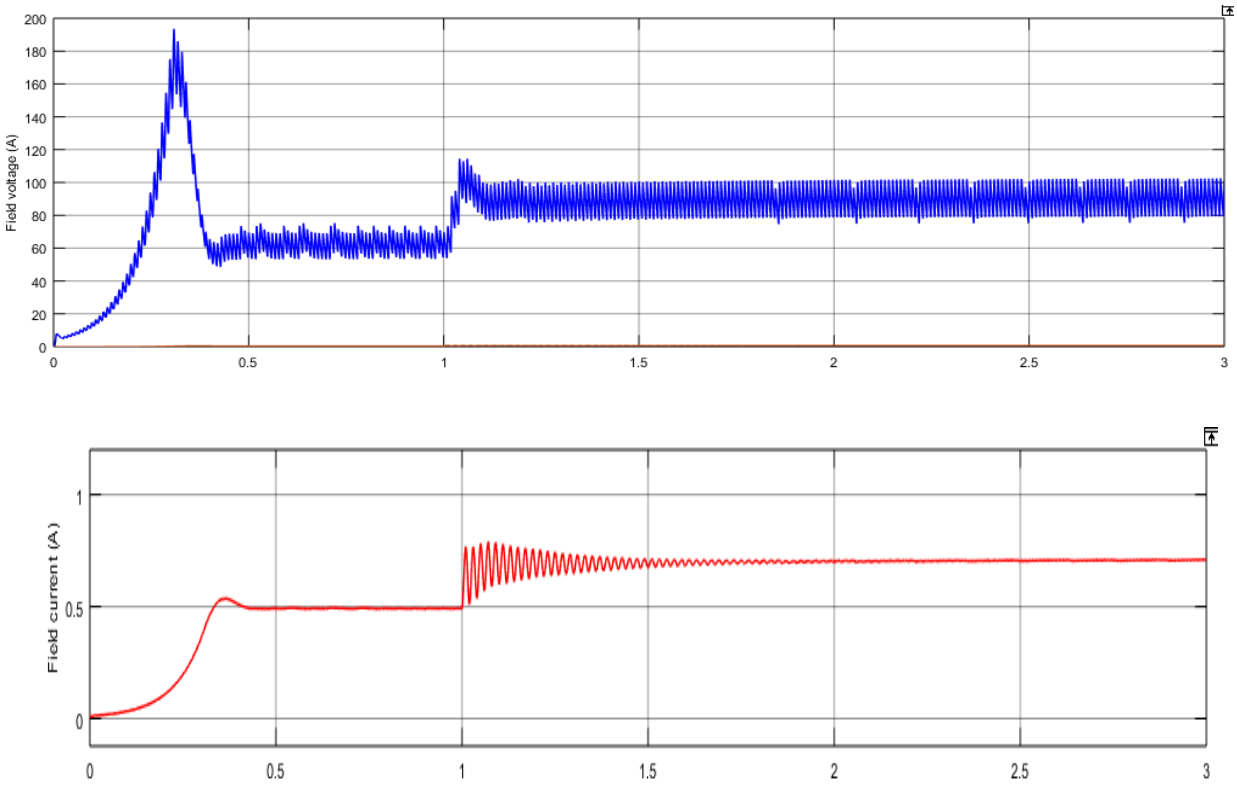

Figure 6.12 Field voltage and field current 3rd case.

When several loads are connected at different times of operation, the response of the system is illustrated in Figure 6.13. It can be noticed that the AVR corrects the connecting first load effect as shown in Figure 6.15 where the field current first rises. Not so long, a second load is connected which influences on the SG. The AVR takes corrective actions again, it increases field current again.

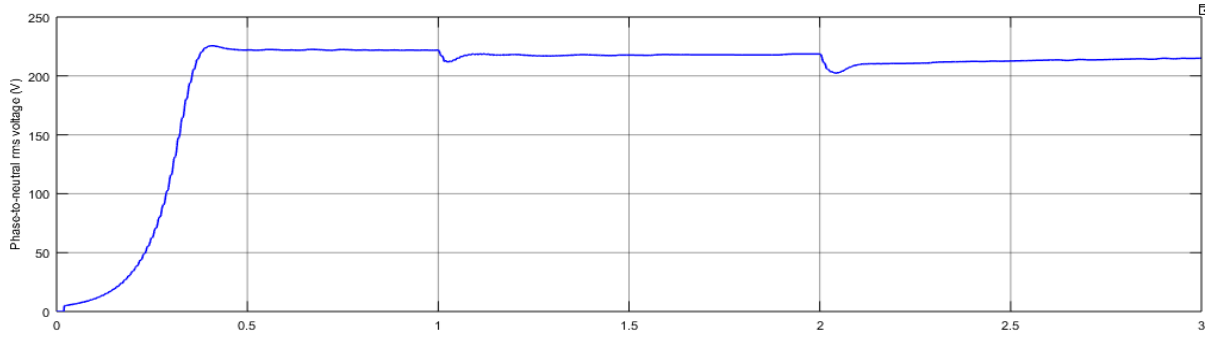

Figure 6.13 Phase-to-neutral rms output voltage. 4thcase

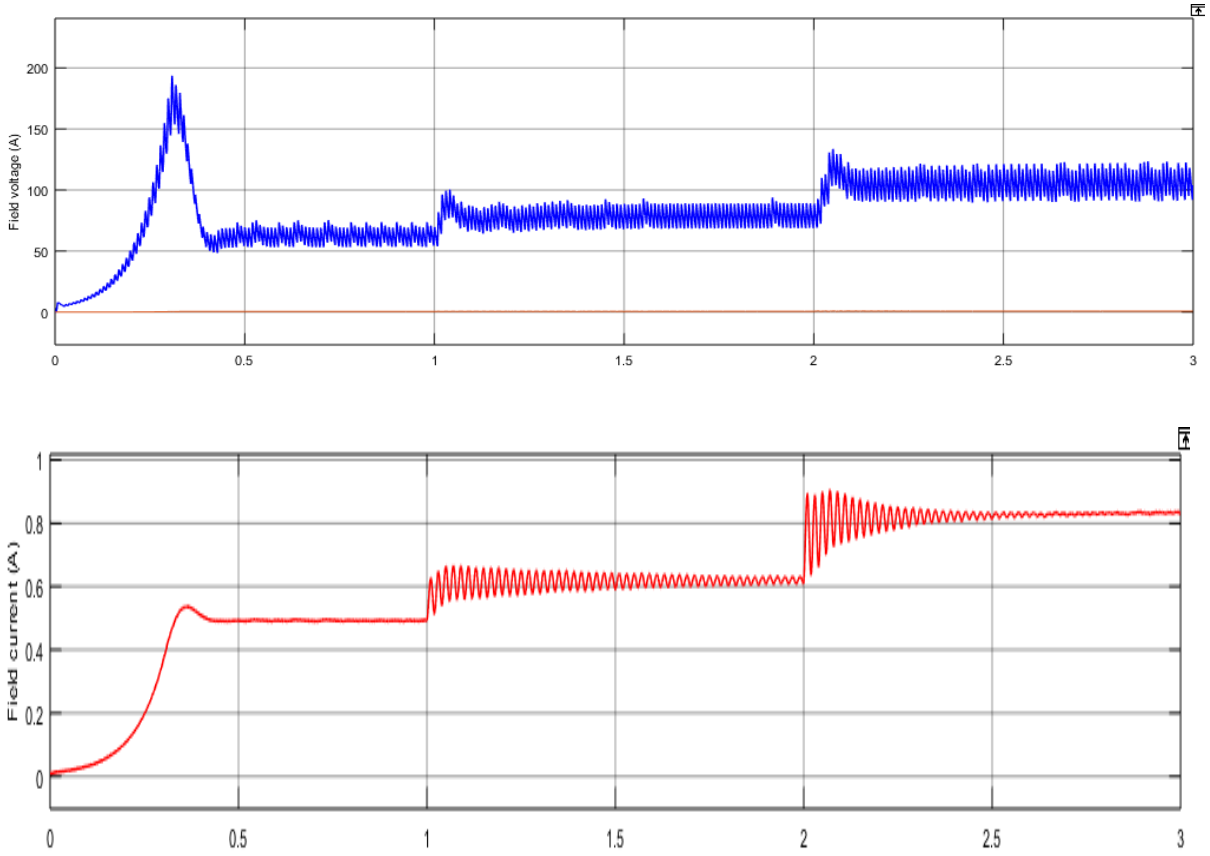

Figure 6.14 Field voltage and field current. 4th case.

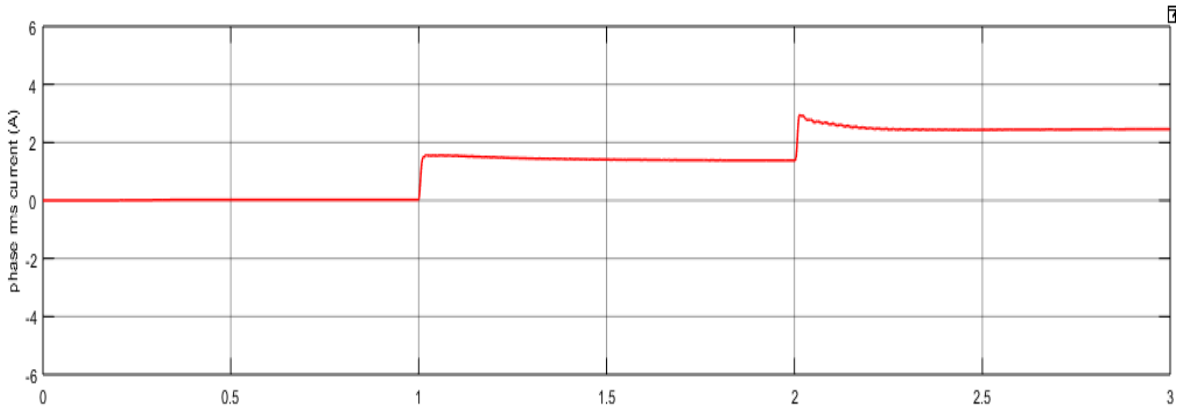

Figure 6.15 Single-phase rms current. 4th case.

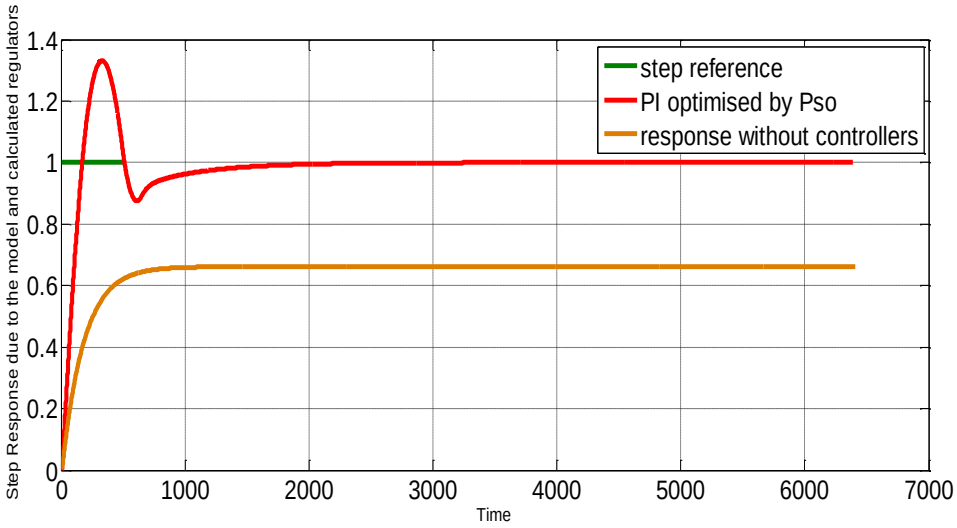

Figure 6.16 Plot of the step response due to the model and calculated regulator.

Figure 6.16 presents the plot of the step response due to the model and calculated regulator parameters using PSO. In the first part, the obtained results encouraged us to extend the study for another type of excitation system and another size of synchronous machine such as the order of 187 MVA as rated power.

6.3.2. PSO tuning results of the second generator

PSO technique has been implemented for obtaining the optimized parameters of the process regulator. The simulation results confirmed that PSO is the optimization technique that gives a good tuning due to its ability to reach the global optimum with relative simplicity and its high convergence speed.

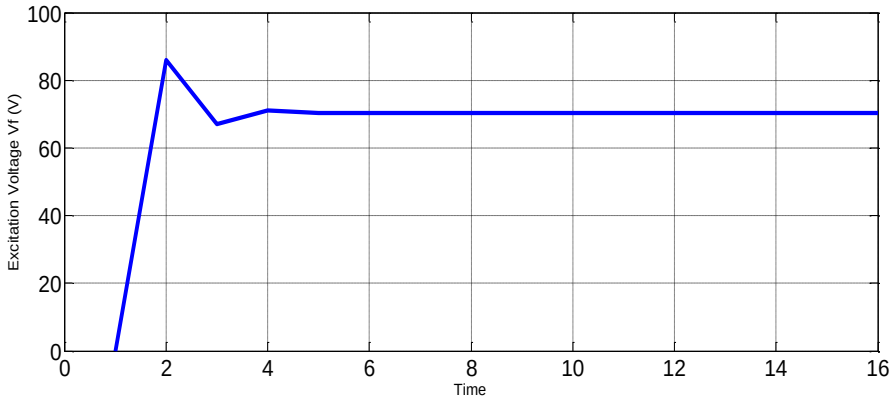

Figure 6.17 Excitation voltage Vf (V).

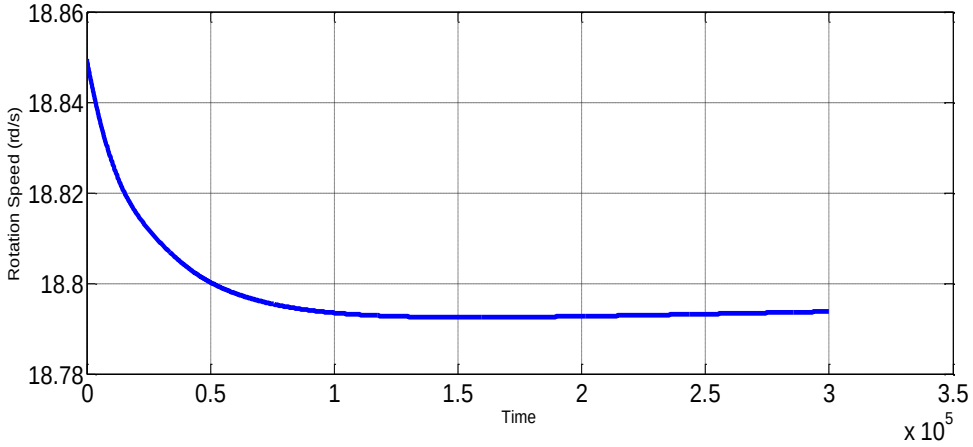

Figure 6.18 Rotation speed (rd/s).

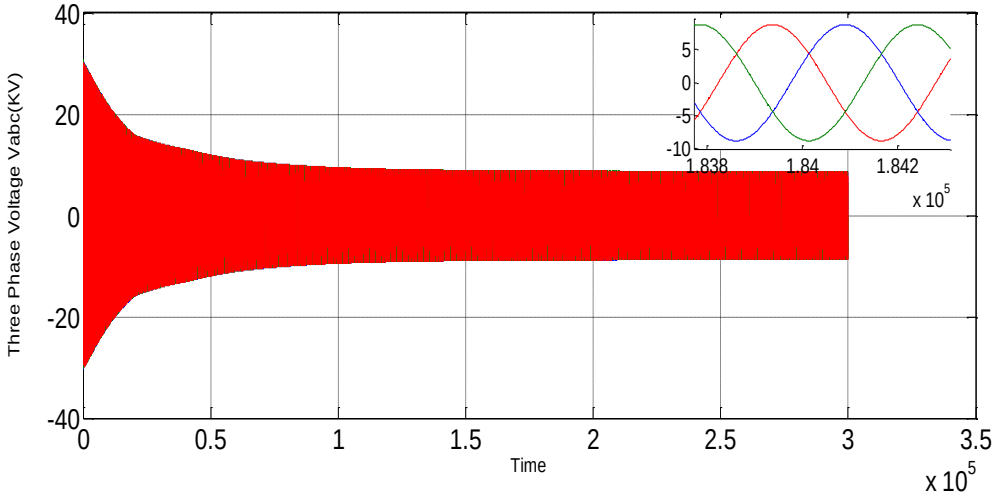

Figure 6.19 Three phase voltage (kV).

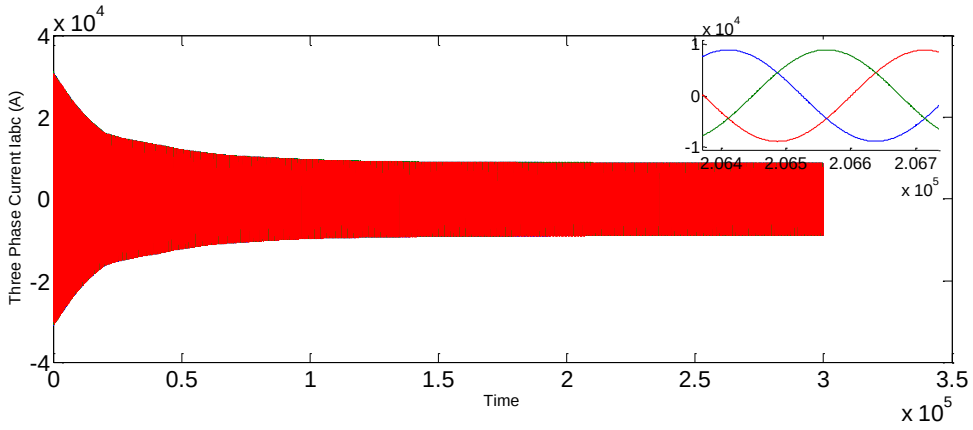

Figure 6.20 Three phase current (A).

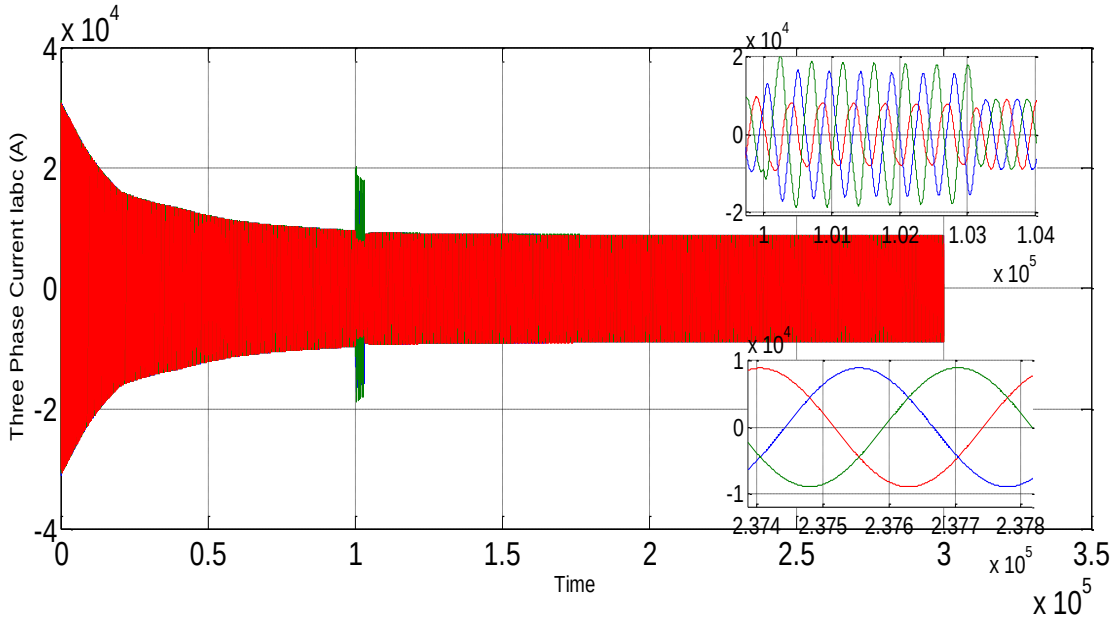

Figure 6.21 Three phase voltage when a fault is applied to phase B at t=1.

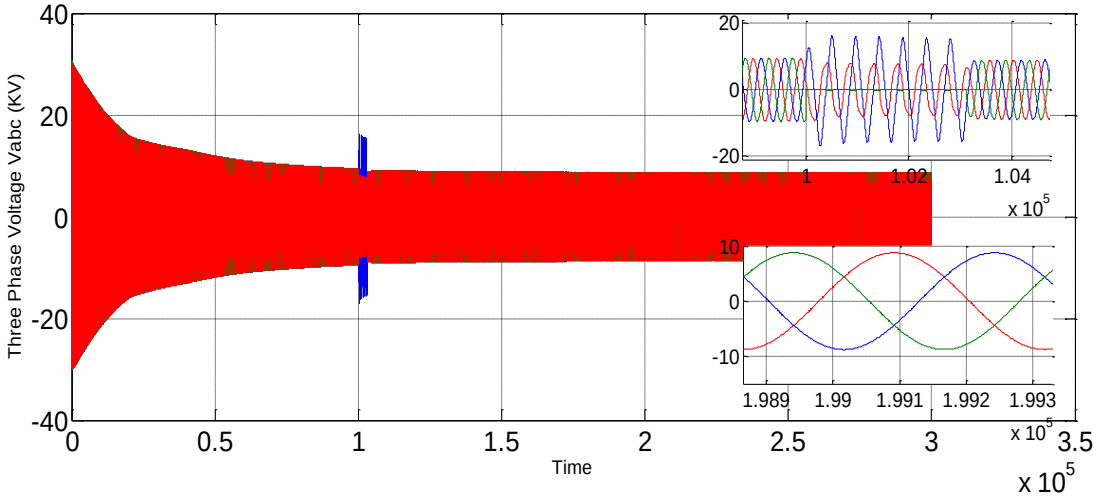

Figure 6.22 Three phase current when a fault is applied to phase B at t=1.

Figures 6.19 and 6.20 represent the application of the load. However, Figs 6.21 and 6.22 show the voltage when a fault is applied on phase B with an earthling resistance R = 1 * 10-3 ohms.

In order to test the performance of the proposed algorithm, a voltage regulation of SM with 187MVA has been carried out. During the optimization process, the possible solutions are evaluated through a function that involves the performance criteria calculated on the response of the overall system. The simulations are carried out on the two systems which show that the PID regulator optimized by the PSO algorithm is efficient.

The advantage of this optimization method compared to other methods is to provide a quick estimation of performance and robustness by taking into consideration the synthesis parameters. This is an important advantage that makes an attempt to satisfy specific regulator objectives.

6.4 Simulation using ADRC Technique

Table 6.2 ADRC parameters settings

	1.5KVA Machine	187MVA Machine
Kp	2.560	0.0025
Kd	2.336	10^{-3}
b	3	19
ω_0	50	1.9
ω_c	1.5	0.05

Withω_c : the controller bandwidth.

6.4.1 1.5 KVA synchronous machine case

SCHEMA OF SIMULATION

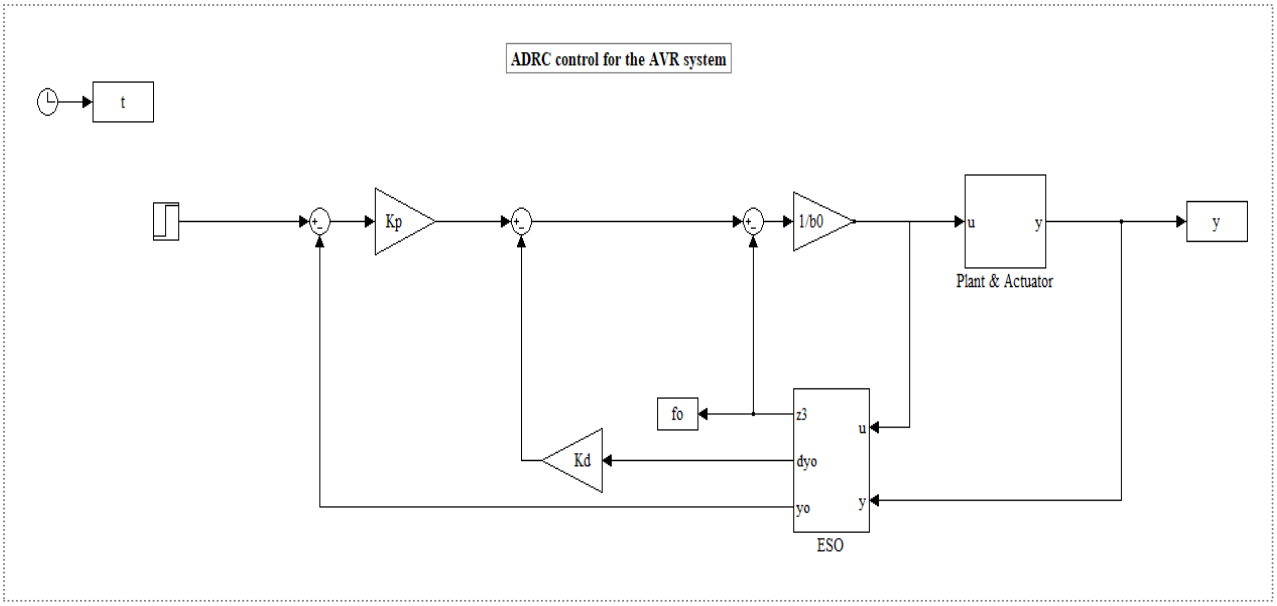

Figure 6.23 Linear ADRC with complete state feedback

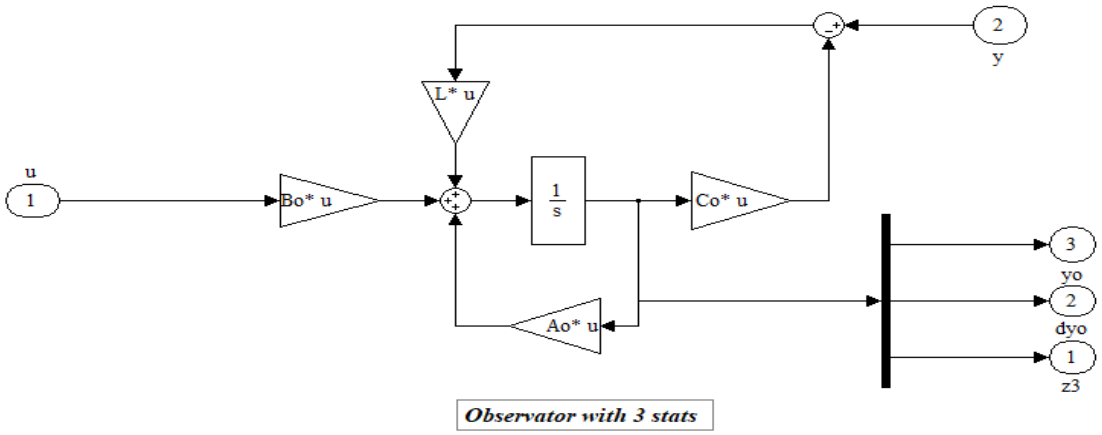

Figure 6.24 Observator Bloc Diagram

As shown in Figure 6.23, the disturbance rejection can be implemented using the estimated variables, and a linear controller can be used to manage the remaining double integrator behavior. A second-order closed loop behavior with tunable dynamics is produced via a modified PD controller (without the derivative part for the reference value). Once more, this is a controller that uses estimation-based status feedback.

ESO gives the estimate value of the object status variable and system's disturbances (Figure 6.24)

Now that we have experimented with different algorithms, it is appropriate to test them against each other in order to better understand the efficiency of each one compared to the other in the case of voltage regulation

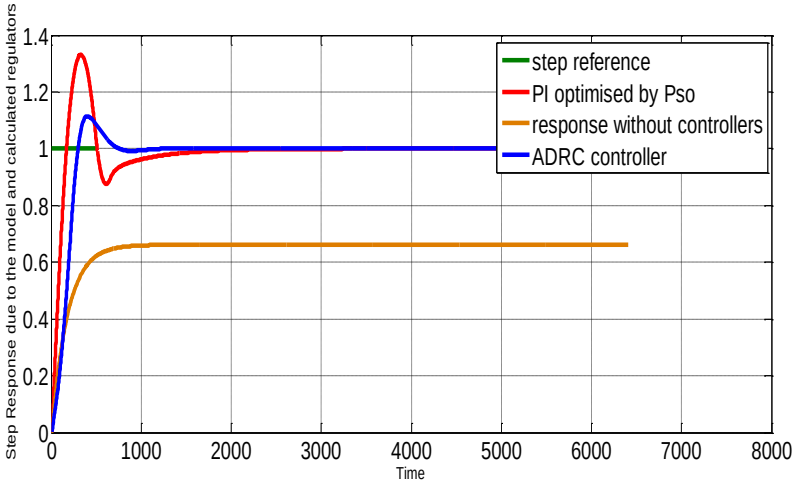

Figure.6.25 Plot of the step response due to the model and calculated regulators for the first system.

For the model's validation, we used the identical input to excite both systems using the both methods, then compared the results (see figure 6.25).

6.4.2 187MVA synchronous machine case

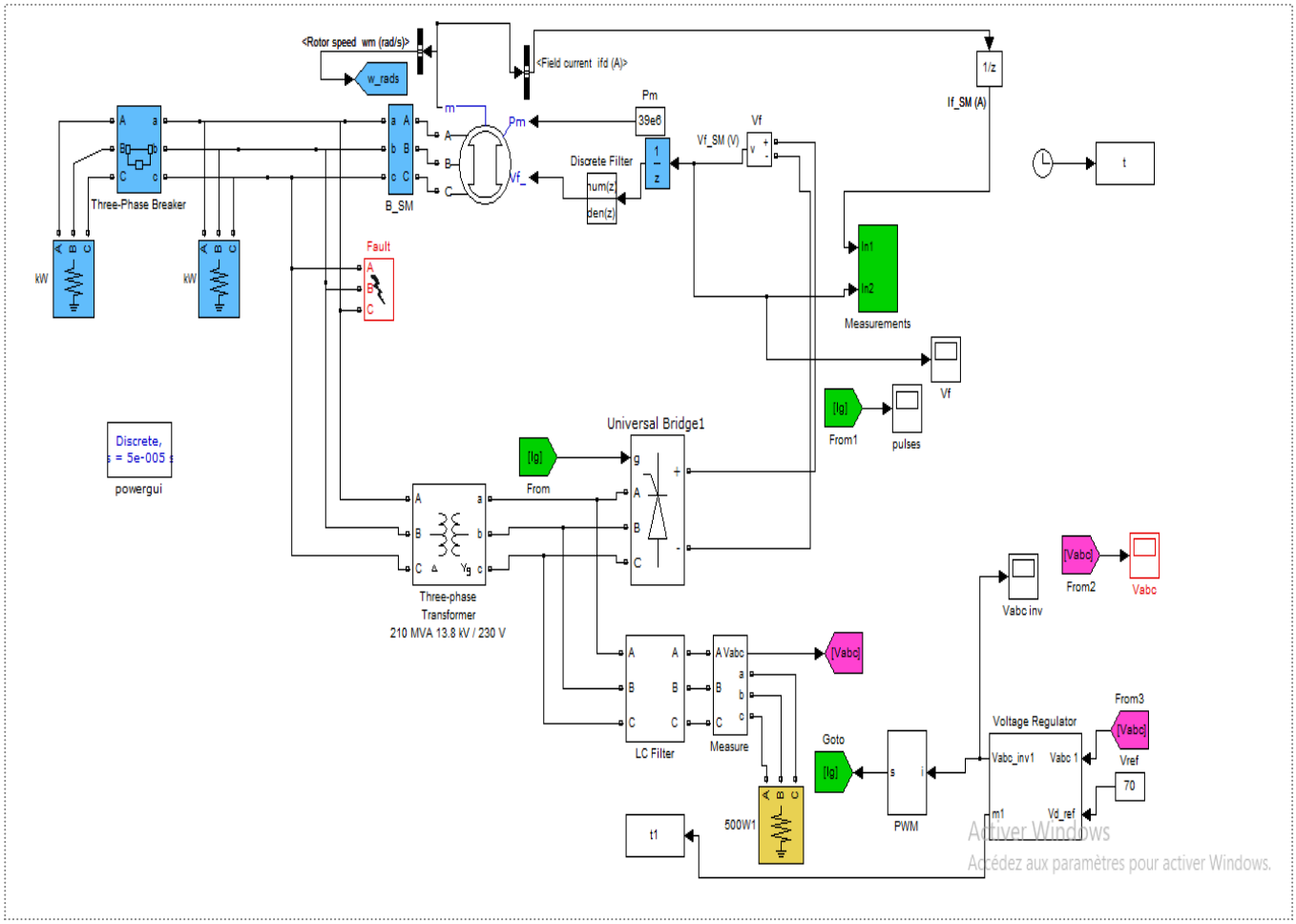

Figure 6.26 Schematic diagram of the ADRC function block.

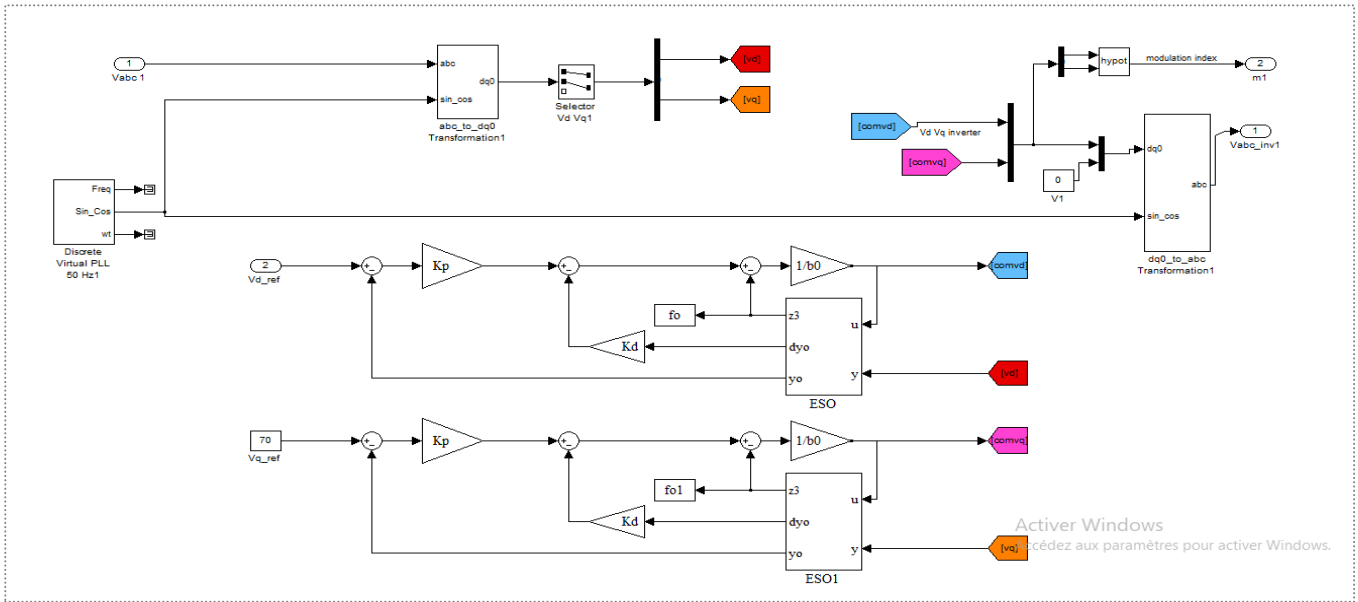

Figure 6.27voltage regulator bloc diagram

The structure of control loop is presented in Figure 6.26.

To show the performance of the proposed controller, a MATLAB/Simulink model has been established.

The performance of the proposed controller is investigated under the following two cases: a) ideal condition; b) load disturbance

The voltage regulator block shown in the figure 6.27 contains the hierarchical control.

The general-purpose ADRC implementation was designed as a building block that was easily accessible and used in a standard way. It encapsulates all process-independent calculations, as well as additional functionality. Its simplified schematic with its input-output specification defined to allow easy parameterization is shown in Figure 6.26. This block also provides error information when errors occur during operation. The ESO calculates the estimation variables and the control law calculates the manipulated variable applied to the process.

For experimental validation, the proposed command structure is implemented and executed. A MATLAB simulation model is built to test the control design, as shown in Fig 6.26

```
%
clear all
clc

%% Modèle d'état de l'observateur à 3 états
   omega0 = 1.9; % pulsation permettant de calculer le gain de l'observateur
   b0 = 19; % instable pour b0 =

   Ao = [0 1 0
         0 0 1
         0 0 0];
   Bo = [0
         b0
         0];
   Co = [1 0 0];

% Observer gain design
 polesobs = [-omega0 -omega0 -omega0];

  L = Acker(Ao',Co',polesobs)';


% Set-point tracking controller design
  omegac =0.05 ; %4.5;
  zz = 0.01;
Kp = omegac^2;
%          0        omegac^2];
  Kd = 2*zz*omegac;
```

Figure 6.28 ADRC program

The controller and observer bandwidths are set from Figure 6.28. For comparison, a PI controller is tuned with a proportional gain and an integral gain. The parameters were tuned to

achieve the best stable response. The same values were used for simulations and measurements.

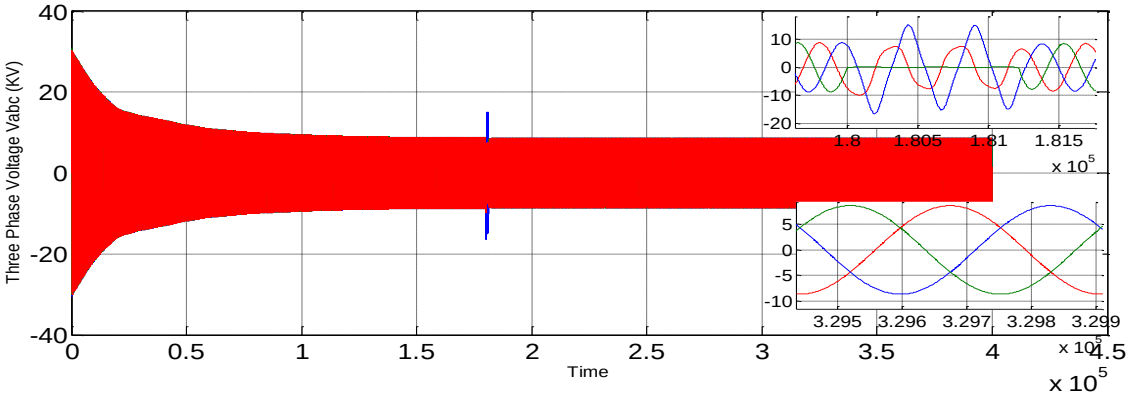

Figure 6.29 Three phase voltage when a fault is applied to phase B at t=1.8 for the second system.

An earthling resistance R = 1 * 10-3 ohms is applied at t=1.8 Sec.

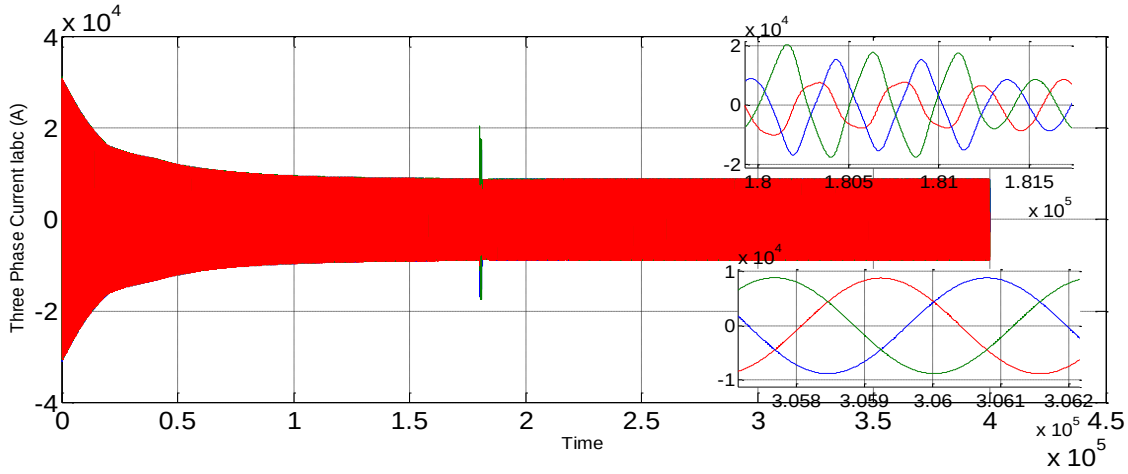

Figure 6.30 Three phase current when a fault is applied to phase B at t=1.8 for the second system.

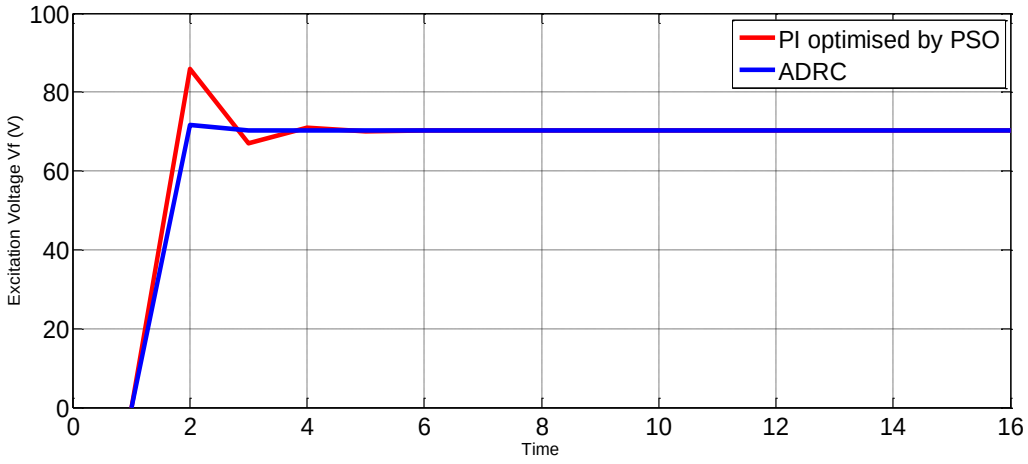

Figure 6.31 Excitation voltage V_f (V) with PSO and ADRC for the second system.

Figure 6.31 represents the layout of the excitation voltage .We observe that for PSO method the response stabilize after ten iterations but for ADRC control the response is faster, which confirms the reliability of the both methods.

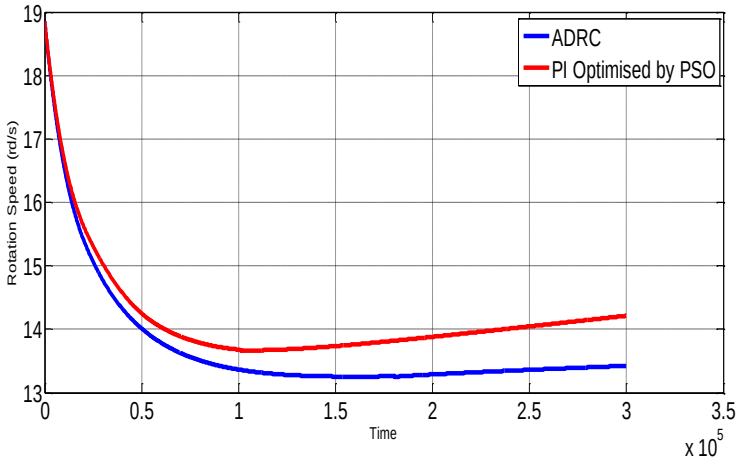

Figure 6.32 Speed w (rd/s) with ADRC and PID- PSO for the second system.

Similar to the first case, it can be noticed that ADRC controller responds quickly when a fault is applied and it offers better performance compared to the PSO technique (see figures 6. 31 – 6.32), and therefore the requirement of voltage regulation is satisfied.

The advantage of this ADRC method over other methods is to provide a quick way to estimate performance and robustness by taking into consideration the synthesis parameters. This is an important advantage that will make it possible to attempt to satisfy specific regulator objectives. Table 6.3 deals with a comparison of the control performance of the AVR system controlled by different controllers.

Table 6.3 AVR system controlled by different controllers.

	overshoot	Settling time	Steady state error
PI optimized by PSO	33%	1.887	0
ADRC control	11%	0.77	0

It is interesting to compare the results obtained by the two methods (Table 6.3). The responses of the controlling system with PID optimized by PSO (PID-PSO) and ADRC controller are illustrated in figure 6.25 and they are given in table 6.3.

The settling time for PID-PSO and ADRC are 1.887 sec and 0.77 sec respectively. PID-PSO of 33%overshoot, but ADRC has 11%of overshoot. The both methods produce a zero error in steady-state.

The comparison is made between the results of PID-PSO and ADRC for same conditions. The objective is to control and maintain the steady state voltage equal to the reference one with a tolerance of ± 2%. The experimental results and the comparative study carried out between the two proposed methods show improvement in the results of the ADRC application.

6.5 Simulation Results Discussion

The Simulation results verify the efficiency of the ADRC which drives the voltage to its nominal value despite the presence of various disturbances. They also demonstrate that ADRC has better set point tracking and robust performance than PID-PSO. The good follow of the reference and the speeds of the dynamics which are ensured by the ADRC controller, compared to the PI regulator can be shown in figures 6.31 and 6.32.

However, the optimization of PI controller by the PSO method has lead to the best performance of PI, which has been proven. But the PI has limits such as in the case of non-linear, noisy and / or uncertain systems. Such complications can be brought by the integral term and the loss of performance in the combination of the proportional and integral terms.

It can be noted that ADRC gives better results without time-consuming adjustment step, knowing that the set point tracking is faster and more accurate. It is ensured by the poles placement.

Therefore the simulations show that the ADRC control is more efficient than the PI-PSO control.

6.6 Conclusion

During the optimization process, the possible solutions are evaluated through a function that involves the performance criteria calculated on the response of the overall system. The simulations that are carried out on the two systems show that the PID regulator

optimized by the PSO algorithm is efficient. The advantage of the ADRC method over other simple methods is to provide a quick way to estimate performance and robustness by playing on the synthesis parameters. This is an important advantage makes it possible to meet specific regulator objectives.

This method has been proven to be used for reducing overshoot. The fast response can be obtained after adjusting the voltage.

Chapter 7

Conclusion

Chapter 7

Conclusion

Minimum voltage deviation and good response at the terminals of the generator in the power plant are both characteristics that are needed in a reliable power system. The used conventional controllers have significant rise time, overshoot……ext. Therefore, many advanced algorithms have been developed in order to be applied to control systems, which show typical characteristics such as fastness and smoothness in their responses.

In first proposed approach of design methods, the PI gains have been tuned using PSO heuristic algorithm. A PSO technique has been implemented to focus on the optimization process. The simulation results using Simulik/ Matlab software have confirmed that PSO is the promising optimization technique due to its ability to reach the global optimum with relative simplicity and its high convergence speed. The AVR has been implemented for the first machine, which is based on Arduino board. However, PI based AVR for the second self-exciting machine application, only the simulation has been carried out. After we are adopting another type of controller relatively recent and still little used to date ADRC. This controllerestimate and cancel or compensates global disturbances directly. It requires very little information about the power plant. Then, the controller uses the information needed from the estimator to control the system instead of being depended on the mathematical model.

Most of the existing control design methods are based on mathematical description of the system. However, many real systems are highly uncertain, the accurate mathematical model is usually not available, and disturbances are unknown.

The ADRC controller is classified among the controllers without model because it doesn’t require the exact knowledge of the system model to be ordered, in our case we have worked on so-called gray box systems where the majority of these parameters are known. This control effectively corrects the voltage level and compensates for disturbances of the complex and nonlinear system[31].

ADRC uses two laws to control the system the first to provide regulation by compensating for the generalized disturbance previously estimated by ESO. The second is a control by a state feedback which makes it possible to ensure stability and closed-loop set point tracking.

Indeed we know that the control of systems by state feedback based on an observer, the dynamics of the ESO must always be faster than the dynamics of the closed loop. The choice of wc is not at all obvious if does not know all system parameters. This can be seen as a disadvantage of this command.It can be noted that, assuming that the parameters relative degree and b are known or correctly estimating the adjustment of the ADRC command, requires the choice of two pulsations which are w0 the pulsation of the observer and wc the

pulsation of the feedback of state. If the choice of w0 seems easy to make, since it depends on wc, therefore, this command is simple to implement and easy to adjust in the real world.

Besides, the modeling of the synchronous machine in the natural reference frame as well as in stator reference frame is presented in this work. Identification tests were performed on the laboratory 1.5kVA salient pole SG to extract the machine parameters. Resulting graphsof tests were explained. Validation of the obtained model has been done based on comparison between the graphs obtained by simulation and those obtained experimentally.The study is extended to another machine with nominal power of 187MVA power

The simulations have been carried out using Matlab software. The obtained simulation results are finally discussed. Every part of the used excitation system is functioning correctly and satisfactorily for both generators and controllers.

Further work

The improvement that can be made to this work would be:

- Online tuning parameters of PI controller of the AVR.
- Advanced control (optimal; adaptive and robust) of synchronous machines with use of digital modes (finite element finite volume and finite differences).
- Apply mathematical solution methods for the synthesis of robust optimal stabilizers.
- Improved technical performance offered by hybridization with other advanced control and optimization techniques.
- Carry out measurements on the electrical parameters of the various elements of the system to be studied using experimental benches in order to satisfy the optimization.
- Implementation ADRC based AVR using a powerful microcontroller.
- validation on an experimental plan with real-time simulations and technical-economic studies

References

1. Ahcene,F.Bentarzi, H. Automatic voltage regulator design using particle swarm optimization. International conference on electrical engineering (2020).
2. Ygzaw, A.Banteyirga. B.; Darsema, M. Generator excitation loss detection on various excitation systems and excitation system failure, ICST 2020 Springer nature swizerland AG. LNICST308(2020) 382 :394.
3. Wei,Y. Zheng, Xu. Excitation System Parameters Setting for Power System Planning. Power Engineering Society Summer Meeting, IEEE (2002).
4. Bendjegh, O.Boushaki,I. Bat, S.Algorithm for optimal tuning of PID controller in AVR system. International conference on control, Engineering and and information technology (2014) 158:170.
5. Gaiang, Z.L. A particle swarm optimization approach for optimum design of PID controller in AVR system, IEEE Transactions on Energy Conversion 19 (2004) 348:391.
6. Kim, D.H. Cho, J.H. A biologically inspired intelligent PID controller tuning for AVR systems. International Journal of Control Automatic and Systems 4 (2006) 624:636
7. Mukherjee, V. Ghoshal, S.P. Intelligent particle swarm optimized fuzzy PID controller for AVR system. Electric Power System Research 77 (2007) 1689:1698.
8. Wong, C.C.Li, S.A Y. Wang, H. Optimal PID controller design for AVR system. Tamkang Journal of Science and Engineering; 12 (2009) 259:270.
9. Shayeghi, H.Dadashpour, J. Anarchic Society Optimization Based PID Control of an Automatic Voltage Regulator (AVR) System. Electrical and Electronic Engineering 2 (2012) 199:207.
10. Hasanien, H. M. Design optimization of PID controller in automatic voltage regulator system using taguchi combined genetic algorithm method. *IEEESystems Journal*7 (2013) 825:831.
11. Han,J.A class of extended state observers for uncertain systems control and decision 10 (1995) 85:88.
12. Han,J. From PID to active disturbance rejection control. IEEE Transactions on industrial electronics 56(2009) 900:906.
13. Wisniewski, T. Modélisation non-linéaire des machines synchrones pour l'analyse en régimes transitoires et les études de stabilité. Paris-Saclay University. 2019
14. DERRAR, A. Resolution du probleme d'optimisation h∞ des stabilisateurs pss robustes par les approches metaheuristiques. SIDI BEL ABBES University. 2016
15. Baouali, B. Chibane, A. Etude du système de régulation automatique de la tension AVR+PSS des alternateurs de grande puissance, application : alternateur 176 MW de la centrale de Cap-Djinet. Boumerdes University. 2017
16. Barakat, A.M. Contribution à l'amélioration de la régulation de tension des générateurs synchrones: nouvelles structures d'excitation associées à des lois de commandes H∞. Poitiers University (2011).
17. BOUCHAMA, Z. Stabilisateurs Synergétiques des Systèmes de Puissance thèse de doctorat en science option réseau électrique. Ferhat Abbas – SETIFuniversity 12/2013.
18. https://www. specialautom.net. Régulation PID par les méthodes empiriques
19. https://www.engie.com(access on January 2022)
20. VAN CUTSEM, T. Introduction to electric power and energy systems. Liege university. 2019
21. IEEE Guide for Synchronous Generator Modeling Practices and Applications in Power System Stability Analyses.2003

22. https://www.electroniclinic.com(access on January 2022)
23. Machowski,J. Bialek,J. and Bumby,D. J. Power System Dynamics: Stability and Control. John Wiley & Sons, (2011).
24. Sauer,P. W. Power System Dynamics and Stability. Prentice Hall, 1998.
25. Barret,P. Régimes transitoires des machines tournantes électriques. Eyrolles, 1987.
26. Arjona, MA Parameter calculation of a turbogenerator during an open-circuit transient excitation. IEEE Trans Energy Convers 19(1):46–52(2004)
27. Ban, D.Žarko, D.Maljkovi´c, Z. The application of finite element method for more accurate calculation and analysis of turbogenerator parameters. Electric Power Compon Syst 26(10):1081–1093(1998)
28. Bastos, JPA. Sadowski, N. Electromagnetic modeling by finite element methods. Marcel Dekker, Inc. (2003)
29. Berhausen, S. Paszek, S. Use of the finite element method for parameter estimation of the circuit model of a high power synchronous generator. Bull Pol Acad Sci 63(3):575–582(2015)
30. Berhausen, S. Paszek, S. Calculation of selected parameters of synchronous generators of different construction based on the analysis of the waveforms for a two-phase short-circuit. Paper presented at the international symposium on electrical machines, SME, Andrychów, Poland, 10-13 June 2018, pp 1–5
31. Gao, J. Zhang, L. Wang, X. AC machine systems, mathematical model and parameters, analysis, and system performance. Springer, Berlin-Heidelberg.(2009)
32. Salon, SJ. Finite element analysis of electrical machines. Kluwer Academic Publishers, New York.(2000)
33. Zhou, P-B. Numerical analysis of electromagnetic fields. In: Electric energy systems and engineering series. Springer, New York.(1993)
34. Anderson, PM. Fouad, AA. Power system control and stability. Wiley Inc.(2003)
35. Ong, C-M. Dynamic simulation of electric machinery using Matlab/Simulink. Prentice Hall, New Jersey. (1998)
36. Chi Choon, Lee. Synchronous Machine Modeling by Parameter Estimation. Louisiana State University LSU Digital Commons. 1976
37. Ghomi, M. Najafi, YS. Review of synchronous generator parameters estimation and model identification. Paper presented at the 42nd international universities power engineering conference, UPEC, September 2007, pp 228–235
38. Krause, PC. Wasynczuk,O and Sudhoff, S. Analysis of electric machinery and drive systems. E nd edition Willey interscience. 2002
39. Nocon, A. Bobon, A. Paszek, S. Pasko, M. Pruski, P. Majka, Ł.Szuster, D. Bojarska, M. Measurement parameter estimation of the model of a synchronous generator working in thermal electric power plant. Paper presented at the 10th international conference on “advanced methods in the theory of electrical engineering, AMTEE, 6–9 Sept 2011, Klatovy, Czech Republic, pp VI-3-4
40. Paszek, S. Bobon, A.Kudła, J.Białek, J. Abi-Samra, N. Parameter estimation of the mathematical model of a generator, excitation system and turbine. Przegl˛adElektrotechniczny 81(11):7–12. (2005).

41. Kundur, P. Power system stability and control. McGraw-Hill, Inc(1994)
42. Padiyar, KR. Analysis of subsynchronous resonance in power systems. Springer, Boston, MA.(1999)
43. Jerkovic, Vedrana; Miklosevic, Kresimir; Spoljaric Zeljko . Excitation System Models of Synchronous Generator Faculy of Electrical Engineering Osijek, Croatia 2010
44. Manoj Kumar Sharma1 , R.P. Pathak2 , Manoj Kumar, Jha , Qureshi,M.F. Excitation control of a power plant alternator using interval type-2 fuzzy logic controller. Advances in Modelling and Analysis C Vol. 73, No. 4, December, 2018, pp. 182-188
45. Zeljko, S.Kresimir,M. VedranaJ.Synchronous Generator Modeling Using Matlab. 2013 http://bib.irb.hr/datoteka/475823.Final_paper-_Spoljaric_Miklosevic_Jerkovic-SIP-2010.pdf
46. Bose,B.K. Modern Power Electronics and AC Drivers. Prentice Hall PTR, ISBN 0-13-016743-6, Upper Saddle River, New Jersey, USA. 2012.
47. Yousif, I. Mashhadany,Al. Farqad, A, Najlaa, A. Modeling, Simulation and Analysis of Excitation System for Synchronous Generator. Asian Journal of Engineering and Technology (ISSN: 2321 – 2462) Volume 02 – Issue 05, October 2014.
48. Chen,Q.Wan,L.Zhou,K. Ding,KJun,HYuchuan, H. Modeling and Simulation of Large Synchronous Generator Excitation System with PSASP. 4th International Conference on Mechatronics, Materials, Chemistry and Computer Engineering (ICMMCCE 2015)
49. Basler Electric Power Systems Group. Basler offers pre-packaged excitation system to replace silverstat regulator. In Note d'application, EX-SILV1, 1999.
50. Chambers,G.S. Rubenstein, A.S. and Temoshok,M. Recent development in amplidyne regulator excitation systems for large generators. AIEE Transactions on Power Apparatus and Systems, vol. 80:pp. 1066–1072, 1961.
51. Bobo,P.O. Carleton,J.Y.Horton,W.F. A new regulator and excitation system. AIEE Transactions on Power Apparatus and Systems, vol. 72 :pp. 175–183, 1953
52. Wetzer,P. Machines synchrones - excitation. Techniques de l'ingénieur, D3545, 1997.
53. Barnes,H.C. Oliver,J.A. Rubenstein,A.S. Temoshok,M. Alternatorrectifier exciter for cardinal plant. IEE Transactions on Power Apparatus and Systems, PAS-87:pp. 1189–1198, 1968.
54. Whitney,E.C. Hoover,D.B. Bobo,P.O. An electric utility brushless excitation system. AIEEE Transactions on Power Apparatus and Systems, vol. 78 :pp. 1821–1824, 1959
55. Ferguson,R.W. Herbst,R. Miller,R.W. Analytical studies of the brushless excitation system. IEEE Transactions on Power Apparatus and Systems, vol. 78, no. 4:pp. 1815 –1821, 1959.
56. Richardson,P. Hawley,R.Wood,J.W. Insulation level for turbogenerator rotors. In IEEE Winter Power Meeting, 1972.
57. AIEE Committee Report. Proposed excitation system definition for synchronous machines. AIEE Transactions on Power Apparatus and Systems, PAS-88, no. 8:pp. 1248–1258, 1969.

58. Wright,W.F. Hawley,R. Dinely,J.L. Parsons,C.C. Brushless thyristor excitation systems. IEEE Transactions on Power Apparatus and Systems, PAS 91, no. 5:pp. 1848–1854, 1972.
59. Umans,S.D. Driscoll,D.J. Excitation System for Rotating Synchronous Machines, United States patent, US 6,362, 588, B1, Mar. 26, 2002.
60. Wetzer,P. Machines synchrones - excitation. Techniques de l'ingénieur, D3545, 1997.
61. Haj agos, L.M. Basler, M.J. Recommended practice for excitation system models for power system stability studies. Changes to IEEE 421.5 Power Engineering Society General Meeting 2005 IEEE.
62. Ghazizadeh,M.S. Hughs,F. M. A Generator Transfer Function Regulator for Jmproved Excitation Control. IEEE Trans on. Power Systems, Vo1.13, N°2, May 1998, pp. 437-441.
63. Prepared by the IEEE Working Group on Computer Modelling of Excitation Systems. Excitation system models for power system stability studies. IEEE committee report, February 1981.
64. Chuvychin,V.Petrichenko, R. Gurov, N. Optimization of Excitation System Parameters for Kegums Hydra Power Plant of Latvia. 126 Environment and Electrical Engineering (EEEIC), 2011,lOth International Conference on.
65. Ouramdane, KH. Modélisation et optimisation du système d'excita ti on du groupe turbine-alternateur du simulateur analogique d'hydro-quebec , université du québec en abitibi-témiscamingue , 2015.
66. Farkh, R. Commande PID Des Systèmes À Retard. Automatique / Robotique. École Nationale d'Ingénieurs de Tunis, 2011. Français.
67. Young-Hyun, M and al. Fuzzy Logic based extended integral control for load frequency control. Proc. of IEEE Power Eng. Society winter meeting, Vol.3. Issue 1, 2001, 1289-1293.
68. Vinod Kumar,D.M.Intelligent Controllers for Automatic Generation Control. Proc. of IEEE region 10 International conference on global connectivity in Energy, Computer, Communication and Control, 1998, p557-574.
69. Fogel,D.B. Evolutionary Computation: Towards a New Philosophy of machine Intelligence, 2nd Edition, IEEE Press, New York.2000.
70. Gaing,Z-L. A Particle swarm optimization approach for optimum design of PID Controller in AVR system. IEEE Transactions on Energy Conversion , Vo.19, No.2, 2004
71. Duan, H-B and al.Novel Approach to Nonlinear PID parameter optimization using Ant Colony Optimization Algorithm. Journal of Bionic Engineering, 2006,p 73-78.
72. LabibAwad, M. Modeling of Synchronous Machines for System Studies, University Of Toronto, Toronto, Canada, 1999.
73. Paszek, S. Bobon, A. Berkausen, S. Majka, L. Nocon, A. Pruski, P. Synchronous generator and excitation systems operating in power system», Springer 631(2020) 49:149.

74. Xu, X. Mathur, R. M. Rogers, G. J. and Kundur, P., Modeling of Generators and their Controls in Power System Simulations Using Singular Perturbations, IEEE Transactions on Power Systems, vol. 13, no. 1, pp.109–114, February 1998.
75. El Serafi, AM. Wu, J.Determination of the parameters representing the cross-magnetizing effect in saturated synchronous machines IEEE Transactions on Energy Conversion (Volume: 8,Issue: 3, Sep 1993.
76. Warmkeue, R. Modélisation Et Identification Statistique Des Machines Synchrones: Outils Et Concepts. Ecole technique de montreal. 1998.
77. Tsai,H. h'eyhani, SM J. Deincko, SM R. G. Farmer, F. On-Line Synchronous Machine Parameter Elstimation from Small Disturbance Operating Data. IEEE Transactions on Energy Conversion (Volume: 10, Issue: 1, Mar 1995
78. Heffron,W. G. Phillips,R. A. Effect of a Modern Amplifying Voltage Regulator on Under excited Operation of Large Turbine Generators [includes discussion] Power Apparatus and Systems (Volume: 71, Issue: 3, Aug. 1952)
79. Vibergt, M. Subspace-based Methods for the Identification of Linear Time-invariant Systems.automaticaVolume 31, Issue 12, December 1995, Pages 1835-1851
80. Peter Van Overschee Subspace identification for linear systems. Theory, implementation, applications. Incl. 1 disk Kluwer Academic Publishers Group 1996.
81. Karrari,M. Malik, OP. sunchronous generator model identification using on line measurements. Power plant and power system control seoul Korea 2003
82. Mouni, E. Tnani, S.Gérard, C. Synchronous generator modelling and parameters estimation using least squares method. Simulation Modelling Practice and Theory 16 (6), 678–689.
83. Fard, RasoolDalirrooy, Karri, M. Synchronous generator model identification for control application using Volterra series. IEEE Transaction on Energy Conversion 20 (4), 852–858. 2005
84. Melgoza,J-J-R.Heydt,G-T.Keyhani, A.Agrawal,B-L. Douglas, S. Synchronous Machine Parameter Estimation Using the Hartley Series. IEEE TRANSACTIONS ON ENERGY CONVERSION, VOL. 16, NO. 1, MARCH 2001.
85. Dehghani, M., Karrari, M., Rosehart, W., Malik, O.P., 2010. Synchronous machine model parameters estimation by a time-domain identifcation method. Electrical Power and Energy Systems 32 (5), 524–529.
86. Hamidreza, M. Alireza, A. Mohammad-Mehdi, F. Parameter identification of chaotic dynamic systems through an improved particle swarm optimization. Expert Systems with Applications 37 (5), 3714–3720. 2010a
87. Hazem, M-A . Bayoumi, M, 2004. Volterra system identification using adaptive genetic algorithms. Applied Soft Computing 5 (1), 75–86
88. Wang, Z., Gu, H., 2007. Parameter identification of bilinear system based on genetic algorithm. In: Proceedings of the International Conference on Life System Modeling and Simulation, pp. 83–91.
89. Tavakolpour, A-R. Darus, I- Z. Mat-Tokhi, O. Mailah, M. Tavakolpour, A.R., et al. 2010. Genetic algorithm-based identification of transfer function parameters for a

rectangular flexible plate system. Engineering Applications of Artificial Intelligence. doi:10.1016/j.engappai.2010.01.005.

90. Sabat Samrat, L. Udgata Siba, K. Murthy, K.P.N. Small signal parameter extraction of MESFET using quantum particle swarm optimization. Microelectronics Reliability 50 (2), 199–206. 2010.
91. Liu, L. Liu, W. Cartes, D-A..Particle swarm optimization-based parameter identification applied to permanent magnet synchronous motors. Engineering Applications of Artificial Intelligence 21 (7), 1092–1100.2008.
92. Pangao, K. Jianzhong Z-N.Changqing, W. Han, X.Huifeng, Z.Chaoshun, L. Parameters identification of nonlinear state space model of synchronous generator. Engineering Applications of Artificial Intelligence ELSEVIER 2011.
93. Jadric,M. Francic,B. Dynamic of Electric Machines. Graphis,Zagreb, Croatia, 1995, ISBN 953-96399-2-1.
94. Boldea, I. Synchronous Genrators -Second edition- Timisoara: CRC Press, 2016.
95. Barakat, A. Analysis of synchronous machine modeling for simulation and industrial applications, Article, University of Poitiers, Poitiers, France, 2010.
96. Ghanim, D. Experimental Dtermination of Equivalent Circuit Parameters for a Laboratory Salient-pole SynchrnousGenerator,University of Newfoundland,Newfoundland,Canada, 2012.
97. Ygzaw, A. Banteyirga. B.Darsema, M. Generator excitation loss detection on various excitation systems and excitation system failure, ICST 2020 Springer nature swizerland AG. LNICST308(2020) 382:394.
98. Shi, Y. Eberhart, R. A modified particle swarm optimizer. Proceedings of IEEE World Congress on computational intelligence international conference on evolutionary computation (1998) 69:73.
99. Sen,P.C. Modern Power Electronics, Wheeler Publishing, 1998.
100. Ashlock, D. Evolutionary Computation for Modeling and Optimization. New York NY 10013. USA– 2005.
101. Colletto, Y. Siarry, P. Optimisation Multi-objectif. EYROLLES. November 2002.
102. SlimanI, L. Contribution à l'application de l'optimisation par des méthodes métaheuristiques à l'écoulement de puissance optimal dans un environnement de l'électricité dérégulé BatnaUniversity. 2009
103. Hashemi, F. Mohammadi, M. Combination of continous action reinforcement learning automata on PSO to design PID controller for AVR system. IJE TRANSACTIONS 28 (2015) 52:59.
104. Yuanchang, Z. Xu, H. Pu, M. Fachuan, L. PSO-RBF Neural Network PID Control Algorithm of Electric Gas Pressure Regulator. Hindawi Publishing Corporation Abstract and Applied Analysis Volume. Article ID 731368, p7. 2014.
105. Coello,CA ; Salazar Lechuga,M. MOPSO : A Proposal for Multiple Objective Particle Swarm Optimization. IEEE Congress on Evolutionary Computation 2. 2002.
106. Fregoso, J. Gonzalez, CI. Martinez, GE. Optimization of Convolutional Neural Networks Architectures Using PSO for Sign Language Recognition. Axioms 10, 139. 2021.

107. Singh, B. Al-Haddad, K and Chandra, A. Review of active filters for power quality improvement. IEEE Transactions on Industrial Electronics, vol. 46, no. 5, pp. 960–971, 1999.
108. Larfi, O.Aisset, A. Développement d'un algorithme intelligent pour la commande des robots mobiles. TEBESSA University. 2016.
109. Carlisle, A. Dozier,G. An Off-The-Shelf PSO. Workshop Particle Swarm Optimization. Indianapolis. 2001.
110. Kennedy, J. Eberhart, R. Particle Swarm Optimization. Proceedings of the IEEE International Conference on Neural Networks, 4, pp 1942:1948 1995
111. Clerc, M. Kennedy, J. The particle swarm explosion, stability, and convergence in a multidimensional complex space. IEEE Transactions on Evolutionary Computation, 6(1): pp. 58-73. 2002.
112. AIT KAID, Dj. Commande d'une machine asynchrone sans capteur mécanique, à l'aide des régulateurs fractionnaires. Mouloud Mammeri University. 2011.
113. Mansouri, R. Contribution à l'analyse et la synthèse des systèmes d'ordre fractionnaire par la représentation d'état. Mouloud Mammeri University. 2008.
114. Rehouma, R.Bekakra, Y. Commande Optimisée du GADA Par La Méthode Essaim de Particules (PSO). El-Oued University. 2015.
115. Meissner, M. Schmuker, M. Schneider, G. Optimized Particle Swarm Optimization (OPSO) and its application to artificial neural network training. BMC Bioinformatics 7:125. 2006.
116. Chowdhury, S. Tong, W. Messac, A. Zhang, J. A mixed-discrete Particle Swarm Optimization algorithm with explicit diversity-preservation. Struct Multidisc Optim 47:367–388. 2013.
117. Bekakra, Y. Contribution à l'Etude et à la Commande Robuste d'un Aérogénérateur Asynchrone à Double Alimentation. Biskra University. 2014.
118. Han,J.Control theory: Model approach or control approach.*Syst. Sci. Math.*, vol. 9, no. 4, pp. 328–335, 1989, (in Chinese).
119. Han,J. Active disturbances rejection control technique. *Frontier Sci.*, vol. 1, no. 1, pp. 24–31, 2007, (in Chinese).
120. Gao,Z. Huang,Y. and Han,J. An alternative paradigm for control M system design. in *Proc. 40th IEEE Conf. Decis. Control*, 2001, vol. 5, pp. 4578–4585.
121. She, J.-H. Mingxing,F. Ohyama,Y. Hashimoto,H. and Wu,M. Improving disturbance-rejection performance based on an equivalent input- disturbance approach," *IEEE Trans. Ind. Electron.*, vol. 55, no. 1, pp. 380–389, Jan. 2008.
122. Gao,Z. Active disturbance rejection control: A paradigm shift in feedback control system design. in *Proc. Amer. Control Conf.*, 2006, pp. 2399–2405.
123. Sun,D. Comments on active disturbance rejection control.*IEEE Trans. Ind. Electron.*, vol. 54, no. 6, pp. 3428–3429, Dec. 2007.
124. Valenzuela,M. Bentley,J. M. Aguilera,P. C. and Lorenz,R. D. Improved coordinated response and disturbance rejection in the critical sections of paper machines. *IEEE Trans. Ind. Appl.*, vol. 43, no. 3, pp. 857–869, May/Jun. 2007.

125. Vincent, D. Commande d'un quadrioptère par rejet de perturbations. Ecole polytechnique de Montréal (2008).
126. Ahcene,F. Bentarzi,H. Ouadi,A.Automatic voltage regulator design enhancement taking into account different operating conditions and environment disturbances",Algerian Journal Of Environmental Science And Technology.2020.
127. Wen,T. Caifen,F. Linear Active Disturbance-Rejection Control: Analysis and Tuning via IMC, IEEE Transactions on Industrial Electronics, vol. 63, no. 4, april 2016.
128. Fliess ,M. Join, C. Two competing improvement of PID controllers. IST Open science London UK (2017).
129. Gonzalez, J. Estimation et controle des systems dynamiques à entrée inconnues et energies renouvelables. Centralle Lille (2019).
130. Gao,Z. Scaling and bandwidth-parameterization based controller tuning," in *Proc. Amer. Control Conf.*, Denver, CO, USA, 2003, pp. 4989–4996.
131. Zhengrong,Ch.Active disturbance rejection control: applications, stability analysis, and tuning method, Manitoba University, 2018.
132. Zheng,Q.Dong,L. Lee,D. H. and Gao,Z. Active disturbance rejection control for MEMS gyroscopes. *IEEE Trans. Control Syst. Technol.*, vol. 17, no. 6, pp. 1432–1438, Nov. 2009.
133. Dong,L. Zhang,Y. and Gao,Z. A robust decentralized load frequency controller for interconnected power systems," *ISA Trans.*, vol. 51, no. 3, pp. 410–419, 2012.
134. Huang, C.-E. Li, D. and Xue,Y. Active disturbance rejection control for the ALSTOM gasifier benchmark problem," *Control Eng. Pract.*, vol. 21, no. 4, pp. 556–564, 2013.
135. Erenturk,K. Fractional-order PIλDμ and active disturbance rejection control of nonlinear two-mass drive system.*IEEE Trans. Ind. Electron.*, vol. 60, no. 9, pp. 3806–3813, Sep. 2013.
136. Xia, Y. Dai, L. Fu, M. Li,C. and Wang,C. Application of active disturbance rejection control in tank gun control system.*J. Franklin Inst.*, vol. 351, no. 4, pp. 2299–2314, 2013.
137. Madoski,R. Kordasz,M. and Sauer,P. Application of a disturbance rejection controller for robotic-enhanced limb rehabilitation trainings," *ISA Trans.*, vol. 53, no. 4, pp. 899–908, 2014.
138. Ramorez-Neria, M. Sira-Ramorez, H. Garrido-Moctezuma,R. and Luviano-Jurez,A. Linear active disturbance rejection control of underactuated systems: The case of the furuta pendulum. *ISA Trans.*, vol. 53, no. 4, pp. 920–928, 2014.
139. Criens,C-H-A. Willems,F-P-T. VanKeulen, T-A-C. and Steinbuch,M. Disturbance rejection in diesel engines for low emissions and high fuel efficiency," *IEEE Trans. Control Syst. Technol.*, vol. 23, no. 2, pp. 662–669, Mar. 2015.
140. Chang, X. Li, Y. Zhang, W. Wang,N. and Xue,W. Active disturbance rejection control for a flywheel energy storage system. *IEEE Trans. Ind. Electron.*, vol. 62, no. 2, pp. 991–1001, Feb. 2015

141. Tian,G. Gao,Z. Frequency response analysis of active disturbance rejection based control system. in *Proc. IEEE Int. Conf. Control Appl.*, Singapore, Oct. 1–3 2007, pp. 1595–1599.
142. Zheng,Q. Gao,L. Q. Gao,Z. On stability analysis of active disturbance rejection control for nonlinear time-varying plants with unknown dynamics. in *Proc. 46th IEEE Conf. Decision Control*, New Orleans, LA, USA, Dec. 12–14, 2007, pp. 3501–3506.
143. Godbole,A. Kolhe,J. Jaywant,J. and Talole,S. Performance analysis of generalized extended state observer in tackling sinusoidal disturbances," *IEEE Trans. Control Syst. Technol.*, vol. 21, no. 6, pp. 2212–2223, Nov. 2013.
144. Wu,D. Chen,K. Frequency-domain analysis of nonlinear active disturbance rejection control via the describing function method. *IEEE Trans. Ind. Electron.*, vol. 60, no. 9, pp. 3906–3914, Sep. 2013.
145. Guo,B.-Z. Zhao,Z.-L. On convergence of the nonlinear active disturbance rejection control for MIMO systems.*SIAM J. Control Optim.*, vol. 51, no. 2, pp. 1727–1757, 2013.
146. Sira-Ramorez, H. Linares-Flores, J. Garcoa-Rodroguez, C. Contreras-Ordaz, M. A. On the control of the permanent magnet synchronous motor: An active disturbance rejection control approach.*IEEE Trans. Control Syst. Technol.*, vol. 22, no. 5, pp. 2056–2063, Sep. 2014.
147. Castaneda, L. Luviano-Juarez, A. and Chairez,I. Robust trajectory tracking of a delta robot through adaptive active disturbance rejection control.*IEEE Trans. Control Syst. Technol.*, vol. 23, no. 4, pp. 1387– 1398, Jul. 2015.
148. Huang,Y. and Xue,W. Active disturbance rejection control: Methodology and theoretical analysis.*ISA Trans.*, vol. 53, no. 4, pp. 963–976, 2014.
149. Wolf,A. Swif,J. B. Swinney,H. L. and Vastano,J-A.Determining Lyapunov exponents from a time series.Physica D: Nonlinear Phenomena, vol. 16, no. 3, pp. 285–317, Jul. 1985.
150. Oseledec,V. I. A multiplicative ergodic theorem: Lyapunov characteristic numbers for dynamic system. Trans. Moscow Math. Soc., vol. 19, pp. 197–231, 1968.
151. Yang,C. Balance control of constrained bipedal standing and stability analysis using the concept of' Lyapunov exponents. Ph. D thesis, University of Manitoba, 2007.
152. Sun,Y. Wu,C. Stability analysis via the concept of Lyapunov exponents: a case study in optimal controlled biped standing. International Journal of Control, vol. 85, no. 12, pp. 1952-1966, Aug. 2012.
153. Sadri,S.On Dynamic and Stability Analysis of the Nonlinear Vehicle Models Using the Concept of Lyapunov Stability. Ph. D thesis, University of Manitoba, 2015.
154. Martini,A.Leonard,F. ABBA, G. Modélisation et commande d'un hélicoptère drone soumis à des rafales de vent. 18ème congrésfrancais de mécanique (2007).
155. Xing, C. Donghai, L. Zhiqiang, G. and Chuanfeng, W. Tuning method for second-order active disturbance rejection control. In Proceedings of the 30th Chinese Control Conference, pages 6322–6327, 2011.
156. Herbst,G. A Simulative Study on Active Disturbance Rejection Control (ADRC) as a Control Tool for Practitioners. Electronics, vol. 2, no. 3, pp. 246–279, Aug. 2013.

157. Xue. W. Huang, Y. On performance analysis of ADRC for nonlinear uncertain systems with unknown dynamics and discontinuous disturbances. In: Proceedings of the 2013 Chinese control conference, Xi'an; 2013
158. Zhao, C. Huang, Y. ADRC based input disturbance rejection for minimum-phase plants with unknown orders and/or uncertain relative degrees. J Syst Sci Complex 2012;25:625–40.

Appendices

Appendices

Appendix (A)

Table 1:1.5kVA salient-pole Lab-Volt SG parameters

Nominal rms line-to-neutral voltage	U_n	*220 v*
Frequency	f_n	*50 Hz*
Stator resistance	R_s	*2.2 Ω*
Rotor resistance	R_f	*127 Ω*
Direct-axis synchronous reactance (unsaturated)	X_d	*75.443 Ω*
Quadrature-axis synchronousreactance (unsaturated)	X_q	*46.556 Ω*
Direct-axis open-circuit time constant	T_{do}'	*0.235 s*
Direct-axis transient reactance	X_d'	*10.309 Ω*
Direct-axis transient time constant	T_d'	*0.0776 s*
Direct-axis sub-transient reactance	X_d''	*8.5298 Ω*
Quadrature-axis sub-transient reactance	X_q''	*5.2637 Ω*
Direct-axis sub-transient time constant	T_d''	*0.0147 s*

Table 2:187M VA SG parameters.[matlab bloc parameters]

Nominal power	P_n	$187*10^6 VA$
Nominal rms line-to-neutral voltage	U_n	*13800 v*
Frequency	f	*60 Hz*
Statorresistance	R_s	$2.9*10^{-3}$ Ω
Rotor resistance	R_f	$5.9*10^{-4}$ Ω
Stator leakage inductance	Ll	$3.089*10^{-4} H$
Direct-axis synchronous magnetizing inductance	Lmd	$3.21*10^{-3}$ H
Quadrature-axis synchronous magnetizing inductance	Lmq	$9.71*10^{-4} H$
Field leakage inductance referred to the stator	$Llfd'$	$3.0712*10^{-4}$ H
Direct-axis damper resistance	RKd'	$1.019\ 10^{-2}$ Ω
Direct-axis damperleakage inductance	$LlKd'$	$4.91*10^{-4}$ H
Quadrature-axis damper resistance	$RKq1'$	$2.008\ 10^{-2}$ Ω
Quadrature-axis damperleakage inductance	$LlKq1'$	$1.03*10^{-3} H$
inertia	J	$3.89*10^6 Kg.m^2$
Pole pair	p	*20*

Appendix (B)

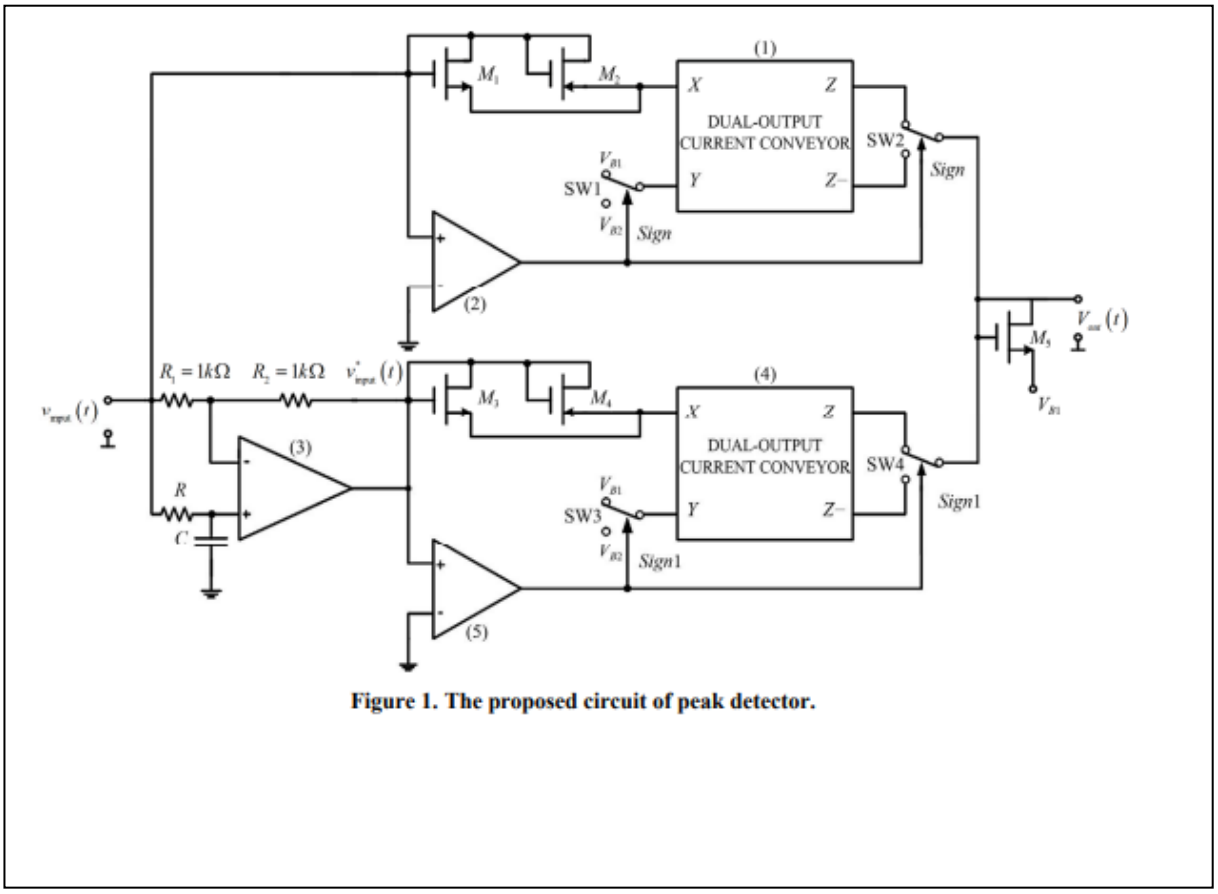

Figure 1. The proposed circuit of peak detector.

The phase shift of the input signal is realized using an all-pass filter. The phase of the input sinusoidal signal: $V_{input}\ (t) = V_m$Sin (2πft) ((where Vm is amplitude and f is frequency) is shifted by 90˚ by adjusting the resistance (R) and capacitor (C) of the RC network of the all-pass filter (using AD844) in which the amplitude of the 90˚ phase-shifted signal is kept equal to the amplitude of the input sinusoidal signal. The all-pass filter passes the input signal with unity gain and without attenuation.

For more information see the following document

Predrag B. Petrović. A New Precision Peak Detector/Full-Wave Rectifier. Journal of Signal and Information Processing, 2013, 4, 72-81